Università degli Studi di Ferrara

DOTTORATO DI RICERCA IN BIOCHIMICA, BIOLOGIA MOLECOLARE E BIOTECNOLOGIE

CICLO XXIV

COORDINATORE Prof. Francesco Bernardi

From cell signalling to cell death: endoplasmic reticulum-mitochondria calcium transfer and its remodelling for cancer cell survival

Settore Scientifico Disciplinare MED/04

Dottorando
Dott. Bononi Angela

Tutore
Prof. Pinton Paolo

Anni 2009/2011

A mia sorella Martina,

e a chi verrà...

…perchè anche se ancora non so dove tutto questo mi porterà,

ci sono legami che resistono a tutto, per sempre.

Contents

ABSTRACT

The tight interplay between endoplasmic reticulum (ER) and mitochondria is a key determinant of cell function and survival through the control of intracellular calcium (Ca^{2+}) signalling. The physical platform for the association between the ER and mitochondria is a domain of the ER called the "mitochondria-associated membranes" (MAMs). MAMs are crucial for highly efficient transmission of Ca^{2+} from the ER to mitochondria, thus controlling fundamental processes involved in energy production and also determining cell fate by triggering or preventing apoptosis.

In particular, we show that: i) despite different roles in cell survival, all three isoforms of the outer mitochondrial membrane protein voltage-dependent anion channels (VDAC) are equivalent in allowing mitochondrial Ca^{2+} loading upon agonist stimulation, vice versa VDAC1, by selectively interacting with the inositol trisphosphate receptors (IP3Rs) - an interaction that is further strengthened by apoptotic stimuli - is preferentially involved in the transmission of the low-amplitude apoptotic Ca^{2+} signals to mitochondria, highlighting a non-redundant molecular route for transferring Ca^{2+} signals to mitochondria in apoptosis; ii) the promyelocytic leukemia (PML) tumor suppressor exerts its extranuclear proapoptotic action by its unexpected and fundamental role at MAMs, where PML was found in protein complexes with the type 3 IP3R, the protein kinase Akt and the phosphatase PP2a, which are essential for Akt- and PP2a-dependent modulation of IP3R phosphorylation and in turn for IP3R-mediated Ca^{2+} release from ER; iii) the PTEN (phosphatase and tensin homolog deleted on chromosome 10) tumor suppressor localizes at the ER and MAMs, and ER-localized PTEN is specifically involved in increasing both Ca^{2+} transfer from the ER to mitochondria and cell sensitivity to Ca^{2+}-mediated apoptosis.

The improved knowledge of the functioning of proteins involved in regulating Ca^{2+} signalling may reveal novel unexplored pharmacological targets, and help in treating cancer as well as other pathologies.

ABSTRACT (Italiano):

L'accoppiamento funzionale tra reticolo endoplasmatico (ER) e mitocondri è un fattore determinate per la funzionalità e la sopravvivenza cellulare, in quanto determina il controllo del segale calcio (Ca^{2+}) intracellulare. Dal punto di vista fisico, la base per l'associazione tra ER e mitocondri risiede in un dominio dell'ER definito "membrane associate ai mitocondri" (MAMs). Le MAMs sono fondamentali per una trasmissione altamente efficiente degli ioni Ca^{2+} dall'ER ai mitocondri, e per questo controllano processi indispensabili coinvolti nella produzione di energia, ed inoltre determinano il destino della cellula facilitando o ostacolando l'apoptosi.

Specificamente, abbiamo dimostrato che: i) nonostante svolgano diversi ruoli nella sopravvivenza cellulare, tutte e tre le isoforme del canale anionico voltaggio dipendente (VDAC, "voltage-dependent anion channels", una proteina della membrana mitocondriale esterna) hanno un ruolo equivalente nell'accumulo mitocondriale di Ca^{2+} indotto da stimolazione con agonista, viceversa VDAC1, attraverso l'intrerazione selettiva con i recettori dell'inositolo trifosfato (IP3Rs) – un'interazione ulteriormente rafforzata dagli stimoli apoptotici – è preferenzialmente coinvolto nella trasmissione ai mitocondri di stimoli apoptotici Ca^{2+} mediati che hanno entità inferiore, evidenziando un'esclusiva via molecolare per il trasferimento del segnale Ca^{2+} ai mitocondri durante l'apoptosi; ii) l'oncosoppressore PML (leucemia promielocitica), quando localizzato al di fuori del nucleo, è comunque in grado di esercitare una funzione proapoptotica mediante la sua inaspettata localizzazione alle MAMs, dove PML è stato trovato in complessi proteici con i recettoti IP3R di tipo 3, la proteina chinasi Akt e la proteina fosfatasi PP2a, che sono essenziali per la modulazione dello stato di fosforilazione dell'IP3R mediata da Akt e PP2a, e di conseguenza del rilascio di Ca^{2+} dall'ER attraverso l'IP3R; iii) l'oncosoppressore PTEN ("phosphatase and tensin homolog deleted on chromosome 10") localizza all'ER e alle MAMs, e la quota di PTEN presente al reticolo è quella specificamente coinvolta nell'aumento sia del trasferimento di Ca^{2+} dall'ER ai mitocondri che nella suscettibilità a stimoli apoptotici mediati da Ca^{2+}.

L'avanzamento nella conoscenza del funzionamento di proteine coinvolte nel segnale Ca^{2+} potrà rivelare nuovi inesplorati bersagli farmacologici ed aiutare nel trattamento del cancro ed altre patologie.

Abbreviations:

$\Delta\Psi_m$, mitochondrial membrane potential difference;
AEQ, aequorin;
ArA, arachidonic acid;
ANT, adenine nucleotide translocase;
Bap31, B-cell receptor-associated protein 31;
BiP, Binding immunoglobulin Protein;
Ca^{2+}, calcium ions;
$[Ca^{2+}]$, Ca^{2+} concentration;
$[Ca^{2+}]_c$, cytosolic Ca^{2+} concentration;
$[Ca^{2+}]_m$, mitochondrial Ca^{2+} concentration;
CABPs, intraluminal Ca^{2+}-binding proteins;
CaMKII, calmodulin-dependent protein kinase II;
Cyp D, cyclophilin D;
Drp1, dynamin-related protein 1;
ER, endoplasmic reticulum;
ERp44, endoplasmic reticulum resident protein 44;
ETO, etoposide;
FACL4, long-chain fatty acid-CoA ligase type 4;
FAD, familial Alzheimer's disease;
Fis1, Fission 1 homologue;
FRET, fluorescence resonance energy transfer;
GFP, green fluorescent protein;
GM1, GM1-ganglioside;
grp75, glucose-regulated protein 75;
HK, hexokinase;
IMM, inner mitochondrial membrane;
IMS, intermembrane space;
IP3, inositol 1,4,5-trisphosphate;
IP3R, inositol 1,4,5-trisphosphate receptor;
Letm1, leucine zipper-EF-hand containing transmembrane protein 1;
MAMs, mitochondria-associated membranes;
MCU, mitochondrial Ca^{2+} uniporter;
MICU1, mitochondrial calcium uptake 1;
Mfn, mitofusin;
VDAC, voltage-dependent anion channel;
UCP, uncoupling protein;
MEN, menadione;
mHCX, mitochondrial H^+/Ca^{2+} exchanger;
mNCX, mitochondrial Na^{2+}/Ca^{2+} exchanger;
MOMP, mitochondrial outer membrane permeabilization;
MPT, mitochondrial permeability transition;
NCX, Na^{2+}/Ca^{2+} exchanger;
OA, okadaic acid;
OMM, outer mitochondrial membrane;
OPA1, optic atrophy 1;
OXPHOS, oxidative phosphorylation;
p66shc, 66-kDa isoform of the growth factor adapter shc;
PACS-2, phosphofurin acidic cluster sorting protein 2;
PAMs, plasma membrane associated membranes;
PDH, pyruvate dehydrogenase;
PI3K, phosphatidylinositol 3-kinase;
PIP2, phosphatidylinositol 4,5-bisphosphate;
PIP3, phosphatidylinositol 3,4,5-trisphosphate;
PKA, protein kinase A;
PKC, protein kinase C;
PLC, phospholipase C;
PMCA, plasma membrane Ca^{2+} ATPase;
PML, promyelocytic leukemia protein;
PP2a, protein phosphatase 2a;
PS1, presenilin;
PSS-1, phosphatidylserine synthase-1;
PTEN, phosphatase and tensin homolog deleted on chromosome 10;
PTP, permeability transition pore;
ROS, reactive oxygen species;
RyR, ryanodine receptor;
SERCA, sarco-endoplasmic reticulum Ca^{2+} ATPase;
Sig-1R, Sigma-1 receptor;
SOCE, store-operated Ca^{2+} entry;
SR, sarcoplasmic reticulum;
TIRF, total internal reflection fluorescence;
TG, thapsigargin;
TN, tunicamycin;

1. INTRODUCTION:

Changes in the levels of intracellular calcium ions (Ca^{2+}) provide dynamic and highly versatile signals that regulates several processes as diverse as energy transduction, fertilization, secretions, muscle contraction, chemotaxis and neuronal synaptic plasticity in learning and memory (1). However, under certain conditions increases in intracellular Ca^{2+} are cytotoxic and lead to apoptosis (programmed cell death). Consequently, Ca^{2+} needs to be used in an appropriate manner to determine cell fate; if this balancing act is compromised, pathology may ensue (2).

Ca^{2+} signalling proteins and organelles are emerging as additional cellular targets of oncogenes and tumour suppressors. The Ca^{2+} signal has major roles in the regulation of processes relevant to tumorigenesis, including migration, invasion, proliferation, and apoptotic sensitivity (3). Intracellular Ca^{2+} homeostasis has been the focus of researchers characterizing changes in Ca^{2+} signalling in cancer cells. In order for the cancer cells to proliferate at higher rates and still protect themselves from apoptosis, many cancer cells remodel the expression or activity of their Ca^{2+} signalling machinery. Spatially restricted Ca^{2+} signalling within specific cellular compartments or discrete cytosolic domains provides an additional layer of complexity in the regulation of cellular processes important in tumorigenesis. . In normal cells, the Ca^{2+} signalling is highly regulated spatially such as between endoplasmic reticulum (ER) and mitochondria, two intracellular organelles which play crucial roles in Ca^{2+} signalling and may decide the ultimate fate of the cell. Indeed, by adjusting the load of Ca^{2+} imposed upon the mitochondrion, the same Ca^{2+} efflux from ER (the main intracellular Ca^{2+} store) that is responsible for regulating processes for maintaining life could also act as a death-inducing signal.

Since ER and mitochondria play significant roles in the regulation of cell proliferation and apoptosis, the remodelling of Ca^{2+} signalling machinery in ER and mitochondria in cancer cells seems imminent during oncogenic transformation. Therefore, targeting of the Ca^{2+} signalling apparatus in cancer cells could specifically disrupt their Ca^{2+} homeostasis, and so decrease cancer cell proliferation and increase cancer cell apoptosis. Such novel and highly innovative strategies can provide rationale and approaches for the design and development of novel technologies based on Ca^{2+} waves for the diagnosis and treatment of cancer, as well as other disease.

1.1 The Ca^{2+}-signalling toolkit

At the beginning of life, Ca^{2+} mediates the process of fertilization and regulates the cell cycle events during the early developmental processes. Once the cells differentiate to perform specific functions, changes in the levels of intracellular Ca^{2+} provide dynamic and highly versatile signals that control a plethora of cellular processes, yet under certain conditions increases in intracellular Ca^{2+} are cytotoxic (4). For this reason, the intracellular concentration of Ca^{2+}, $[Ca^{2+}]_i$, in resting cells is usually maintained very low, at ~100 nM.

In cells, due to the presence of several charged molecules, the Ca^{2+} diffusion rates are slow. In order to utilize Ca^{2+} as a second messenger, cells have devised an ingenious mechanism of signalling that has overcome the inherent problems associated with lower diffusion rates and potential cytotoxicity of Ca^{2+}, by presenting changes in Ca^{2+} concentration as brief spikes which are often organized as regenerative waves (1). The universality of Ca^{2+}-based signalling depends on its enormous versatility in terms of amplitude, duration, frequency and localization. The formation of the correct spatio-temporal Ca^{2+} signals is dependent on an extensive cellular machinery named the Ca^{2+} toolkit, which includes the various cellular Ca^{2+}-binding and Ca^{2+}-transporting proteins, present mainly in the cytosol, plasma membrane, ER and mitochondria (5).

To provide for a very fast and effective Ca^{2+}-signaling, the cells use a great amount of energy to maintain an almost 20 000-fold Ca^{2+}-gradient between their intracellular (~100 nM free) and extracellular (~1 mM) Ca^{2+} concentrations. To maintain this Ca^{2+} gradient, the cells chelate, compartmentalize, or remove Ca^{2+} from the cytoplasm through its active extrusion by the plasma membrane Ca^{2+} ATPase (PMCA) and the Na^+/Ca^{2+} exchanger (NCX) (6, 7)

The increase of intracellular $[Ca^{2+}]$ can be elicited by two fundamental mechanisms (or a combination of both). The first involves Ca^{2+} entry from the extracellular milieu, through the opening of plasma membrane Ca^{2+} channels (traditionally grouped into three classes: voltage operated Ca^{2+} channels (VOCs) (8), receptor operated Ca^{2+} channels (ROCs) (9) and second messenger operated Ca^{2+} channels (SMOCs) (10)). The second universal mechanism for Ca^{2+} signaling is the release of Ca^{2+} from intracellular Ca^{2+} stores, mainly the ER and its specialized form in muscle, the sarcoplasmic reticulum (SR). In these intracellular stores, two main Ca^{2+}-release channels exist that, upon stimulation, release Ca^{2+} into the cytosol, thus triggering Ca^{2+} signalling: the inositol 1,4,5-trisphosphate (IP3) receptors (IP3Rs) and the ryanodine receptors (RyRs) (11, 12). IP3Rs are ligand-gated channels that function in releasing Ca^{2+} from ER Ca^{2+} stores in response to IP3 generation. G protein coupled receptors (GPCRs) can activate phospholipase C β (PLCβ), and tyrosine-kinase receptors (TKR) can activate PLCγ, which then

cleave PIP2 into IP3 and diacylglycerol (DAG). IP3 binding to the IP3Rs that are present in the ER, causes efflux of Ca^{2+} from the ER to the cytoplasm resulting in increase in cytosolic Ca^{2+} concentration ($[Ca^{2+}]_c$) from ~100 nM to ~1 μM for several seconds (13, 14). This rise in $[Ca^{2+}]_c$ results in various Ca^{2+}-dependent intracellular events (Figure 1). A variety of cellular proteins with Ca^{2+}-binding affinities ranging between nM to mM are utilized by the cells to buffer the cellular Ca^{2+} increase as well as to regulate cellular processes via Ca^{2+}-signaling. The exact cellular outcome depends on the spatiotemporal characteristics of the generated Ca^{2+} signal (15).

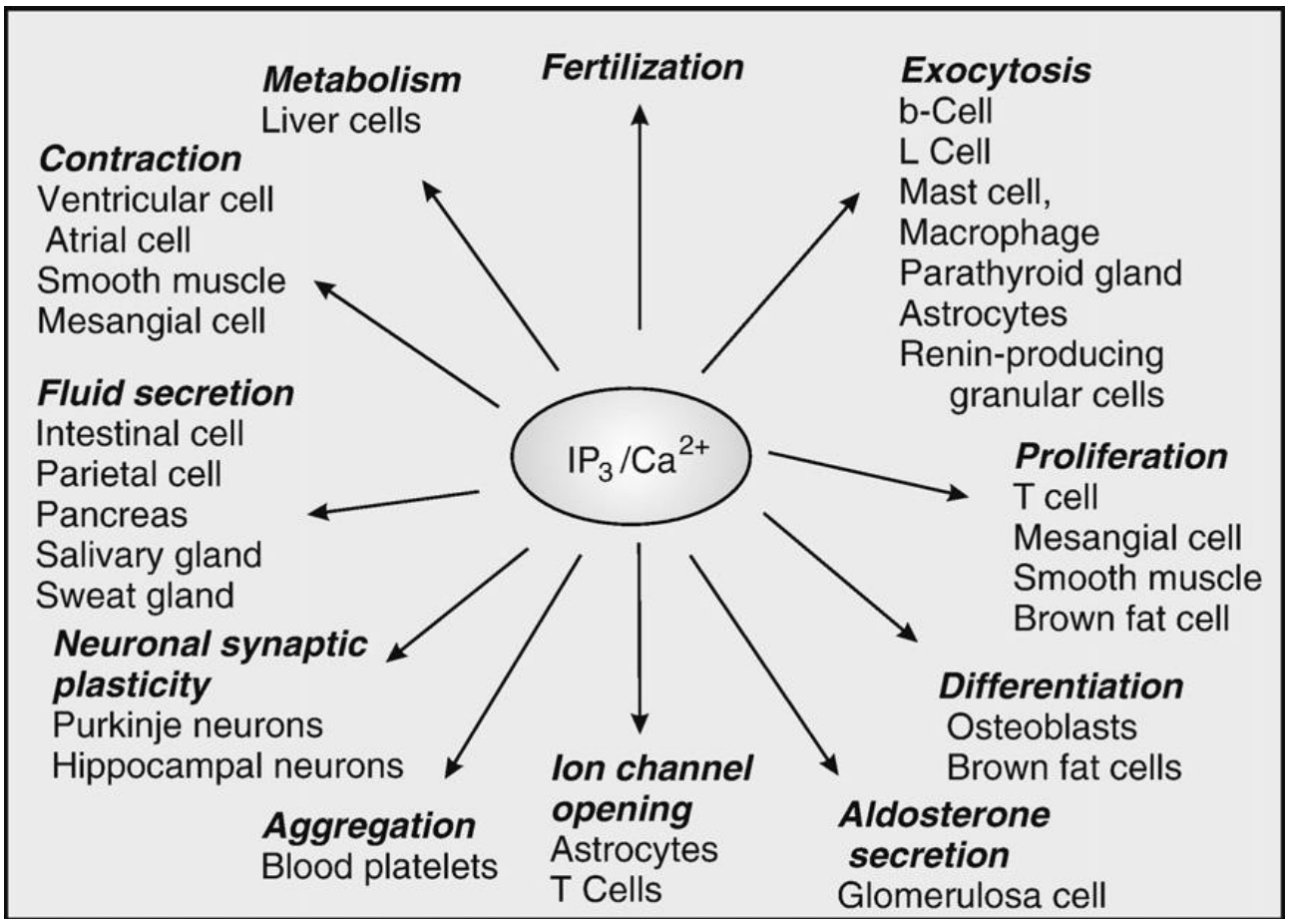

Figure 1. Regulation of multiple cellular processes by the IP3/Ca^{2+} signalling pathway. *(figure from (16))*

Once its downstream targets are activated, basal $[Ca^{2+}]_c$ levels are regained by the combined activity of Ca^{2+} extrusion mechanisms, such as PMCA and NCX, and mechanisms that refill the intracellular stores, like sarco-endoplasmic reticulum Ca^{2+} ATPases (SERCAs) (6). Due to SERCA activity and intraluminal Ca^{2+}-binding proteins (CABPs), *i.e.*, calnexin and calreticulin (17), the ER can accumulate Ca^{2+} more than a thousand-fold excess as compared to the cytosol. Given that

PMCAs pump Ca^{2+} out of the cell faster than it can be repleted, IP3R mediated efflux of Ca^{2+} from the ER in response to receptor activation empties the ER, thus a Ca^{2+} entry mechanism is activated. This mechanism is called "Store-operated Ca^{2+} entry" (SOCE). The molecular determinants of SOCE have been identified in the very last few years and include the ER Ca^{2+} sensors STIM (stromal interaction molecule) 1 and 2, and the specialized plasma-membrane channels Orai1, Orai2 and Orai3 (for a recent review (18)).

Although the ER (and its specialized form in muscle, the SR) is generally considered the main intracellular Ca^{2+} store, almost all other organelles play a role in Ca^{2+} signalling: mitochondria (see below) (19), the Golgi apparatus (20), secretory vesicles (21), lysosomes (22), endosomes (23) and peroxisomes (24, 25).

Specificity in decoding Ca^{2+} signals can be provided by the affinity of Ca^{2+} sensor as well as its duration, amplitude and intracellular location: in this way a particular Ca^{2+} signal can specifically regulate many different cell functions (26).

1.2 ER-mitochondria crosstalk: local microdomains support mitochondrial Ca^{2+} uptake

While the role of the ER as a physiologically important Ca^{2+} store has long been recognized, a similar role for mitochondria have seen a reappraisal only in the past two decades (27). The uptake of the Ca^{2+} ions into the mitochondrial matrix implies different transport systems responsible for the transfer of Ca^{2+} across the outer and the inner mitochondrial membrane (OMM and IMM respectively). It has long been known that mitochondria can rapidly accumulate Ca^{2+} down the large electrochemical gradient (mitochondrial membrane potential difference, $\Delta\Psi_m$ = -180 mV, negative inside) generated by the respiratory chain (28). Indeed, based on the chemiosmotic theory, the translocation by protein complexes of H^+ across an ion-impermeable inner membrane generates a very large H^+ electrochemical gradient and mitochondria employ the dissipation of this proton gradient not only to run the endoergonic reaction of ATP synthesis by the H^+-ATPase, but also to accumulate cations into the matrix.

For a long time, however, due to the low affinity of the mitochondrial Ca^{2+} uptake system under physiological conditions (an apparent K_d of 20 to 30 μM under conditions thought to mimic the cytoplasm, estimated in the earlier work with isolated organelles) and the submicromolar global $[Ca^{2+}]_c$ briefly reached after physiological stimulation (which rarely exceed 2-3 μM), this process was considered to take place only in conditions of high-amplitude, prolonged $[Ca^{2+}]_c$ increases, i.e.

in the Ca^{2+} overload that is observed in various pathological conditions (such as, for example, excitotoxic glutamate stimulation of neurons) (19). Mitochondrial Ca^{2+} returned to the limelight in 1992 when Rizzuto, Pozzan and colleagues generated a novel, genetically encoded chemiluminescent indicator, aequorin. This probe, specifically targeted to the mitochondrial matrix, allowed dynamic, accurate and specific monitoring of the $[Ca^{2+}]$ within the matrix of mitochondria in living cells (29). With this new tool they could show that mitochondria in living cells undergo very fast and large increases in their matrix Ca^{2+} levels (mitochondrial Ca^{2+} concentration, $[Ca^{2+}]_m$) upon cell stimulation, reaching peaks similar or even larger than those in the cytoplasm, even for normal physiological cytoplasmic Ca^{2+} rises (30). Similar conclusions could be reached also with fluorescent indicators, such as the positively charged Ca^{2+} indicator rhod-2 (that accumulates within the organelle) (31) and the more recently developed GFP-based fluorescent indicators (32).

While enlivening the interest in mitochondrial Ca^{2+} homeostasis, these data raised an apparent contradiction between the prompt response of the organelle (where $[Ca^{2+}]_m$ rise, in a few seconds, to values above 10 μM, and in some cell types up to 500 μM) and the low affinity of the Ca^{2+} uptake system together with the low concentration of global Ca^{2+} signals observed in cytoplasm. Based on a large body of experimental evidence, it is now generally accepted that the key to the rapid Ca^{2+} accumulation rests in the strategic location of a subset of mitochondria, close to the opening ER or plasma membrane Ca^{2+} channels (30, 31, 33). The hypothesis, called "microdomain hypothesis" (26), proposes that microdomains of high $[Ca^{2+}]$ (10-20 μM) can be transiently formed in regions of close apposition between mitochondria and Ca^{2+} channels of the ER/SR or of the plasma membrane (33). These high Ca^{2+} microdomains rapidly dissipate (due to diffusion) insuring that mitochondria do not overload with Ca^{2+} (Figure 2).

The "microdomain hypothesis" received a number of indirect confirmations in the last 20 years by different groups. More recently, such microdomains in selected regions of contact between ER and mitochondria were finally measured directly, by two complementary studies that demonstrated the existence and amplitude of high Ca^{2+} microdomains on the surface of mitochondria. Giacomello *et al.* (34) targeted a new generation of FRET-based Ca^{2+} sensors (35) to the OMM and, through a sophisticated statistical analysis of the images, revealed the existence of small OMM regions where $[Ca^{2+}]$ reaches values as high as 15-20 μM. The probe detected Ca^{2+} hotspots on about 10% of the OMM surface that were not observed in other parts of the cell. The Ca^{2+} hotspots were not uniform, and their frequency varied among mitochondria of the same cell. Moreover, classical epifluorescence and total internal reflection fluorescence (TIRF) microscopy experiments were combined in order to monitor the generation of high Ca^{2+} microdomains in mitochondria located near the plasma membrane. With this approach, it could be shown that Ca^{2+} hotspots on the surface

of mitochondria occur upon opening of VOCs, but not upon SOCE. Csordás *et al.* (36) used a complementary approach in which they generated genetically encoded bifunctional linkers consisting of OMM and ER targeting sequences connected through a fluorescent protein, including a low-Ca^{2+}-affinity pericam, and coupled with the two components of the FKBP-FRB heterodimerization system (37), respectively. Using rapamycin-assembled heterodimerization of the FKBP-FRB-based linker, they detected ER/OMM and plasma membrane/OMM junctions (the latter at a much lower frequency). In addition, the recruited low-Ca^{2+}-affinity pericam reported Ca^{2+} concentrations as high as 25 μM at the ER/OMM junctions in response to IP3-mediated Ca^{2+} release, which is in excellent agreement with the values obtained by Giacomello *et al.*.

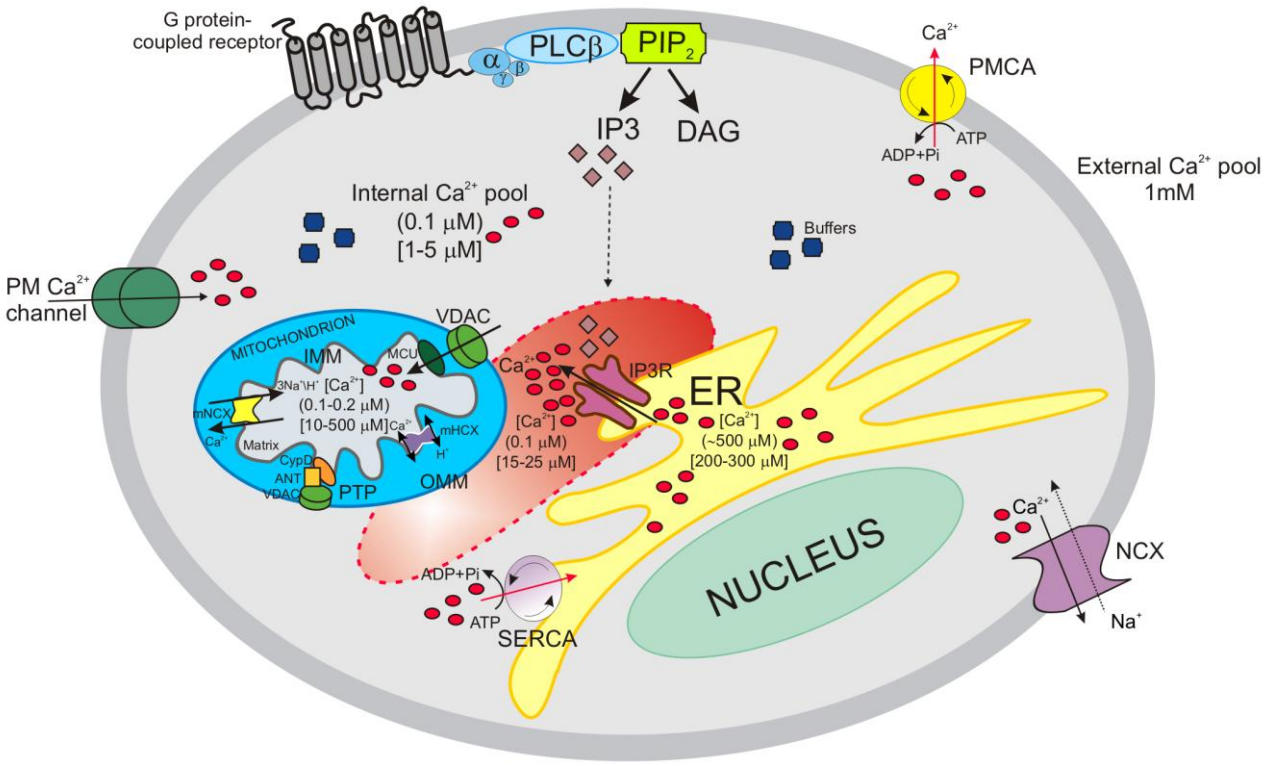

Figure 2. Intracellular Ca^{2+} signalling. *Schematic model of intracellular Ca^{2+} homeostasis. Plasma membrane G-protein coupled receptors activate phospholipase C-β (PLC-β) to promote the generation of inositol 1,4,5-trisphosphate (IP3) and the release of Ca^{2+} from the endoplasmic reticulum (ER) into the cytosol. Mitochondrial surface directly interacts with the ER through contact sites defining hotspots Ca^{2+} signalling units. Ca^{2+} import across the outer mitochondrial membrane (OMM) occurs by the voltage-dependent anion channel (VDAC), and then enters the matrix through the mitochondrial Ca^{2+}+ uniporter (MCU), the main inner mitochondrial membrane (IMM) Ca^{2+}-transport system (Ca^{2+} levels reached upon stimulation are indicated in square brackets). Mitochondrial Ca^{2+} exchangers present in the IMM export Ca^{2+} from the matrix once mitochondrial Ca^{2+} has carried its function; another mechanism for Ca^{2+} efflux from mitochondria is the permeability transition pore (PTP). Ca^{2+} levels return to resting conditions (indicated in round brackets) through the concerted action of cytosolic Ca^{2+} buffers, plasma membrane Ca^{2+}-ATPase (PMCA) and the Na^{+}/ Ca^{2+} exchanger (NCX) that permit the ion extrusion in the extracellular milieu. Sarco-endoplasmic reticulum Ca^{2+} ATPase (SERCA) restablishes basal Ca^{2+} levels in intracellular stores. ANT adenine nucleotide translocase, Cyp D cyclophilin D, DAG diacylglycerol, PIP2 phosphatidylinositol 4,5-bisphosphate.*

While based on cell morphology the close proximity between the mitochondria and the ER is expected and indeed often observed, i.e. in neuronal prolongings, a close interaction between ER-resident Ca^{2+} channels and mitochondria in non-excitable cells implies the assembly of a dedicated signaling unit at the organelle interphase (see section 1.7).

1.3 Calcium release from cellular store: structure and function of the IP3R

The ER is possibly the largest individual intracellular organelle comprising a three dimensional network of endomembranes arranged in a complex grid of microtubules and cisternae. It is made up of functionally and structurally distinct domains (reviewed extensively by a number of authors (38-41), in relation to the variety of cellular functions played by the organelle, primarily concerning protein synthesis, maturation and delivery to their destination (42, 43). Moreover, the ER is a dynamic reservoir of Ca^{2+} ions, which can be activated by both electrical and chemical cell stimulation (44, 45) making this organelle an indispensable component of Ca^{2+} signalling (46-48).

Modern analysis methods enabled the determination of the molecular profile of the ER. This profile reflects the ER's role in signalling, as it comprises a number of components constituting the Ca^{2+} signalling pathway. It contains IP3Rs, RyRs, SERCAs, and in addition to these release channels and pumps, there are buffers (calnexin, calreticulin) and a number of ancillary proteins (FK 506-binding proteins, sorcin, triadin, phosholamban) that contribute to the ER Ca^{2+} signalling system (49).

Many extracellular stimuli, such as hormones, growth factors, neurotransmitters, neutrophins, odorants, and light, function generating IP3 through the phospholipase C isoforms, activated in different manners: G-protein coupled receptors (acting via PLC-β), tyrosine-kinase coupled receptors (PLC-γ), an increase in Ca^{2+} concentration (PLC-δ) or activated by Ras (PLC-ε) (50, 51). The final effector are the IP3Rs, nonselective cationic channels that conduct Ca^{2+}.

A functional IP3R Ca^{2+} channel is composed of tetramers with six transmembrane domains (of ~3000 amino acids) that can be either homotetramers or, to a lesser extent, heterotetramers of different isoforms. From the structural point of view, several domains are recognized in the protein sequence, with different functions. These include the IP3-binding domain (IP3-BD), i.e. the minimal sequence sufficient for IP3 binding, located near the N-terminus of the protein (aa 226-578). Interestingly, this protein domain contains armadillo-repeat protein structures that are engaged in protein-protein interactions, and mediates intramolecular interactions with other IP3R domains as well as the association with other regulatory proteins. N-terminally to the IP3-BD, i.e. within aa 1-222, a suppressor region is located that inhibits ligand binding and thus lowers the global receptor IP3 affinity in the physiological range. The six transmembrane-spanning domain is at the very C-

terminal end of each subunit, and, between them, an internal coupling domain assures the signal of IP3 binding is transferred to the channel-forming region, hence triggering its opening (52).

Three isoforms of IP3R encoded by different genes have been identified with different agonist affinities and tissue distribution (53). Given that the affinity of the IP3-binding core to its ligand is similar for the three isoforms, the tuning of the whole receptor's affinity appears to be due to the isotype-specific properties of the N-terminal suppressor domain (54).

The release of Ca^{2+} from the ER is a nonlinear, cooperative process wherein IP3 binds to four receptor sites on the IP3R, one on each subunit of the tetramer (52). IP3Rs are at first potentiated, then inhibited by Ca^{2+}. Small perturbations in conditions, such as basal $[Ca^{2+}]_i$, [IP3], and various regulators can cause uncoordinated bursts of local release across a cell. The brief opening of IP3R channels gives rise to localized Ca^{2+} pulses, called “sparks” or “blips” and “puffs” (1). The smallest Ca^{2+} release events, “blips”, probably reflect random openings of single IP3R. Spontaneous clustering of IP3Rs (in particular of IP3R2, due to its higher IP3 affinity) have been proposed to be the underlying mechanism responsible for Ca^{2+} “puffs” observed in the cytoplasm (55). Recruitment of neighboring IP3Rs and combination of Ca^{2+} “puffs” results in Ca^{2+} waves, ensuring that the Ca^{2+} signal propagates to the entire cell (56), or remains confined to specific subcellular regions (57).

Ca^{2+} oscillations, depend upon both the spatial organization of IP3Rs and their regulation by Ca^{2+}, although the links between IP3R activities and Ca^{2+} oscillations are not fully understood. Ca^{2+} regulates channel activity in a biphasic manner. Early studies demonstrated inhibition of IP3-mediated Ca^{2+} mobilization by micromolar concentrations of Ca^{2+} (58). Lower concentrations were subsequently found to potentiate the effects of IP3 (59). In addition, also the ER Ca^{2+} content retains the capability to regulate the channel opening: in permeabilized hepatocytes, an increase in $[Ca^{2+}]_{er}$ enhances the sensitivity of IP3R for its ligand, promoting also spontaneous Ca^{2+} release, but the nature of this direct regulation and the protein involved are still a matter of debate (60). In this context, the tight spatial relationship between ER and mitochondria, and the capacity of the latter to rapidly clear the high $[Ca^{2+}]$ microdomain generated at the mouth of the IP3R, makes mitochondria an active player in the control of IP3R function. The first clear demonstration of this concept came from the fine work of Lechleiter et al., who demonstrated that energized mitochondria, by regulating the kinetics of ER Ca^{2+} release, finely tune the spatio-temporal patterning of Ca^{2+} waves in Xenopus oocytes. Then, the observation that Ca^{2+} uptake by mitochondria controls the $[Ca^{2+}]$ microdomain at the ER/mitochondrial contacts and thus the kinetics of IP3R activation/inactivation was extended to a variety of mammalian cell lines, e.g. hepatocytes, astrocytes and BHK-21 cells, thus highlighting its general relevance (61).

Whereas IP3 and Ca^{2+} are essential for IP3R channel activation, other physiological ligands, such as ATP, are not necessary but can finely modulate the Ca^{2+}-sensitivity of the channel (62). As for Ca^{2+}, the modulation of IP3R by ATP is biphasic: at micromolar concentrations, ATP exerts a stimulatory effect, while inhibiting channel opening in the millimolar range (63, 64).

Finally, in their coupling/suppressor domains, the IP3Rs possess consensus sequences for phosphorylation by numerous kinases; currently, at least 12 different protein kinases are known to directly phosphorylate the IP3R (65), among them: Akt (66), protein kinase A (cAMP-dependent) (67), protein kinase G (cGMPdependent) (68), calmodulin-dependent protein kinase II (CaMKII) (69), protein kinase C (PKC) (70), and various protein tyrosine kinases (71).

1.4 Mitochondria: cell physiology and molecular nature of the mitochondrial Ca^{2+} uptake and release machinery

Mitochondria: the basics

The mitochondrion represents a unique organelle within the complex endomembrane systems that characterize any eukaryotic cell. Complex life on earth has been made possible through the "acquisition" of mitochondria which provide an adequate supply of substrates for energy-expensive tasks. The mitochondrion is a double membrane-bounded organelle thought to be derived from an α-proteobacterium-like ancestor, presumably due to a single ancient invasion occurred more than 1.5 billion years ago. The basic evidence of this endosymbiont theory (72) is the existence of the mitochondrial DNA (mtDNA), a 16.6 Kb circular double-stranded DNA molecule with structural and functional analogies to bacterial genomes (gene structure, ribosome). This mitochondrial genome encodes only 13 proteins (in addition to 22 tRNAs and 2 rRNAs necessary for their translation), all of which are components of the electron transport chain (mETC) complexes (I, III and IV), while the whole mitochondrial proteome consists of more than 1000 gene products. Thus, one critical step in the transition from autonomous endosymbiont to organelle has been the transfer of genes from the mtDNA to the nuclear genome. At the same time, eukaryotes had to evolve an efficient transport system to deliver nuclear-encoded peptides inside mitochondria: TIM (Transporters of the Inner Membrane), TOM (Transporters of the Outer Membrane) and mitochondrial chaperones (such as hsp60 and mthsp70) build up the molecular machinery that allows the newly-synthesized unfolded proteins to enter mitochondrial matrix (73).

Mitochondria are defined by two structurally and functionally different membranes: the plain outer membrane, mostly soluble to ions and metabolites up to 5000 Da, and the highly selective inner membrane, characterized by invaginations called *cristae* which enclose the mitochondria matrix. The space between these two structures is traditionally called intermembrane space (IMS), but recent advances in electron microscopy techniques shed new light on the complex topology of the inner membrane. *Cristae* indeed are not simply random folds but rather internal compartments formed by profound invaginations originating from very tiny "point-like structures" in the inner membrane (74). These narrow tubular structures, called *cristae junctions*, can limit the diffusion of molecule from the intra-*cristae* space towards the IMS, thus creating a micro-environment where mETC complexes (as well as other proteins) are hosted and protected from random diffusion.

Mitochondria were identified as the powerhouse for energy production in eukaryotic cells thanks to decades of extensive biochemical work on carbohydrate metabolism and organelle morpho-functional characterization, carried out in the first half of the 20th century by leading scientific figures such as Krebs, Corey, Claude, Palade and many others. Mitochondria are the main site of ATP production. When glucose is converted to pyruvate by glycolysis, only a small fraction of the available chemical energy has been stored in ATP molecules; the main enzymatic systems involved in this process are the tricarboxylic acid (TCA) cycle and the mETC. Products from glycolysis and fatty acid metabolism are converted to acetyl-CoA which enters the TCA cycle where it is fully degraded to CO_2. More importantly, these enzymatic reactions generate NADH and $FADH_2$ which provide reducing equivalents and trigger the electron transport chain. mETC consists of five different protein complexes: complex I (NADH dehydrogenase), complex II (succinate dehydrogenase), complex III (ubiquinol cytochrome c reductase), complex IV (cytochrome c oxidase) and complex V that constitutes the F_1F_0-ATP synthase. Electrons are transferred from NADH and $FADH_2$ through these complexes in a stepwise fashion: as electrons move along the respiratory chain, energy is stored as an electrochemical H^+ gradient across the inner membrane, thus creating a negative mitochondrial membrane potential (estimated around -180 mV against the cytosol). H^+ are forced to reenter the matrix mainly through complex V which couples this proton driving force to the phosphorylation of ADP into ATP, according to the chemiosmotic principle. ATP is then released to IMS through the electrogenic Adenine Nucleotide Translocase (ANT) which exchange ATP with ADP to provide new substrate for ATP synthesis. Finally, ATP can easily escape the IMS thanks to the mitochondrial porin of the outer membrane, VDAC (voltage-dependent anion channel).

With the general acceptance of the chemiosmotic hypothesis, it has became clear that the $\Delta\Psi$ across the mitochondrial inner membrane is the driving force for mitochondrial Ca^{2+} accumulation (75).

Thus, Ca^{2+} enters the mitochondrial matrix down its electrochemical gradient, that can be generated either by the electron flow in the mETC or by reversal of the ATP synthase. Mitochondrial Ca^{2+} accumulation plays a key role in the regulation of many cell functions, ranging from ATP production to cell death. Mitochondrial Ca^{2+} uptake and release is central not only for the regulation of cellular Ca^{2+} homeostasis, but is vital also for the regulation of intramitochondrial enzymes concerned with the utilization of oxidizable substrates. However, excess Ca^{2+} accumulation by mitochondria is a common event in the process of cell death, by both necrosis and apoptosis (76) (see , sections 1.5 and 1.6).

Despite the basic mechanisms of mitochondrial Ca^{2+} homeostasis have been firmly established for decades, the molecular identities of the channels and transporters responsible for Ca^{2+} uptake and release (schematized in Figure 3) have remained mysterious until very recently.

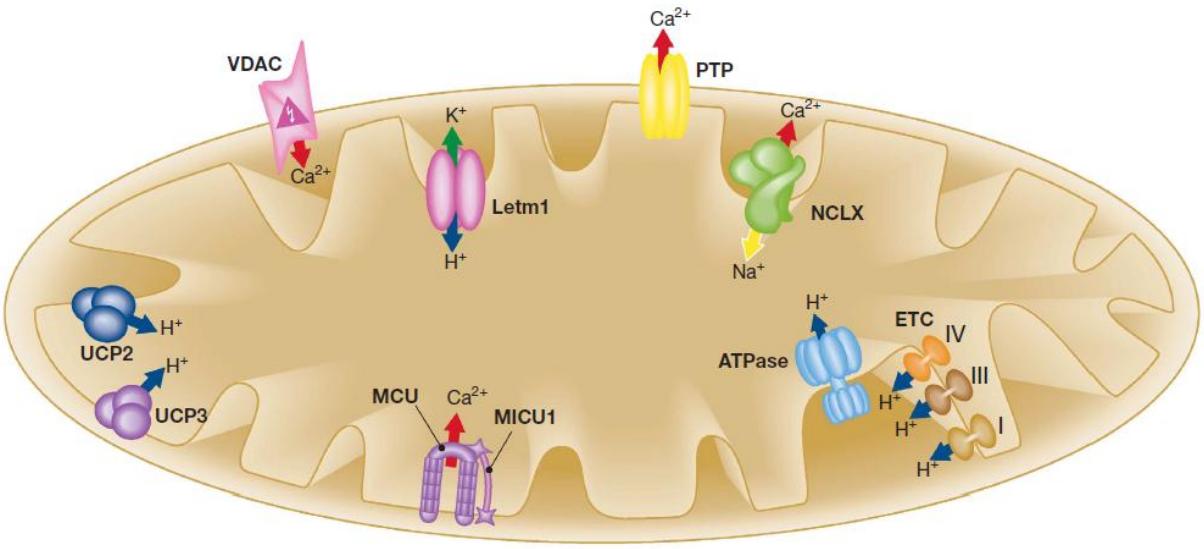

Figure 3. Schematic representation of the mitochondrial Ca^{2+}, Na^{+} and H^{+} handling machinery. *Ion fluxes are indicated by arrows. Red arrow, Ca^{2+}; blue arrow, H^{+}; green arrow, K^{+}; yellow arrow, Na^{+}. ETC, electron transport chain; Letm1, Leucine-zipper EF-hand containing transmembrane protein 1; MCU, mitochondrial Ca^{2+} uniporter; MICU1, mitochondrial calcium uptake 1; NCLX, Na^{+}/Ca^{2+} exchanger; PTP, permeability transition pore; UCP2/3, uncoupling protein 2/3; VDAC, voltage-dependent anion channel (figure from (77)). See text for details.*

We and other groups extensively worked on this topic and what emerged was that the outer mitochondrial membrane (OMM, although traditionally considered freely permeable) is a critical determinant of the mitochondrial Ca^{2+} accumulation (78). Thus, the mitochondrial Ca^{2+} uptake machinery will be discussed, starting from the channels of the OMM, to the last identified components of the IMM.

Ca^{2+} transfer across the OMM

The OMM was previously thought to be freely permeable for ions and small molecules, but now it is clear that the so-called voltage-dependent anion channels, VDAC, also reffered to as the mitochondrial porin, are major regulators of the various ion, nucleotide and molecule fluxes across this membrane, including the Ca^{2+} fluxes (79).

Yeast possesses only one VDAC isoform (but has also another VDAC gene that correctly inserts into OMM showing no channel activity), while higher multicellular organisms and mammals have three distinct VDAC genes (VDAC1, VDAC2 and VDAC3), with VDAC1 representing the best characterized one. These three isoforms show a substantial sequence homology (from 65 to 75% in identity) and similar structure, with the only exception of VDAC2 that has a longer (11 aminoacids) N-terminal tail (80). Yeasts lacking VDAC gene cannot grow on non-fermentable medium, thus highlighting the relevance of this channel in mitochondrial function: reintroduction of any of the mammalian VDAC genes in this yeast strain can promptly restore growth defects (81, 82).

VDAC can exist in multiple conformational states with different selectivity and permeability. This 30-35 kDa protein, is traditionally considered as a large, high-conductance, weakly anion-selective channel, fully opened (pore diameter about 2.5 nm) at low potential (<20-30 mV), but switching to cation selectivity and lower conductance (the so-called "closed" state, with a smaller pore diameter of about 1.8 nm) at higher potentials (both positive and negative). When reconstituted into liposomes, each isoform induced a permeability with a similar molecular weight cut-off (between 3400 and 6800 Da based on permeability to polyethylene glycol). Its structure, as determined by NMR and X-ray crystallography, consists of a 19-stranded β-barrel forming a pore with an inner diameter of about 1.5×1 nm and an N-terminal α-helix domain residing inside the pore: this segment most likely represents the voltage sensor since it is ideally positioned to regulate the conductance of ions and metabolites passing through the VDAC pore (83-85). As the main function of VDAC is assumed to be the gateway for ATP and metabolites, its "open" or "closed" states are defined with respect to those molecules (80, 86). However, the physiological relevance of the voltage gating properties of VDAC is still obscure and a matter of debate, since it requires the existence of a potential across the OMM. The existence of any membrane potential across the OMM has never been directly demonstrated (although some have assumed such a potential is not possible, others have proposed several clues in support of this hypothesis, as discussed in (87)). Despite this, a number of reports show that numerous cytosolic components can significantly modulate VDAC gating properties, including NADH (88), members of Bcl-2 protein family (89), metabolic enzymes (90), chaperones (91) and cytoskeletal elements (92).

A recent work by Tan and Colombini describes the higher permeability of VDAC to Ca^{2+} in the closed states (with low permeability to anionic metabolites), rather than the opened state. So VDAC closure seems to promote Ca^{2+} flux into mitochondria, with consequent permeability transition and cell death (see section 1.5), accordingly with previous observations that VDAC closure is a pro-apoptotic signal (93, 94). These notions have a direct impact on mitochondrial Ca^{2+} transport, as variations in OMM permeability to Ca^{2+} can represent a bottleneck for the efficient ion transfer from the high [Ca^{2+}] microdomain generated by the opening of the IP3R to the intermembrane space. Indeed, transient expression of VDAC in various cell types enhanced the amplitude of the agonist-dependent increases in mitochondrial matrix Ca^{2+} concentration by allowing the fast diffusion of Ca^{2+} from ER release sites to the inner mitochondrial membrane (78). As to the functional consequences, VDAC overexpressing cells are more susceptible to ceramide-induced cell death, thus confirming that mitochondrial Ca^{2+} uptake has a key function in the process of apoptosis.

VDAC has been considered a master regulator of the apoptotic process: on one hand it was thought to be one of the main component of the permeability transition pore (PTP), the megachannel mediating the collapse of mitochondrial membrane potential during apoptosis; on the other side it has long been believed a key mediator of Bax-mediated release of cytochrome c (see sections 1.5 and 1.6). However, despite the huge amount of work carried out on this protein, several recent papers (95-97) have raised serious doubt about our functional understandings of this channel. Indeed, new approaches mainly based on mice knockout models failed to clearly confirm any of the above mentioned functions and rather suggest that a substantial rethinking of VDAC roles is needed.

Ca^{2+} transfer across the IMM

Many attempts were made to identify the molecular nature of the mitochondrial Ca^{2+} uniporter (MCU), starting in the early 1970s, that is, soon after the discovery of mitochondrial Ca^{2+} function.

MCU has always been described as an highly selective ion channel located in the IMM, with a dissociation constant ≤2 nM over monovalent cations, reaching saturation only at supraphysiological $[Ca^{2+}]_c$. Also Sr^{2+} and Mn^{2+} are conducted by MCU and the relative ion conductance is: $Ca^{2+}\approx Sr^{2+}\geq Mn^{2+}\approx Ba^{2+}$. Studies performed on isolated mitochondria allowed the identification of some regulatory molecules acting on MCU, in particular the most effective inhibitors are the hexavalent cation Rutenium Red (RuR) and its related compound RuR360; MCU is also modulated by aliphatic polyamines, such as spermine and aminoglycosides, and by the adenine nucleotides, in the order of effectiveness ATP>ADP>AMP (whereas the nucleoside

adenosine is ineffective) (98) as well as several plant-derived flavonoids (99). Another important regulator of MCU is Ca^{2+} itself. The apparent affinity of the MCU for Ca^{2+}, under physiological conditions (i.e. 1 mM Mg^{2+}), is very low (apparent Kd of 20-30 μM) and the influx rate only becomes substantial when the extramitochondrial [Ca^{2+}] reaches values above 5-10 μM. As demonstrated by Moreau and its group (99), in fact, MCU has a biphasic dependence on $[Ca^{2+}]_c$ increase, that can both activate or inactivate mitochondrial Ca^{2+} uptake. This mechanism allows the mitochondrial Ca^{2+} oscillation, but it prevents an excessive mitochondrial Ca^{2+} accumulation when intracellular Ca^{2+} elevation is prolonged.

The MCU has been molecularly identified only very recently, preceded by the discovery of mitochondrial calcium uptake 1 (MICU1), an uniporter regulator which appears essential for mitochondrial Ca^{2+} uptake (100).

The identification of MICU1 came from the establishment of the so-called MitoCarta database in which about 1000 proteins, specifically present in mitochondria, have been identified (many of them with unknown functions) (101). MICU1 is a 54-kDa protein, with only one putative transmembrane domain, which makes it unlikely that it can function as a Ca^{2+} channel, so it is not known whether it actually forms (part of) a Ca^{2+} channel, or functions as Ca^{2+} buffer, or as a Ca^{2+}-dependent regulatory protein acting as a Ca^{2+} sensor (it has a pair of Ca^{2+}-binding EF-hand domains, the mutation of which eliminates the mitochondrial Ca^{2+} uptake). Taken together the above-mentioned characteristics suggest that MICU1 is not the channel-forming subunit of MCU itself, but rather an associated key subunit.

Finally, last year, two indipendent papers identified the same protein, termed CCDC109A (coiled-coil domaincontaining protein 109A) and renamed MCU, that possesses all the characteristics expected by the elusive Ca^{2+} uniporter of the IMM (102, 103). MCU is a 40-kDa protein ubiquitously expressed in all mammalian tissues and in most eukaryotes, but missing a yeast orthologue. MCU possesses two transmembrane domains and this characteristic makes it reasonable that it forms (through oligomerization) a gated ion channel. Downregulation of MCU drastically reduces mitochondrial Ca^{2+} uptake whereas transfection with the native channel rescues the phenotype of the specific siRNA-treated cells. Moreover, the other classical properties of mitochondria (that is, organelle shape and ER-mitochondrial interactions, O_2 consumption, ATP synthesis and $\Delta\Psi$) are not affected by MCU down-regulation. Just the protein's orientation is the mainly discrepancy between the two papers, one affirming a C-terminus localization in the intermembrane space (102), the other in the matrix (103). Importantly, thanks to the molecular

identification of the MCU, we can now expect a strong acceleration in the search for the functional role of this property of mitochondria, in both physiology and physiopathology.

In the IMM are also present the mitochondrial Na^+/Ca^{2+} exchanger (mNCX) and the H^+/Ca^{2+} exchanger (mHCX). Their main function is probably to export Ca^{2+} from the matrix once mitochondrial Ca^{2+} has carried out its function, to reestablish resting conditions (104). In spite of a few remarkable reports identifying the stoichiometry of the Na^+/ Ca^{2+} exchanger (3 or 4 Na^+ ions per Ca^{2+}) (105), their molecular identity remained, until very recently, completely mysterious. They have yet to be identified, although recently strong evidence has been provided that the Na^+/Ca^{2+} exchanger isoform NCLX (until then considered an isoform of the PM Na^+/ Ca^{2+} exchanger family) fulfils the criteria to be the elusive mitochondrial Na^+-dependent Ca^{2+} efflux (106). They showed that practically all endogenous NCLX localizes in the mitochondrial fraction and knockout of NCLX drastically reduced Na^+-dependent Ca^{2+} efflux in isolated mitochondria; moreover it is sensitive to the classical mitochondrial Na^+/ Ca^{2+} exchanger inhibitor CGP-37157.

Finally, the low conductance mode of the PTP, a channel of still debated nature localized in the IMM (107), can be also considered as a non-saturating mechanism for Ca^{2+} efflux from mitochondria. When open, PTP allows the passage of ions and molecules with a molecular weight up to 1.5 kDa, including Ca^{2+}. Short-time openings may have a physiological function but its long-time activation leads to the demise of the cell, either by apoptosis or by necrosis, depending on whether PTP opening occurs in only a small fraction of the mitochondria or in all of them (see the following section and references (108, 109)).

1.5 Mitochondrial Ca^{2+} function

Physiological functions of Ca^{2+} uptake in the mitochondria

The first role assigned to the Ca^{2+} ions taken up into the mitochondrial matrix was the stimulation of the mitochondrial ATP production since important metabolic enzymes localized in the matrix, the pyruvate-, α-ketoglutarate- and isocitrate-dehydrogenases are activated by Ca^{2+}, with different mechanisms: the first through a Ca^{2+}-dependent dephosphorylation step, the others via direct binding to a regulatory site (110, 111). Those three enzymes represent rate-limiting steps of the Krebs cycle thus controlling the feeding of electrons into the respiratory chain and the generation of the proton gradient across the inner membrane, in turn necessary for ATP production through oxidative phosphorylation (OXPHOS). These events were directly visualized in intact, living cells using a molecularly engineered luciferase probe, which revealed an increase in the [ATP] of the

mitochondrial matrix following agonist stimulation and mitochondrial Ca^{2+} uptake (112). As the ATP produced by mitochondria is subsequently transferred to the cytosol, mechanisms that control ATP production will not only affect overall cell life but, more specifically, will regulate the activity of ATP-sensitive proteins localized in the close vicinity of mitochondria, such as IP3Rs and SERCA, which are stimulated by ATP (113, 114). The bidirectional relation between Ca^{2+} release and ATP production allows for a positive feedback regulation between ER and mitochondria during increased energetic demand (115).

The uptake of Ca^{2+} in mitochondria will also affect Ca^{2+} signalling at both the local and the global level. Assuming the microdomain concept (30, 33), the local [Ca^{2+}] will depend on both the amount of Ca^{2+} released by IP3Rs and that taken up by mitochondria. Since both SERCA pumps and IP3Rs are also regulated by Ca^{2+}, the local [Ca^{2+}] in the vicinity of mitochondria will determine the refilling of the ER and eventually the spatiotemporal characteristics of the subsequent Ca^{2+} signals (116). This will in turn depend on the exact subcellular localization of mitochondria, as well as the efficiency of the coupling between the ER and the mitochondrial network (117). In some conditions, the presence of mitochondria can completely block the further propagation of a Ca^{2+} signal through the cytoplasm. In pancreatic acinar cells, the mitochondria serve as efficient firewalls, absorbing cytosolic Ca^{2+} signals. As a result, the propagation of the Ca^{2+} signal will be limited to the apical pole of the cell and will be prohibited from entering the nucleus (117). The local Ca^{2+} concentration can also affect mitochondrial motility and ER-mitochondria associations in various ways, hence the connection between mitochondria and the ER can be highly dynamic (118). Proteins involved in mitochondrial movement along microtubules, dynein and kinesin, are prone to high $[Ca^{2+}]_c$ mediated by a Ca^{2+} sensor. As the mitochondrial motility is inhibited by Ca^{2+} levels in the low micromolar range, it means that mitochondria will be trapped in the neighbourhood of active Ca^{2+}-release sites allowing for a more efficient Ca^{2+} uptake (119, 120). Apart from organelles movement, mitochondria also continuously remodel their shape. Many of the gene products mediating the fission and fusion processes have been identified in yeast screens, and most are conserved in mammals, including the fission mediators dynamin-related protein 1 (Drp1, Dnm1 in yeast) and Fis1 (Fission 1 homologue), as well as the fusion mediators mitofusins (Mfn) 1 and 2 (Fzo1 in yeast) and optic atrophy 1 (OPA1, Mgm1 in yeast) (121). Several previous studies have indicated that elevation of $[Ca^{2+}]_c$ perturbs mitochondrial dynamics (122), and more recent works have clearly demonstrated that mitochondrial shape can be controlled by an ER-dependent signalling pathway (123, 124). Mitochondria also undergo a more ‘macroscopic’ remodelling of their shape during programmed cell death: after apoptosis induction, mitochondria become largely fragmented, resulting in small, rounded and numerous organelles. However, the relationship

between mitochondrial fusion/fission and apoptosis is complex and mitochondrial fragmentation is not necessarily related to apoptosis (125).

Finally, mitochondria may play an even more active part in Ca^{2+} signaling since the ions can propagate through the mitochondrial network, allowing for mitochondrial release of Ca^{2+} at a distance of the original uptake site (126).

Mitochondrial Ca^{2+} overload

Although Ca^{2+} uptake in the mitochondria is crucial for vital cell functions, there exists a risk of mitochondrial Ca^{2+} overload, which may result in the induction of cell death (Figure 4). There are two pathways that can lead to apoptosis, the death receptor pathway (extrinsic apoptotic pathways) and the mitochondrial pathway (intrinsic apoptotic pathways), both converging on the activation of the executioner caspases (127).

The mitochondrial IMS contains many pro-apoptotic factors such as cytochrome *c*, apoptosis-inducing factor (AIF), Smac/Diablo, HtrA2/Omi and endonuclease G (EndoG). These are released from mitochondria to the cytosol in response to apoptotic signals (for a review see (128)). Released pro-apoptotic proteins can initiate three signalling cascades leading to apoptosis: i) released cytochrome *c*, together with pre-existing cytosolic apoptosis protease activating factor 1 (APAF-1) forms the "apoptosome", which results in the activation of procaspase-9 and in turn activation of effector caspases (caspases-3, -6, and -7), the primarily responsible for the cleavage of cellular proteins leading to the biochemical and morphological characteristics of apoptosis; ii) released Smac/DIABLO and Omi/HtrA2 favour caspase activation by antagonizing the endogenous inhibitor of apoptosis (IAP) proteins in the cytosol; and iii) released AIF and EndoG favour DNA fragmentation and chromatin condensation.

The release of pro-apoptotic factors is preceded by the OMM permeabilization, a crucial step in apoptosis. However, the exact mechanism of mitochondrial OMM permeabilization is not yet clear (129). Ca^{2+} is a critical sensitizing signal in the pro-apoptotic transition of mitochondria, that plays a key role in the regulation of cell death. At a high concentration, mitochondrial Ca^{2+} stimulates drastic changes in mitochondrial morphology and functional activity due to the opening of a non-specific pore, commonly known as the PTP, a mitochondrial megachannel likely to be located in the inner-outer contact sites of the mitochondrial membranes (108). This event, also known as mitochondrial permeability transition (MPT), leads to osmotic swelling of the mitochondria, loss of their membrane potential, and rupture of the OMM, causing the release of IMS proteins, including cytochrome c, into the cytosol (129, 130). This process can be facilitated by inorganic phosphate, oxidation of pyridine nucleotides, ATP depletion, low pH, and ROS. The PTP is generally believed

to be a multimeric complex, composed of VDAC in the OMM, ANT in the IMM, and a matrix protein, cyclophilin D (CypD). Ca^{2+} binding to cyclophilin D positively regulates PTP opening and in turn cell death (131). However, the molecular nature of the PTP is still unresolved (108). An important point hereby was the demonstration that the MPT was not affected by the genetic ablation of any or all of the 3 VDAC isoforms (95). PTP opening may ultimately also lead to necrosis, if MPT and subsequent uncoupling of mitochondria occur in a large subpopulation of these organelles; indeed the border between apoptotic and necrotic cell death is quite diffuse.

Mitochondrial membrane permeabilization can also result from a distinct, yet partially overlapping process known as mitochondrial outer membrane permeabilization (MOMP) (128). In MOMP, pro-apoptotic members of the B-cell CLL/lymphoma-2 (Bcl-2)-protein family may form protein-permeable pores in the OMM (for example, by binding to the VDAC channels and regulating their properties or by forming multimeric channel complexes (132)), causing the release of IMS proteins into the cytosol. Moreover, Bcl-2 family members function as regulators of Ca^{2+} signalling; this important aspect will be discussed in the following section (the interested reader should also refer to (133)).

1.6 Remodelling ER-mitochondria Ca^{2+} transfer in cell survival and death

ER and mitochondria functions are intimately connected. A major area of functional interaction between the ER and mitochondria is the control of Ca^{2+} signalling, that is a topic of major interest in physiology and pathology. These two organelles form a highly dynamic interconnected network within which they cooperate to generate Ca^{2+} signals. The mitochondria play an important role in shaping the Ca^{2+} signal released from the ER. During normal signalling, there is a continuous flow of Ca^{2+} between these two organelles. The normal situation is for most of the Ca^{2+} to reside within the lumen of the ER except during Ca^{2+} signalling when a small bolus is periodically released to the cytoplasm and is then re-sequestered with a proportion passing through the mitochondria. At equilibrium, therefore, the bulk of internal Ca^{2+} is in the ER where it not only functions as a reservoir of signal Ca^{2+} but it also plays an essential role in maintaining the activity of the chaperones responsible for protein processing (26). However, despite controlling many processes essential for life, Ca^{2+} arising from the ER can be a potent death-inducing signal (134, 135).

The release of Ca^{2+} from ER stores by IP3Rs has been implicated in multiple models of apoptosis as being directly responsible for massive and/or a prolonged mitochondrial Ca^{2+} overload. The requirement of IP3Rs for Ca^{2+}-dependent cell death is exemplified by the resistance to apoptosis of cells in which InsP3R expression has been ablated or reduced (136, 137). Mitochondria seem to be

the downstream effectors of this pathway, as KO of IP3R3 significantly decreased agonist-induced mitochondrial Ca^{2+} uptake (138). In this picture, the three isoforms of the IP3R appear to play distinct roles. IP3R3 seems to play a selective role in the induction of apoptosis by preferentially transmitting apoptotic Ca^{2+} signals into mitochondria, whereas IP3R1 predominantly mediates cytosolic Ca^{2+} mobilization (139, 140). However, other studies have shown that the type 1 isoform can also mediate apoptosis (141).

Several observations underline the significance of the role of the ER-mitochondrial Ca^{2+} flux in stimulating apoptosis. Indeed, a wide number of apoptotic stimuli, such as ceramide, arachinodic acid, and oxidative stress induced by H_2O_2 or menadione, trigger both a progressive release of Ca^{2+} from the ER and an activation of the capacitative Ca^{2+} influx (142, 143). This sustained ER Ca^{2+} release, in turn, induced a mitochondrial Ca^{2+} overload with a consequent release of mitochondrial proteins involved in the apoptotic process (Figure 4).

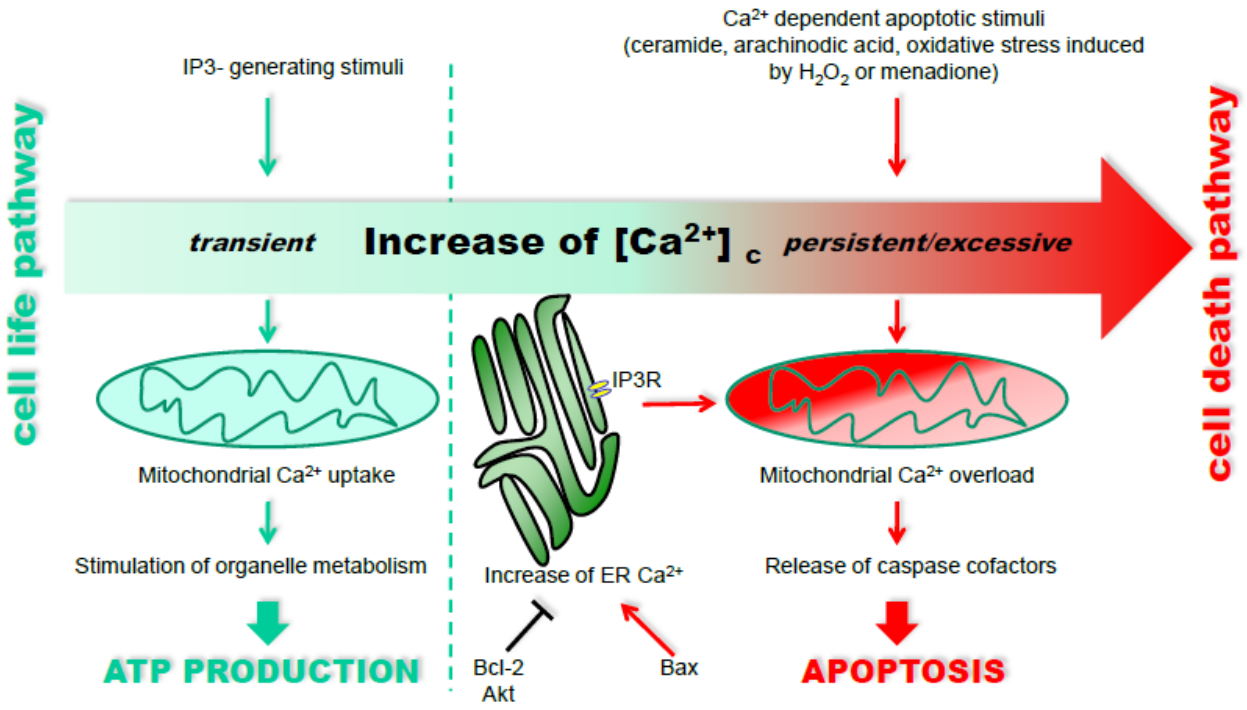

Figure 4. Differential decoding of Ca^{2+}-linked stimuli evoking the activation of cell metabolism or apoptosis. *(figure modified from (135)*

Since ER and mitochondria play significant roles in the regulation of cell proliferation and apoptosis, the remodeling of Ca^{2+} signaling machinery in ER and mitochondria of cancer cells seems imminent during oncogenic transformation, to limit death-inducing Ca^{2+} signals during

cancer. The first indication came from the observation that in cancer cells the increased expression of anti-apoptotic members of the Bcl-2 family of proteins (Bcl-2 and Bcl-X_L), or decreased expression of the pro-apoptotic BH3-only proteins (Bax or Bak) can protect these cells from apoptosis by modulating intracellular Ca^{2+} signals. These proteins reside in the ER, cytosol and mitochondria as homo o heterodimers. Of interest, the proapoptotic protein Bcl-2 affects ER-mitochondrial Ca^{2+} crosstalk, as the over-expression of Bcl-2 reduces the Ca^{2+} content of the ER (144) making the cells resistant to apoptosis. Similarly, genetic ablation of the proapoptotic proteins Bax and Bak that drastically increases the resistance to death signals also results in a dramatic reduction in ER Ca^{2+} content, and consequently in a reduction of the Ca^{2+} that can be transferred to mitochondria (143). The use of a Bax/Bak double-knockout model system demonstrated that Bcl-2 forms a macromolecular complex with the IP3Rs. The decreased level of Bax and Bak hereby correlated inversely with the amount of Bcl-2 bound to the IP3R, the phosphorylation status of the IP3R and the Ca^{2+} leak from the ER, leading to the conclusion that Bcl-2 regulated ER Ca^{2+}-store content by regulating the phosphorylation status and the activity of the IP3R. The phosphorylation of IP3R1 was proposed to be due to protein kinase A, but the role of other kinases could not be dismissed (145).

IP3R phosphorylation appears to be a key common feature for modulation of channel function and, as consequence, apoptotic signalling. IP3Rs possess consensus sequences for phosphorylation by numerous kinases, including the pro-survival protein kinase Akt. The consensus site for phosphorylation by Akt has been identified at the carboxyl terminus (serine 2618) of all three mammalian IP3R isoforms and is conserved from mammals to flies (66). This phosphorylation event decreases IP3-stimulated Ca^{2+} release from the ER and so diminishes flux of Ca^{2+} to the mitochondria following stimulation with pro-apoptotic agonists, thereby reducing apoptosis (146, 147). This is an interesting observation, because in some cancer cells in which Akt is constitutively active (e.g. prostatic carcinoma cells), IP3Rs are hyper-phosphorylated (66). These data suggest that this functional interaction between Akt and IP3Rs is retained in tumour cells, endowing them with a significant survival advantage by limiting Ca^{2+}-dependent death signalling.

ER-mitochondria Ca^{2+} transfer appears to be a key sensitizing in various apoptotic routes. Hence, therapeutic modulation of targets that regulate $[Ca^{2+}]_{er}$ and/or ER-mitochondrial Ca^{2+} transfer may be able to augment apoptosis in cancer cells without disrupting global Ca^{2+} homeostasis. However, the precise molecular definition of this process still awaits a fine clarification of the macromolecular complex assembled at the interphase between the two organelles. As will be discussed shortly, significant research efforts have been made to shed some light on this signalling pathway, and this was also the main aim of this thesis project.

1.7 Mitochondria-associated membranes: role of structural and regulatory proteins in the control of Ca^{2+} transfer between ER and mitochondria

The association between ER and mitochondria was first described by Copeland and Dalton over 50 years ago in pseudobranch gland cells (148). By the beginning of the 70s, the contacts between mitochondria and ER had been visualized by several groups (149, 150). Electron micrograph images of quickly frozen samples (151) and experiments in living cells with the two organelles labelled by means of targeted spectral variants of GFP (mtBFP and erGFP) (33), demonstrated conclusively that such physical interactions between the two organelles indeed exist. These latter experiments revealed the presence of overlapping regions of the two organelles and allowed to estimate the area of the contact sites as 5-20% of the total mitochondrial surface (Figure 5). The distance between the ER and the OMM was originally estimated to be approximately 100 nm (152, 153). More detailed morphological studies, carried out by Achleitner *et al.* in 1999, indicated that the distance between the ER and mitochondria in the areas of interaction varied between 10 and 60 nm (154). Importantly, a direct fusion between membranes of the ER and mitochondria was not observed in any case, and the membranes invariably maintained their separate structures. The authors of this pioneering paper proposed that a distance of less than 30 nm between the two organelles could be considered as an association. More recently, electron tomography techniques allowed to estimate that the minimum distance is even shorter (e.g., 10-25 nm) (155). This distance thus enables ER proteins to associate directly with proteins and lipids of the OMM. Further development of microscopic techniques enabled detailed analysis of such contacts with high resolution in three dimensions (156).

The interactions between ER and mitochondria at the contact sites are so tight and strong, that upon subcellular fractionation (at the step of mitochondria purification), a unique fraction, originally named ‘mitochondria-associated membranes” (MAMs), can be isolated (157, 158). More recently, the isolation procedures was improved and adapted to isolate the MAMs fraction from yeast, different organs, tissues, and various cell lines (154, 159, 160). The molecular analysis of both “crude” mitochondria and MAMs fractions demonstrated that, apart from specific ER and mitochondrial proteins, they also contain proteins which are abundant in the plasma membrane. However, research on the morphological organization of mitochondria and ER with respect to the plasma membrane is much less extensive. Modifications in the subcellular fractionation procedure enabled the isolation of the “plasma membrane associated membranes” (PAMs) fraction. In general, PAMs fractions have been described as the center of interactions between plasma membrane and

the ER (161, 162), but the presence of mitochondrial proteins in these fractions indicates that mitochondria interact actively also with the plasma membrane (163, 164).

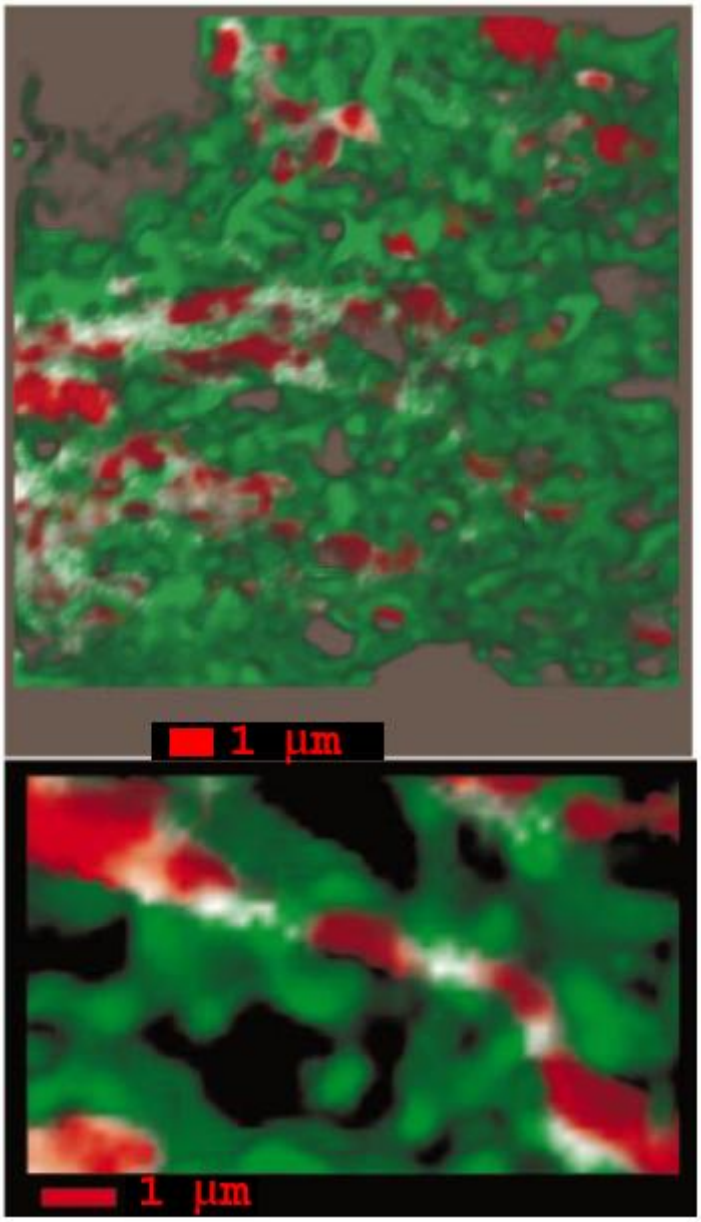

Figure 5. High-resolution 3D imaging of ER-mitochondria contact sites. *Combined 3D imaging of mitochondria and ER in a HeLa cell transiently expressing mtGFP(Y66H,Y145F) and erGFP(S65T). The mitochondrial and ER images are represented in red and green, respectively; the overlaps of the two images are white. On the bottom, a detail of the main image (80-nm pixel) (figure from (33)*

The MAMs have a pivotal role in several cellular functions related to bioenergetics and cell survival. MAMs have been originally shown to be enriched in enzymes involved in lipid synthesis and trafficking between ER and mitochondrial membranes, including long-chain fatty acid-CoA ligase type 4 (FACL4) and phosphatidylserine synthase-1 (PSS-1) (158, 165, 166). The MAMs

have since been shown to be enriched in functionally diverse enzymes involved not only in lipid metabolism but also in glucose metabolism (for recent reviews, see (167, 168)).

More recently, the same subcellular fraction has been shown to contain Ca^{2+}-sensing ER chaperones and oxidoreductases, as well as key Ca^{2+} handling proteins of both organelles (169, 170). Together, these data have led to the conclusion that the MAMs are not only a site of lipid synthesis and transfer, but also function as a fundamental hub of cellular signalling that controls a growing number of processes associated with both organelles, ranging from ER chaperone-assisted folding of newly synthesized proteins to the fine-tuning of physiological and pathological Ca^{2+} signals from ER to mitochondria.

Ca^{2+}-handling proteins such as IP3Rs (especially type 3 IP3Rs) and VDAC are highly compartmentalized at MAMs (139), identifying these zones as 'hotspots' of Ca^{2+} transfer from the ER to the closely adjacent mitochondrial network (31, 33). Ca^{2+} signals arising from the ER are vital for regulating Ca^{2+} levels in mitochondria, and so the activation of cell metabolism or apoptosis. Therefore, ER Ca^{2+} handling at MAMs acts as a double-edged sword, suggesting the existence of still not fully elucidated regulatory mechanisms, that are capable of discriminating between signals of life or death.

Several proteins may participate in the stabilization of MAMs and, in this way, affect Ca^{2+} transfer between ER and mitochondria, while other proteins may be directly involved in regulating Ca^{2+}-transport proteins. During the last years, research has focused on the identification of connecting structures between the ER and mitochondria at the MAMs, revealing that the interactions between the two organelles seem to be modulated both by a family of chaperone proteins and by a family of "mitochondria-shaping proteins". One of the first advances was made in 2006, when Csordás *et al.* showed by electron tomography that ER and mitochondria are adjoined by tethers seemingly composed of proteins, since the *in vitro* incubation with proteinase not only detached the ER from mitochondria, but also disrupted Ca^{2+} transfer. Tightening of the connections sensitized mitochondria to Ca^{2+} overloading, ensuing permeability transition, and seemed relevant for several mechanisms of cell death. Thus, these results revealed an unexpected dependence of cell function and survival on the maintenance of a proper spacing between the ER and mitochondria (155).

At the same time, Szabadkai *et al.* found that the mitochondrial chaperone grp75 (glucose-regulated protein 75) mediates the molecular interaction of VDAC with the ER Ca^{2+}-release channel IP3R. It was demonstrated that grp75 not only induces a chaperone-mediated conformational coupling of the proteins, but also allowed for a better transfer of the Ca^{2+} ions from the ER to the mitochondrial matrix (171). In support of this view, we previously demonstrated that the overexpression of VDAC enhances Ca^{2+} signal propagation into the mitochondria, increasing the extent of mitochondrial Ca^{2+}

uptake (also leading to a higher susceptibility for ceramide-induced cell death), acting at the ER-mitochondria contact sites (78). Moreover, one aim of my PhD Programme was the analysis of the contribution of the different VDAC isoforms to global cellular Ca^{2+} homeostasis, in order to establish the role of this non-redundant molecular route in transferring Ca^{2+} signals to mitochondria in apoptosis. The results (presented in section 3.1 and in Reference (172)) demonstrate that VDAC1, but not VDAC2 and VDAC3 isoforms, selectively interacts with IP3Rs; this interaction is further strengthened by apoptotic stimuli and thus VDAC1 is preferentially involved in the transmission of the low-amplitude apoptotic Ca^{2+} signals to mitochondria (172).

Also, ER chaperones, particularly the Ca^{2+}-binding chaperones calnexin, calreticulin, Sigma-1 receptor (Sig-1R) and Binding immunoglobulin Protein (BiP, also known as the glucose-regulated protein GRP78), have been found to be compartmentalized at the MAMs, yielding a new picture whereby chaperone machineries at both ER and mitochondria orchestrate the regulation of Ca^{2+} signalling between these two organelles. For instance, calnexin reversibly interacts with SERCA2b to block Ca^{2+} import (173). Similarly, calreticulin inhibits Ca^{2+} uptake by inhibiting its affinity for the SERCA2b pump, but also regulates IP3-induced Ca^{2+} release (17, 174). *In vivo*, these functions of calreticulin may be more crucial for survival than its chaperone activity, since calreticulin-deficient cells have impaired Ca^{2+} homoeostasis (175, 176).

Back in 2005, Simmen *et al.* reported the identification of a multifunctional cytosolic sorting protein, PACS-2 (phosphofurin acidic cluster sorting protein 2), that partially resides in the MAMs and maintains their integrity (177). PACS-2 depletion induces mitochondria fragmentation and uncouples these organelles from the ER, raising the possibility that, in addition to mediating MAMs formation, PACS-2 might also influence Ca^{2+} homeostasis and apoptosis. Indeed, it has been shown that IP3Rs (and RyRs) possess potential PACS-2-binding sites (178); hence, disruption of PACS-2 may cause mislocalization of IP3Rs, resulting in reduced Ca^{2+} transfer from the ER to mitochondria. Moreover, in response to apoptotic stimuli, PACS-2 has been demonstrated to be capable of inducing Bid recruitment to mitochondria, an event that leads to cytochrome *c* release and caspase 3 activation (177). PACS-2 also interacts with and regulates the distribution and activity of calnexin. Under control conditions, >80% of calnexin localizes to the ER, mainly at the MAMs. However, through a protein-protein interaction, PACS-2 causes calnexin to distribute between the ER and the plasma membrane, affecting ER Ca^{2+} homeostasis (179). PACS-2 and calnexin also interact with the MAMs-resident ER cargo receptor Bap31 (B-cell receptor-associated protein 31) and regulate its cleavage during the triggering of apoptosis (180). Despite these observations, the exact role of PACS-2 in the regulation of Ca^{2+} transfer from the ER to the mitochondria remains to be further investigated.

Recently, Simmen's group have also shown that the GTPase Rab32, a member of the Ras-related protein family of Rab, localizes to the ER and mitochondria and identified this protein as a regulator of MAMs properties. Its activity levels control MAMs composition, destroying the specific enrichment of calnexin at the MAMs, and consequently ER calcium handling. Furthermore, as a PKA-anchoring protein, Rab32 determines the targeting of PKA to mitochondrial and ER membranes, resulting in modulated PKA signalling. Together, these functions result in a delayed apoptosis onset with high Rab32 levels and, conversely, accelerated apoptosis with low Rab32 levels, explaining the possible mechanism by which it could act as an oncogene (181).

Also Sig-1R, an ER chaperone serendipitously identified in cellular distribution studies by Hayashi and Su, is enriched in the MAMs and seems to be involved in Ca^{2+}-mediated stabilization of IP3Rs (138). Under normal conditions in which the ER luminal Ca^{2+} concentration is at 0.5-1.0 mM, it selectively resides at the MAMs and forms complexes with the ER Ca^{2+}-binding chaperone BiP. Upon the activation of IP3Rs, which causes the decrease of the Ca^{2+} concentration at the MAMs, Sig-1R dissociates from BiP to chaperone IP3R, which would otherwise be degraded by proteasomes. Thus, Sig-1R appears to be involved in maintaining, on the ER luminal side, the integrity of the ER-mitochondrial Ca^{2+} cross-talk, as demonstrated by the fact that its silencing leads to impaired ER-mitochondrial Ca^{2+} transfer. Sig-1R has been implicated in several neuronal and non-neuronal pathological conditions (182), and is also upregulated in a wide variety of tumour cell lines (183). Therefore, degenerative neurons or tissue might benefit by Sig-1R agonists which promote cell survival (184, 185); conversely, its antagonists inhibit tumour-cell proliferation (186).

Another example of a folding enzyme regulating ER Ca^{2+} content is the oxidoreductase ERp44 (endoplasmic reticulum resident protein 44) that interacts with cysteines of the type 1 IP3R, thereby inhibiting Ca^{2+} transfer to mitochondria when ER conditions are reducing (187). Recent results suggest that another oxidoreductase, Ero1α, might also perform such a function, since Ero1α interacts with the IP3R and potentiates the release of Ca^{2+} during ER stress (188). This function of Ero1α could impact the induction of apoptosis that critically depends on ER-mitochondria Ca^{2+} communication (139, 189). Gilady *et al.* showed that, despite Ero1α being an ER luminal protein, the targeting of Ero1α to the MAMs is quite stringent (>75%), consistent with its role in the regulation of Ca^{2+} homeostasis. Moreover, they found that localization of Ero1α on the MAMs is dependent on oxidizing conditions within the ER; indeed, hypoxia leads to a rapid and eventually complete depletion of Ero1α from the MAMs (190).

In the increasingly clear but complex picture that is emerging for MAMs, also the mitochondrial fusion protein Mfn2 has been shown to be enriched at contact sites between the ER and mitochondria. Mfn2 on the ER appeared to link the two organelles together: the connection

depended on the interaction of the ER Mfn2 with either Mfn1 or Mfn2 on the OMM (156). Moreover, its absence changes not only the morphology of the ER but also decreased by 40% the interactions between ER and mitochondria, thus affecting the transfer of Ca^{2+} signals to mitochondria. This may contribute to the Charcot-Marie-Tooth neuropathy type 2a in which missense mutations occur in Mfn2 (191). A too strong ER-mitochondria interaction, and the concomitant improved Ca^{2+} transfer between the two organelles, may also be detrimental as overexpression of Mfn2 led to apoptosis in vascular smooth-muscle cells (192). A recent report also propose the keratin-binding protein Trichoplein/mitostatin (TpMs), often downregulated in epithelial cancers (193), as a new regulator of mitochondria-ER juxtaposition in a Mfn2-dependent manner (194).

Also the mitochondrial fission protein Fis1 has been involved in ER-mitochondria coupling. Fis1 physically interacts with Bap31, an integral membrane protein expressed ubiquitously and highly enriched at the outer ER membrane, to bridge the mitochondria and the ER, setting up a platform for apoptosis induction. It appeared that the Fis1-Bap31 complex is required for the activation of procaspase-8. Importantly, as this signalling pathway can be initiated by Fis1, the Fis1-Bap31 complex establishes a feedback loop by releasing Ca^{2+} from the ER that is able to transmit an apoptosis signal from the mitochondria to the ER (195).

Apoptosis is a process of major biomedical interest, since its deregulation is involved in the pathogenesis of a broad variety of disorders (neoplasia, autoimmune disorders, viral and neurodegenerative diseases, to name a few). The key process connecting apoptosis to ER-mitochondria interactions is an alteration in Ca^{2+} homeostatic mechanisms that results in massive and/or a prolonged mitochondrial Ca^{2+} overload (Figure 6).

Mitochondrial Ca^{2+} is therefore a central player in multiple neurodegenerative diseases such as Alzheimer's disease (AD), Parkinson's disease and Huntington's disease (196). It is noteworthy that alteration in Ca^{2+} homeostasis in sporadic AD patients started being reported in the middle of the 1980s, albeit in contrasting ways. Interestingly, very recent data have revealed that presenilin-1 (PS1) and presenilin-2 (PS2), two proteins that, when mutated, cause familial AD (FAD), have a strong effect on Ca^{2+} signalling (sometimes yielding contradictory experimental findings, as recently reviewed in (197)). Of particular interest on this topic, is the report that MAMs are the predominant subcellular location for PS1 and PS2, and for γ-secretase activity (198). Moreover, it has recently been found that PS2 over-expression increases the interaction between ER and mitochondria and consequently Ca^{2+} transfer between these two organelles, an effect that is greater in FAD variants (199). It is possible to speculate that this favoured interaction could potentially result in a toxic mitochondrial Ca^{2+} overload. A defect in Ca^{2+} signalling due to altered MAMs

function could explain the well-known disturbances in Ca^{2+} homeostasis in AD (200, 201). It also opens the door to new ways of thinking about complementary treatment; in addition, it may be possible to exploit aberrant MAMs function as a useful marker for the development of a diagnostic tool for AD (202).

Sano *et al.* also demonstrated that in GM1-gangliosidosis, a neurodegenerative disease, GM1-ganglioside (GM1) accumulates in brain within the MAMs, where it specifically interacts with phosphorylated IP3R1, influencing its activity (203). GM1 has been previously shown to modulate intracellular Ca^{2+} flux (204, 205). As such, the recent discovery that MAMs are the sites where GM1 accumulates and influences ER-to-mitochondria Ca^{2+} flux, leading to Ca^{2+} overload and activation of the mitochondrial apoptotic pathway, explains the neuronal apoptosis and neurodegeneration that occurs in patients with GM1-gangliosidosis (203). These findings may have important implications for targeting checkpoints of the GM1-mediated apoptotic cascade in the treatment of this catastrophic disease.

Modulation of the progression of cell death may therapeutically be very important also for the inhibition of tumour growth. A tumour cell must harness the Ca^{2+} signalling machinery to promote proliferation yet protect itself from apoptosis. Owing to their principal roles in the control of cell death and Ca^{2+} signalling, the ER and mitochondria are at the frontline of this battle during oncogenic transformation, and are thus sites where significant remodelling of Ca^{2+} signalling apparatus occurs to limit death-inducing Ca^{2+} signals during cancer. Specific stimulation of the Ca^{2+} transfer between the IP3R and mitochondria could specifically destabilize Ca^{2+} homeostasis in cancer cells and sensitize mitochondria towards apoptosis. Treating both normal and cancer cells with an agent that disrupts these pathways may kill the cancer cell, owing to the loss of redundancy. Such novel and highly innovative strategies can provide rationale and approaches for the design and development of novel technologies based on ER-mitochondria Ca^{2+} transfer for the diagnosis and treatment of cancer.

During my PhD Programme, we have found that the tumor suppressor promyelocytic leukemia protein (PML) modulates the ER-mitochondria Ca^{2+}-dependent cross-talk due to its unexpected and fundamental role at MAMs, highlighting a new extra-nuclear PML function critical for regulation of cell survival. This was demonstrated to be mediated by a specific multi-protein complex, localized at MAMs, including PML, IP3R3, the protein phosphatase PP2a, and Akt. Our results (presented in section 3.2 and in Reference (206)) show that PML mediates PP2a retention in the MAMs, which dephosphorylates and inactivates Akt. Thus, in the absence of PML, the unopposed action of Akt at the ER, due to an impaired PP2a activity, leads to a hyperphosphorylation of IP3R3 and in turn a

reduced Ca^{2+} flux from ER to mitochondria, rendering cells resistant to apoptotic Ca^{2+}-dependent stimuli (Figure 6).

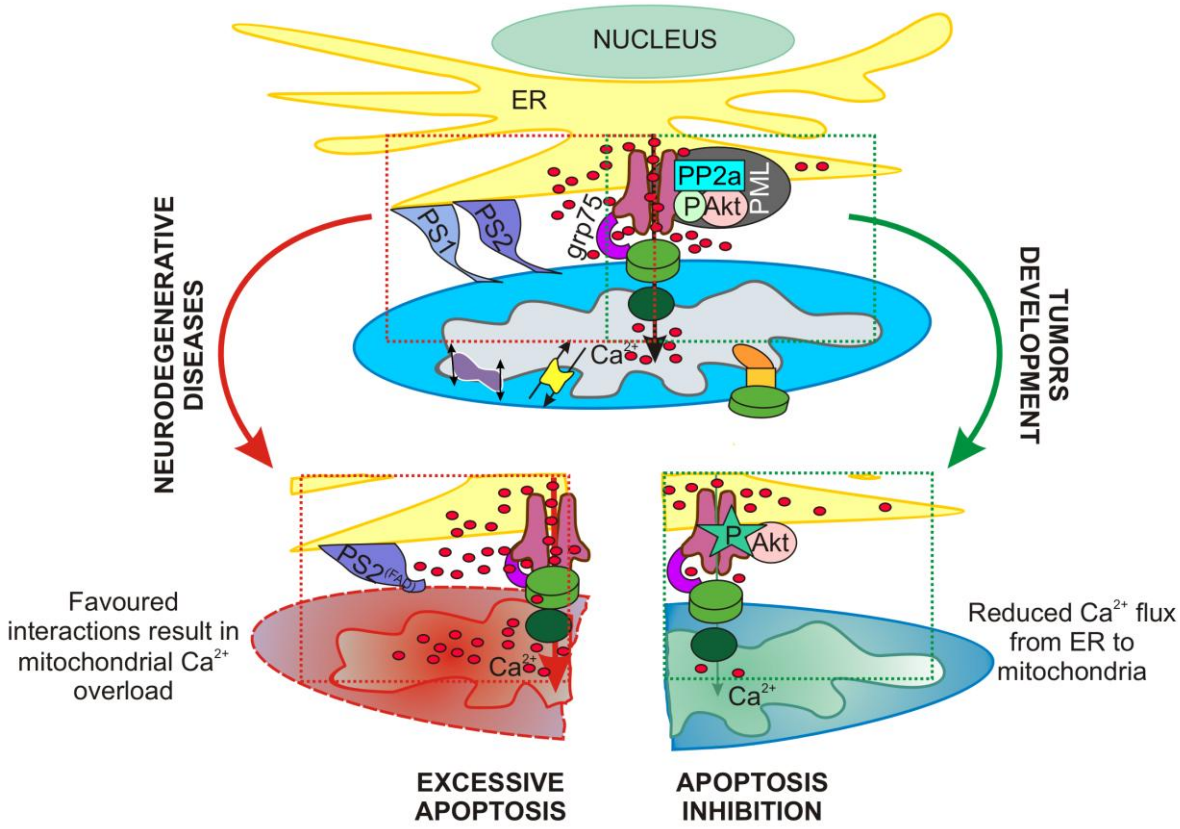

Figure 6. Representation of MAMs proteins involved in ER-mitochondria Ca^{2+} cross-talk and perturbations implicated in cell survival and cell death. *Ca^{2+} release from the ER results in high-Ca^{2+} hot spots at the mitochondrial surface to allow efficient Ca^{2+} uptake through VDAC - which is coupled to the IP3R by the chaperone grp75 - and the MCU. Mitochondrial Ca^{2+} activates organelle metabolism and ATP synthesis but also, when in excess, triggers apoptosis. Apoptosis deregulation is involved in the pathogenesis of neurodegenerative diseases as well as tumors development. Presenelin-1 (PS1) and Presenelin-2 (PS2), two proteins that when mutated cause familial Alzheimer's disease (AD), have been recently found at MAMs, and familial AD (FAD) variants of PS2 ($PS2^{FAD}$) seem to increase ER and mitochondria interaction; this could result in mitochondrial Ca^{2+} overload and subsequent excessive apoptosis. In addition, controlled apoptosis is likely to be important to eliminate cells, thereby avoiding tumor genesis. In this process the tumor suppressor PML localized at ER/MAMs and plays a crucial role as it promotes IP3R-mediated Ca^{2+} transfer from ER into mitochondria. While Akt is known to suppress IP3R-channel activity by its phosphorylation, the recruitment of protein phosphatase PP2a via PML in a specific multi-protein complex (comprising PML, IP3R-3, PP2a, and Akt), dephosphorylates and inactivates Akt. This suppresses Akt-dependent phosphorylation of IP3R-3 and thus promotes Ca^{2+} release through this channel and Ca^{2+} transfer into the mitochondria. In cancer cells, where PML is often missing, IP3R3 are hyper-phosphorylated due to an impaired PP2a activity, as a result the Ca^{2+} flux from ER to mitochondria is reduced and cells become resistant to apoptosis.*

Interestingly, the 66-kDa isoform of the growth factor adapter shc (p66shc) (207), a cytosolic adaptor protein which is involved in the cellular response to oxidative stress, has been recently found also in the MAMs fraction. In particular, the level of p66Shc in MAMs fraction is age-dependent and corresponds well to the mitochondrial ROS production which is found to increase

with age (208). p66shc is one of the key regulators of ROS production, mitochondrial dysfunction, and ageing. The mechanisms by which p66shc increases intracellular ROS levels, inducing apoptosis and the deleterious effects of ageing have recently been clarified by our group. Once imported into mitochondria, p66Shc causes alterations of organelle Ca^{2+} responses and three-dimensional structure, thus inducing apoptosis (209).

Finally, the functional significance of MAMs resident proteins in the regulation of ER-mitochondrial cross-talk is further supported by the finding that several viral proteins, such as the human cytomegalovirus vMIA (210), as well as the p7 and NS5B proteins of hepatitis C virus (211), are targeted to the MAMs and exert anti- or pro-apoptotic effects, respectively.

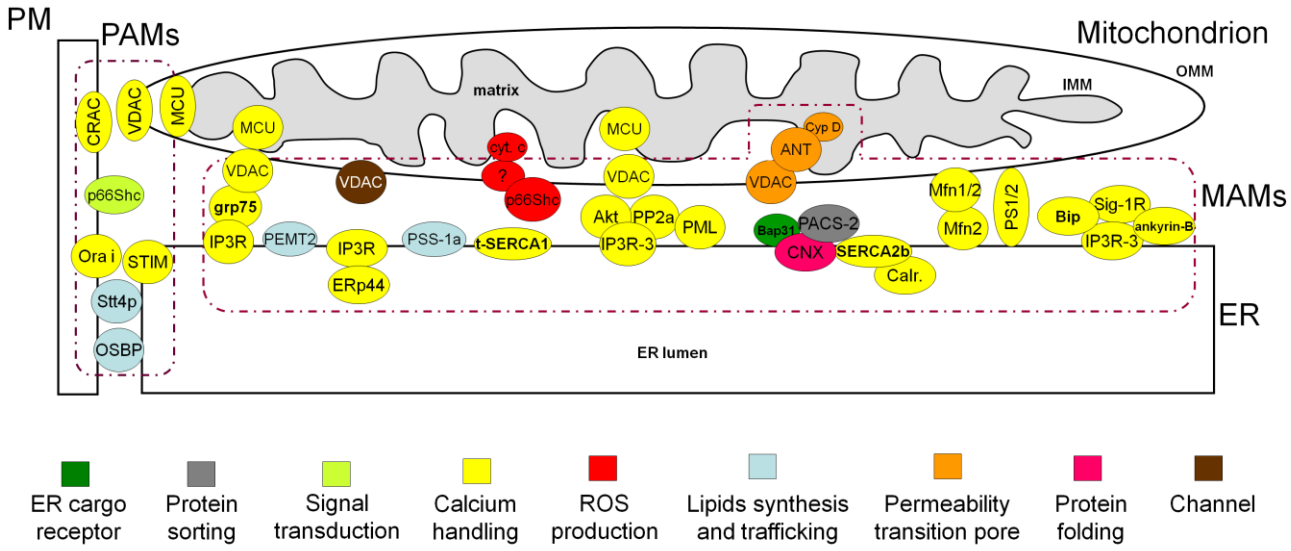

Figure 7. Schematic view of the interorganelle interactions and protein composition of the membranes contact sites.
Possible contact sites between organelles are marked in dotted brown line.
ER, endoplasmic reticulum; ER lumen, endoplasmic reticulum lumen; IMM, inner mitochondrial membrane; MAMs, mitochondria-associated membranes; OMM, outer mitochondrial membrane; PAMs plasma membrane associated membranes; PM, plasma membrane.
The color indicates the function/role of the protein.
Akt, the serine-threonine protein kinase Akt; ANT, adenine nucleotide translocase; Bap31, B-cell receptor-associated protein 31 (or endoplasmic reticulum resident cargo receptor); Calr, carleticulin; CRAC, Ca^{2+} release-activated calcium channel; Cyp D, cyclophilin D; cyt. c, cytochrome c; ERp44, endoplasmic reticulum resident protein 44; grp75, glucose-regulated protein 75 (or mortalin); BiP, Binding immunoglobulin Protein (or 78 kDa glucose-regulated protein (GRP78)); IP3R, inositol 1,4,5-triphosphate receptor; MCU, mitochondrial calcium uniporter; Mfn1/2 mitofusin-1/2; Ora i, ORAI calcium release-activated calcium modulator; OSBP, oxysterol binding protein; p66Shc, 66-kDa isoform of the growth factor adapter shc; PACS-2, phosphofurin acidic cluster sorting protein 2; PEMT2, phosphatidylethanolamine N-methyltransferase 2; PP2a, protein phosphatase 2a; PML, promyelocytic leukemia protein; PS1/2, presenilin-1/2; PSS-1a, phosphatidylserine synthase-1a; SERCA2b, sarco-endoplasmic reticulum calcium ATPase 2b; Sig-1R, Sigma-1 receptor; STIM1, stromal-interacting molecule 1; Stt4p, phosphatidylinositol-4-kinase; t SERCA1, truncated sarco-endoplasmic reticulum Ca^{2+} ATPase; VDAC, voltage-dependent anion channel; ?, unknown protein.

The deeper understanding at the molecular level of the structural and functional links that are established at MAMs and the possibility to modulate them may in the future be of great importance in the treatment of many different human pathologies.

To summarize, a schematic representation of the ER-mitochondria interactions and some of MAM proteins with the assigned functions is presented in figure 7.

2.AIMS:

The communication between the ER and mitochondria is important for bioenergetics and cellular survival. The ER supplies Ca^{2+} directly to mitochondria via IP3Rs at close contacts between the two organelles referred to as MAMs. The disruption of these contact sites has profound consequences for cellular function, such as imbalances of intracellular Ca^{2+} signalling and disrupted apoptosis progression. However, the precise molecular definition of the physical and functional interaction between ER and mitochondria still awaits a fine clarification of the macromolecular complexes assembled at the interphase between the two organelles. This project propose to investigate the molecular aspects that control the dynamics of the organelle-organelle interaction and their relationship with Ca^{2+} signals and control of apoptosis.

The Voltage-dependent anion channel (VDAC), the most abundant protein of the OMM, is in a crucial position in the cell where it forms an important interface between ER and mitochondria. VDAC has been identified at the MAMs and is deeply involved in efficient delivery of Ca^{2+} from the ER to mitochondria. Strikingly, VDAC1 is a pro-apoptotic protein while VDAC2 exert a protective effect. Therefore we analysed the contribution of the different VDAC isoforms to global cellular Ca^{2+} homeostasis, in order to establish the role of this non-redundant molecular route in transferring Ca^{2+} signals to mitochondria in apoptosis

Ca^{2+} signalling proteins and organelles are also emerging as additional cellular targets of oncogenes and tumour suppressors. The ER-to-mitochondria Ca^{2+} transfer is often remodelled or deregulated in tumour cells to sustain proliferation and avoid cell death. The PML and PTEN tumour suppressors have been demonstrated to display uncanonical and different subcellular localization as well as a broad and fundamental role in apoptosis. Therefore we analyzed the role of PML and PTEN in the control of ER-mitochondria Ca^{2+} cross-talk and in induction of apoptosis.

In particular we took advantage from the long standing experience of our group in the analysis of cellular Ca^{2+} signalling, cell fractionation and use of fluorescent probes, in order to precisely characterize the contribution of these proteins to global cellular Ca^{2+} homeostasis and apoptosis.

3.RESULTS:

3.1 VDAC1 selectively transfers apoptotic Ca^{2+} signals to mitochondria

Introduction

VDACs, the most abundant proteins of the OMM, mediate the exchange of ions and metabolites between the cytoplasm and mitochondria, and are key factors in many cellular processes, ranging from metabolism regulation to cell death. Multicellular organisms and mammals have three distinct VDAC genes (VDAC1, VDAC2 and VDAC3), with high sequence homology and similar structure (see Introduction, section 1.4).

Besides its fundamental role as metabolite exchanger, the pleiotropic role of VDACs appears to rely on their ability to engage protein-protein interactions with different partners. Indeed, VDACs have been shown to interact with cytoskeletal elements such as actin and tubulin (212, 213), metabolic enzymes (90), Bcl2-family members including Bak (214), Bad (215), tBid (216) and Bcl-X_L (89), or other channels such as ANT (217), or the IP3R (171, 203). This scenario is further complicated by evidence showing that VDAC contribution to cell death can be isoform and stimulus dependent. Given that VDAC exists in three different isoforms that share similar electrophysiological properties (molecular weight cutoff, voltage dependence, etc.,) (82), one would expect that all three isoforms exert the same effect on apoptosis, i.e. enhancing cell death by increasing mitochondrial Ca^{2+} uptake. Unfortunately, this simple model is contradicted by previous work: indeed, Cheng and colleagues demonstrate that VDAC2 is a potent anti-apoptotic protein, and proposed a molecular mechanism where VDAC2 prevents Bak activation by inhibiting its oligomerization and OMM permeabilisation (218). Thus, two different VDAC isoforms are reported to act on apoptosis in the opposite direction: VDAC1 acts predominantly as a pro-apoptotic protein (78, 219) whereas VDAC2 exerts a protective role against cell death (218).

The notion that these different isoforms are not simply redundant but could potentially being involved in radical different functions is supported by some observations. First of all, the presence of one single archetypical mitochondrial porin in simpler organisms (such as yeasts or *Neurospora Crassa*) and several different isoforms in more complex organisms (ranging from plants to mammals) suggests that gene duplication and divergent evolution likely occurred, conferring

specific functions to different isoforms. Moreover, gene ablation of the different isoforms in mice lead to different phenotypes. VDAC1, VDAC3 KO, as well as VDAC1/3 DKO, are viable but with variable defects (KO of VDAC1 reduces respiratory capacity (81), KO of VDAC3 causes male sterility (220), VDAC1- and VDAC3-KO show deficits in learning behavior and synaptic plasticity (221) and the lack of both VDAC1 and VDAC3 causes growth retardation (220)), while the ablation of VDAC2 is embryonic lethal (81). In any case, apart from these clues, a serious and rigorous assessment of the role of the different VDAC isoforms was still missing.

Given the relevance that mitochondrial Ca^{2+} plays in triggering apoptosis we test whether these differences are due to a diverse channeling capacities toward this cation in living cells. Indeed, mitochondrial Ca^{2+} accumulation acts as a 'priming signal' sensitizing the organelle and promoting the release of caspase cofactors, both in isolated mitochondria as well as in intact cells (189, 222). In this context, ER-mitochondria contacts mediate the tight and efficient Ca^{2+} transmission between the two organelles and thus could represent a potential regulatory site for cell death signals. Here we investigate the role of the different VDAC isoforms in the context of cell sensitivity to apoptosis and their role in regulating ER-mitochondrial Ca^{2+} signals transmission, and demonstrated that VDAC1, by selectively interacting with the IP3Rs, is preferentially involved in the transmission of the low-amplitude apoptotic Ca^{2+} signals to mitochondria.

Results

Silencing of the three VDAC isoforms differentially regulate cellular sensitivity to apoptotic stimuli

In this part of the PhD project, we aimed to correlate the Ca^{2+} channelling properties of the VDAC isoforms with their effects on cell death. We first downregulated the individual isoforms by RNAi silencing (Figure 8c). The siRNA of interest was cotransfected with a GFP reporter, and the effect on cell fate was evaluated by applying an apoptotic challenge (C2-ceramide or H_2O_2) and comparing the survival of transfected and non-transfected cells. In these experiments, the siRNA of interest was co-transfected with a GFP reporter and the percentage of GFP-positive cells was calculated before and after applying an apoptotic stimulus (C2-ceramide or H_2O_2). In mock-transfected cells, although the total number of cells is reduced after cell death induction, the apparent transfection efficiency was maintained (i.e. transfected and non-transfected cells have the same sensitivity to the apoptotic stimulus and thus die to the same extent). However, when GFP-positive cells are co-transfected with a construct influencing their sensitivity to apoptosis, this will be reflected by a change in the fraction of fluorescent cells, that is, in the 'apparent' transfection

efficiency. Thus, protection from apoptosis results into an apparent increase of transfection, whereas a decrease reflects a higher sensitivity to apoptosis. The results of the experiment are shown in Figure 8.

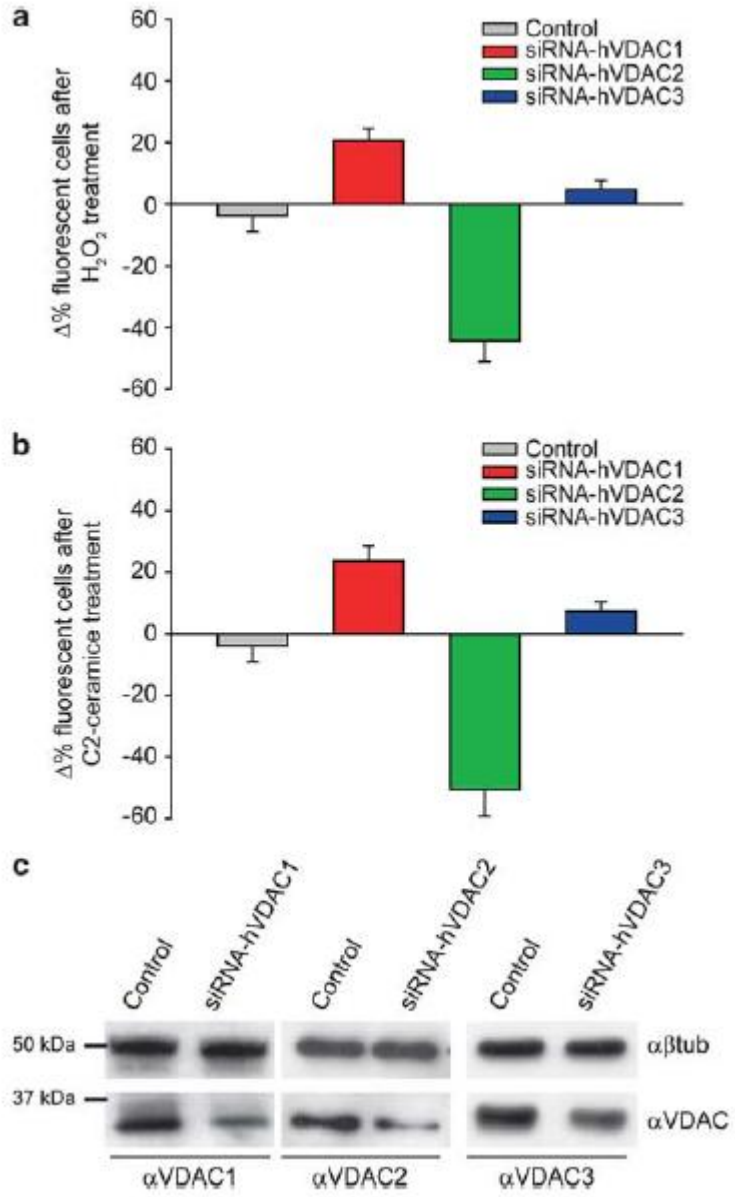

Figure 8. Sensitivity to apoptotic challenges of VDAC-silenced cells. *Cells were co-transfected with a fluorescent marker (GFP) and the siRNA of interest. The graph bar shows the change in percentage of fluorescent cells before the treatment with 100 μM H_2O_2 for 2 h ((a) control -3.7±5.2%; siRNA-hVDAC1 20±4.1%; siRNA-hVDAC2 -44.4±6.8%; siRNA-hVDAC3 +4.7±3.1%) and 30 μM C2-ceramide for 2 h ((b) control -4±5.3%; siRNA-hVDAC1 +24.3±5.1%; siRNA-hVDAC2 -50.1±6.8%; siRNA-hVDAC3 +7.1±2.5%). (c) HeLa cells were transfected for 48 h with control or siRNA-hVDAC encoding plasmid. Cells were harvested, total protein was extracted and subjected to western blotting analysis with antibodies anti-β-tubulin as loading control and anti-VDAC specific antibodies as indicated*

Mocktransfected cells show no difference in the percentage of fluorescent cells after H_2O_2 treatment (-3.7±5.2%), whereas in the same conditions VDAC1-, VDAC2- and VDAC3-silenced GFP-positive cells were varied by 20±4.1%, -44.4±6.8% and 4.7±3.1%, respectively (Figure 8a). Similar results were obtained with C2-ceramide (Figure 8b). This confirms the notion that VDAC1 is pro-

apoptotic and, among the various reported effects of VDAC2, the pro-survival role is prevailing in HeLa cells. Finally, VDAC3 shows no significant effect on apoptosis.

All VDAC isoforms enhance mitochondrial Ca^{2+}

Considering that the enhancement of mitochondrial Ca^{2+} uptake generally correlates with increased sensitivity to apoptosis and that VDAC1 has been shown to be a regulator of OMM permeability to Ca^{2+} , we wondered whether isoform specificity could rely on different Ca^{2+} channeling properties of the VDACs. The individual VDAC siRNAs were thus co-transfected with a mitochondrial Ca^{2+}-probe (mtAEQmut). After aequorin reconstitution with the cofactor coelenterazine, cells were challenged with 100 μM histamine, and luminescence was measured and converted to Ca^{2+}, as described in the Materials and Methods section. VDAC1 silencing significantly reduced the histamine-induced $[Ca^{2+}]_m$ peak (Figures 9a and c, $[Ca^{2+}]_m$ peak values: control, 88.6±2.7 μM; siRNA-hVDAC1, 75.6±3.2 μM; siRNA-hVDAC2, 64.9±3.5 μM; siRNA-hVDAC3, 69±3.8 μM). Interestingly, VDAC2 and VDAC3 silencing had the same effect, if anything greater. To confirm this notion, we carried out overexpression experiments, and, also in this case, VDAC1 showed an enhancement of mitochondrial Ca^{2+} uptake, in agreement with previous data (78). The effect was comparable, if not smaller, than that observed upon overexpression of VDAC2 and VDAC3 (Figures 9b and c, $[Ca^{2+}]_m$ peak values: hVDAC1-EYFP, 97.7±3.3 μM; hVDAC2-EYFP, 102.7±4.2 μM; hVDAC3-EYFP, 112.8±5.5 μM).

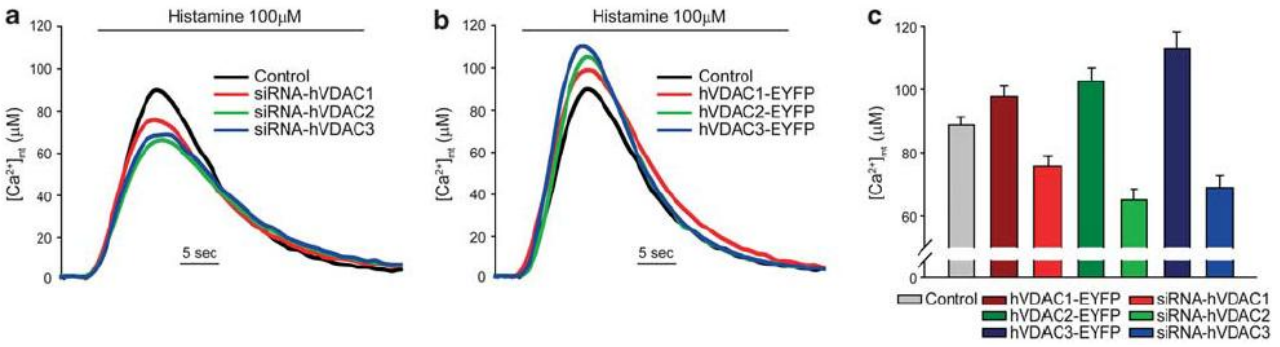

Figure 9. Effect of VDAC isoform silencing or overexpression on mitochondrial Ca^{2+} uptake. *$[Ca^{2+}]_m$ increase evoked by histamine stimulation in VDAC-silenced (a and c) or VDAC-overexpressing (b and c) cells ($[Ca^{2+}]_m$ peak values: control, 88.6±2.7 μM; siRNA-hVDAC1, 75.6±3.2 μM; siRNA-hVDAC2, 64.9±3.5 μM; siRNAhVDAC3, 69±3.8 μM; hVDAC1-EYFP, 97.7±3.3 μM; hVDAC2-EYFP, 102.7±4.2 μM; hVDAC3-EYFP, 112.8±5.5 μM). (a and b) Representative traces, (c) bar graph of the average $[Ca^{2+}]_m$ peak. The traces are representative of >12 experiments that gave similar results. The bar graphs are the average of all experiments performed*

All VDACs do not affect ER Ca^{2+} content and cytosolic Ca^{2+} transients

To rule out a confounding effect on cytosolic Ca^{2+} signaling, we measured ER and cytosolic [Ca^{2+}] with the appropriate aequorin chimeras. Silencing or overexpression of the three VDAC isoforms did not alter significantly the state of filling of the ER store (Figure 10a), nor of its release kinetics (data not shown). Accordingly, the cytosolic [Ca^{2+}] transient evoked by histamine stimulation was not significantly affected when any isoform were silenced (Figure 10b) or overexpressed (Figure 10c). Finally, mtGFP imaging and mitochondrial loading with the potential sensitive dye tetramethylrhodamine methyl ester (TMRM) showed that the effect was not due to changes in mitochondrial morphology or significant reduction of mitochondrial membrane potential (data not shown).

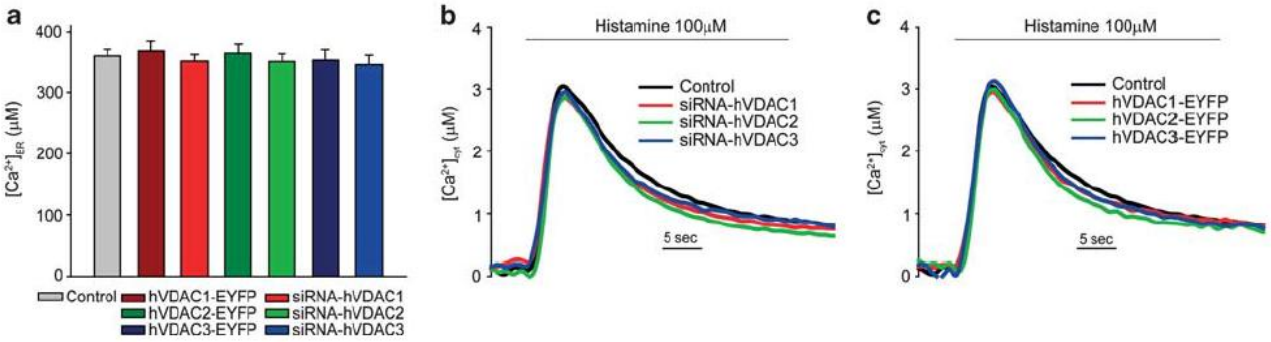

Figure 10. Effect of VDAC isoform silencing or overexpression on ER and cytosolic [Ca^{2+}]. *(a) Effect of the overexpression, or silencing, of individual VDAC isoforms on [Ca^{2+}]er steady-state levels (control, 360.1±10.5 μM; siRNA-hVDAC1, 351.9±10.6 μM; siRNA-hVDAC2, 352.3±12.3 μM; siRNA-hVDAC3, 346.5±15.1 μM; hVDAC1-EYFP, 368±15.6 μM; hVDAC2-EYFP, 364.5±14.4 μM and hVDAC3-EYFP, 353.6±16.6 μM). Transfection with the appropriate aequorin probe, reconstitution and [Ca^{2+}] measurements were carried out as detailed in the methods section. When indicated, the cells were challenged with 100 μM histamine. erAEQ transfection and $[Ca^{2+}]_{er}$ measurements, after ER Ca^{2+} depletion, aequorin reconstitution and ER refilling were carried out as detailed in the methods section. (b and c) Representative traces of cytosolic Ca^{2+} transients evoked by 100 μM histamine in VDAC-silenced (b) and overexpressing (c) cells ($[Ca^{2+}]_c$ peak values: control, 3.06±0.05 μM; siRNA-hVDAC1, 2.85±0.06 μM; siRNA-hVDAC2, 2.81±0.07 μM; siRNA-hVDAC3, 2.98±0.06 μM; hVDAC1-EYFP, 2.94±0.06 μM; hVDAC2-EYFP, 2.97±0.07 μM and hVDAC3-EYFP, 3.08±0.04 μM). The traces and graph bars of this figure are representatives of >12 experiments that gave similar results*

Altogether, these data, while showing a clear effect of VDAC silencing or overexpression on mitochondrial Ca^{2+} handling, argue against the possibility that the pro-apoptotic effect of VDAC1 depends on a greater Ca^{2+} conductance of this isoform. Rather, the data may suggest a preferential role of the VDAC2 and VDAC3 isoforms in Ca^{2+} transport (also considering their lower expression levels (223)), although the real significance of this observation could be hampered by differences in protein stability or trafficking to the OMM.

VDAC1 specific coupling to ER Ca^{2+} releasing channels

The pro-apoptotic activity of VDAC1 thus appears either totally independent of Ca^{2+}, or due to the fine tuning of Ca^{2+} signals in specialized microdomains that may be overlooked in bulk cytosolic measurements (34). We followed the latter possibility, based on growing evidence demonstrating that the mitochondria-ER crosstalk is not merely the consequence of physical neighborhood but relies on the existence of macromolecular complexes linking the two organelles (see Introduction, section 1.7). Specifically, during massive Ca^{2+} release upon maximal agonist stimulation, the existence of discrete signaling units could be overwhelmed and masked by the robustness of the response. Conversely, when an apoptotic stimulus causes a small, sustained Ca^{2+} release the existence of preferential channelling routes could become relevant. Based on previous data, showing the interaction of the IP3R with VDAC mediated by the grp75 chaperone (171), we investigated whether IP3Rs and grp75 preferentially interact with VDAC1, forming privileged signaling units.

We first performed co-immunoprecipitation experiments using the highly expressed IP3R3 as bait. Strikingly, Figure 11a shows that VDAC1 is the only isoform bound to the IP3R in stringent conditions: no VDAC2 or VDAC 3 could be detected, also in long-term exposures. Neither actin, nor hexokinase-I, a known interactor of VDAC1, were co-immunoprecipitated in the assay, whereas the grp75 chaperone did. To confirm the specificity of the interaction, we also carried out the reverse experiment, by immunoprecipitating VDAC1 and revealing the presence of grp75 and IP3R3 in the precipitate. In these experiments, the cells were transfected with an HA-tagged VDAC1 fusion protein, and immunoprecipitation was carried out with anti-HA antibodies. The results, shown in Figure 11b, demonstrate that both IP3R3 and grp75 co-immunoprecipitate with VDAC1 (similarly to previous data with the IP3R1 (171), and see also Figure 12c).

Apoptotic treatment enhances VDAC1 specific coupling to IP3Rs

We then investigated whether the VDAC1-IP3Rs interaction is altered in apoptotic conditions. We thus performed coimmunoprecipitations in cells challenged with H_2O_2 using grp75 or VDAC1-HA as bait. VDAC1 pull-down in H_2O_2-treated cells resulted in a significantly greater amount of both grp75 and IP3R in the immunoprecipitate (Figure 12a), and the relative amount of IP3R co-immunoprecipitating with grp75 was significantly greater in H_2O_2-treated cells (Figure 12b). Moreover, we performed co-immunoprecipitation experiments also with IP3R type 1: as shown in Figure 12c, similarly to IP3R3, also IP3R1 interacts with VDAC1 but not with VDAC2, and H_2O_2 treatment enhance this interaction (although the effect seems weaker than with IP3R3).

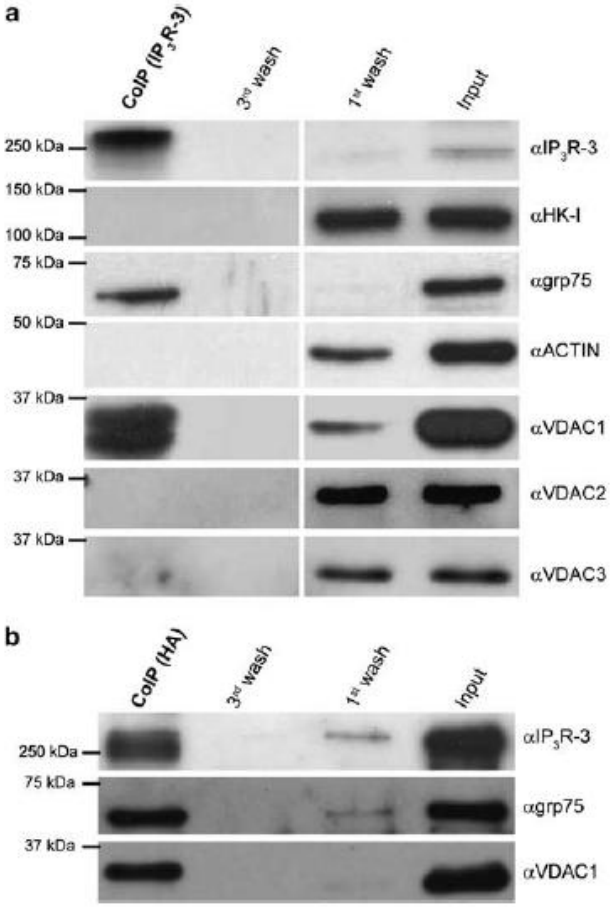

Figure 11. Co-immunoprecipitations of VDAC1 with IP3R3. *Co-immunoprecipitations using IP3R3 (a) and VDAC1-HA (b) as baits. HeLa cells were grown in 10-cm Petri dishes until full confluence. For VDAC1-HA immunoprecipitation, cells were transfected 48 h before experiment. Cells were then detached by scraping, harvested and proteins were extracted in non-denaturing conditions as indicated in the methods section. After protein quantification, 700 μg were incubated overnight at 4 °C with the 3 μg of the indicated antibody. The immunocomplex was then isolated by adding protein G-coated sepharose beads for 2 h at 4 °C. The purified immunocomplex was then washed three times with lysis buffer. Indicated fractions were then subjected to SDS-PAGE and western blotting, and probed with the indicated antibodies*

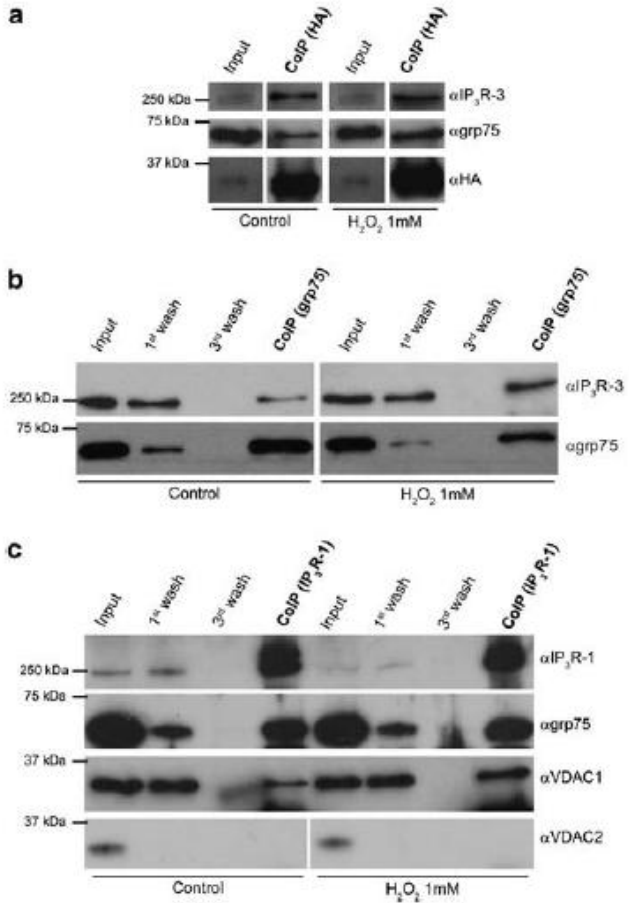

Figure 12. Co-immunoprecipitations of VDAC1 with IP3R3 after H_2O_2 treatment. *Co-immunoprecipitations using VDAC1-HA (a), grp75 (b) and IP3R-1 (c) as baits. HeLa cells were grown in 10-cm Petri dishes until full confluence. For VDAC1-HA immunoprecipitation, cells were transfected 48 h before experiment. Cells were then detached by scraping, harvested, incubated for 10 min with vehicle or 1 mM H_2O_2 and proteins were extracted in non-denaturing conditions as indicated in the methods section. After protein quantification, 700 μg were incubated overnight at 4 °C with the 3 μg of the indicated antibody. The immunocomplex was then isolated by adding protein G- (for anti-HA) or A- (for anti-IP3R-1 and grp75) coated sepharose beads for 2 h at 4 °C. The purified immunocomplex was then washed three times with lysis buffer. Indicated fractions were then subjected to SDS-PAGE and western blotting, and probed with the indicated antibodies*

VDAC1 selectively transfers apoptotic Ca^{2+} signals to mitochondria.

In order to test whether the interaction of VDAC1 and IP3Rs is involved in apoptotic signaling, we investigated the Ca^{2+} transients evoked by apoptotic stimuli in VDAC-silenced cells. We applied an oxidative stress, that is, treated the cells acutely with 1 mM H_2O_2. As previously reported (222), the addition of H_2O_2 caused a $[Ca^{2+}]_c$ increase that is much smaller and more sustained than that evoked by histamine (Figures 13a and b). Under those conditions, mitochondria also undergo a small increase (peak value <1 μM). VDAC1 silencing decreased mitochondrial Ca^{2+} accumulation, while the knock-down of the other isoforms was indistinguishable from controls. We then titrated the histamine concentration in order to elicit a small Ca^{2+} response, comparable to that evoked by H_2O_2 by applying a 0.5 μM histamine challenge. Under those conditions, no difference among the different VDAC isoforms could be revealed (Figure 13c), thus suggesting that besides the slow kinetics the strengthening of the physical coupling of the IP3R and VDAC1 channels by apoptotic challenges may have an important role in the potentiation of mitochondrial Ca^{2+} signals and the induction of cell death.

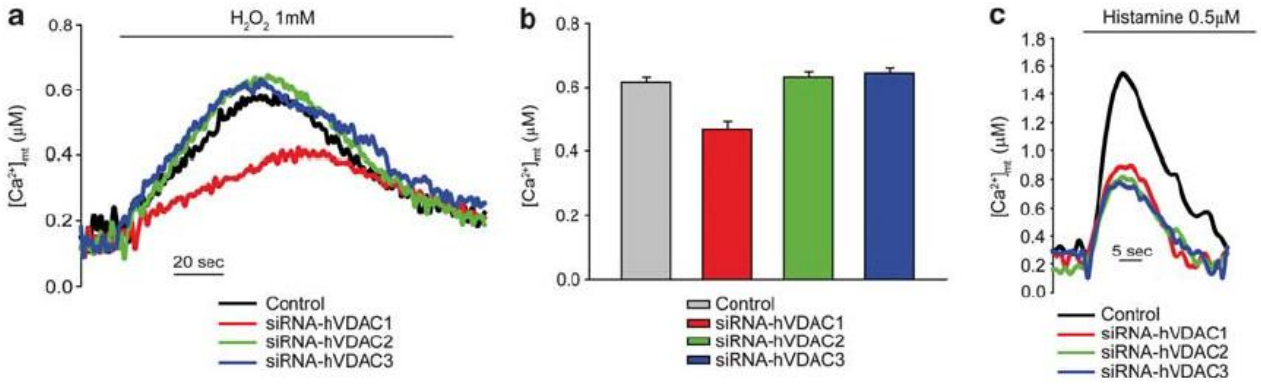

Figure 13. VDAC1 selectively transfers apoptotic Ca^{2+} signals to mitochondria. *Representative traces (a) and statistics (b) of $[Ca^{2+}]_m$ evoked by the acute administration of 1 mM H_2O_2 ($[Ca^{2+}]_m$ peak values: control, 0.617±0.015 μM; siRNA-hVDAC1, 0.469±0.025 μM; siRNA-hVDAC2, 0.632±0.016 μM; siRNA-hVDAC3, 0.644±0.016 μM). (c) $[Ca^{2+}]_m$ increases evoked by 0.5 μM histamine. All other conditions as in Figure 9*

Discussion

Several observations support the notion that VDAC can finely tune cellular processes in an isoform-specific way: (i) selective genetic ablation of the three VDAC genes exhibits different phenotypes (224) (ii) VDAC1 and VDAC2 exert diametrically opposite effects on apoptosis (78, 218, 225) and

a compound acting through VDAC2, erastin, is effective in tumors harboring Ras mutations (226); (iii) apoptotic challenges (227) and genomic programs, such as the PGC1-α pathway (De Stefani and Rizzuto, unpublished), differentially regulate the expression of VDAC isoforms; and (iv) the three isoforms are localized to different sub-domains of the OMM (228). We thus investigated in greater detail the molecular mechanism underlying the different role of VDAC isoforms in apoptosis.

The first, obvious explanation of this diversity relied on different Ca^{2+} channelling capacities, given the sensitizing role of Ca^{2+} in the release of caspase activators. Our results ruled out the possibility, by showing relatively minor differences in Ca^{2+} channelling that cannot account for their differential cell death regulation. These minor differences could potentially be due to small variations in Ca^{2+} transport capacities. However, as in situ VDAC levels after overexpression or gene silencing are quite difficult to rigorously assess, this conclusion is risky. These data simply support the notion that all VDAC isoforms can similarly transport Ca^{2+} in living cells, and this is not correlated with their effect on apoptosis.

How can we then solve the discrepancy between mitochondrial Ca^{2+} transport and apoptosis regulation? An obvious conclusion is the denial (or, at least the reconsideration) of the classic paradigm linking mitochondrial Ca^{2+} to apoptosis. However, this notion is now supported by broad evidence showing that mitochondrial Ca^{2+} loading favors cell death and signalling molecules reducing or increasing Ca^{2+} signals protect from or enhance apoptosis, respectively (135). Ca^{2+} in mitochondria, however, is an intrinsically pleiotropic signal, and the final outcome varies widely depending on both the nature of the stimulus (and hence the 'Ca^{2+} signature') and concomitant signalling pathways. Indeed, while physiological stimuli cause the rapid release of Ca^{2+} from internal stores, and thus a large and transient mitochondrial Ca^{2+} uptake, cell death signals have been shown to induce only a modest (even if sustained) $[Ca^{2+}]_m$ increase (222). This latter event has been proposed to represent a sort of priming signal that conditions and sensitizes mitochondria to otherwise non-lethal stimuli. In this context, the local coupling between ER and mitochondrial Ca^{2+} channels becomes critically relevant: small Ca^{2+} microdomains elicited by apoptotic stimuli such as C2-ceramide strongly relies on the existence of a preferential route transmitting the signal from the ER to the mitochondrion; on the other side, during physiological signals large Ca^{2+} microdomains are generated and this fine channel coupling could be potentially overwhelmed by the vigorous ER Ca^{2+} release. On the ER side, the notion that the accurate discrimination of Ca^{2+} signals mediating diverse effects relies on highly specialized molecular determinants was associated to the observation that the selective knockdown of IP3R3 impairs cell death signals transmission whereas

the silencing of the other two isoforms had almost no effect (139, 140). On the mitochondrial side, we wondered whether a similar selectivity could be associated to the mitochondrial channel repertoire at ER-mitochondria contact sites. The results clearly confirmed this possibility, by demonstrating that VDAC1 is preferentially involved in the transfer of apoptotic stimuli (such as those induced by H_2O_2) rather than physiological responses to agonists. Strikingly, our co-immunoprecipitation studies showed that IP3R selectively interacts with VDAC1, providing a molecular route for the higher sensitivity of the Ca^{2+} transfers. Moreover, this selective interaction appears not static but finely tuned by cellular conditions, as demonstrated by the fact that H_2O_2 strengthens the coupling between the ER and mitochondrial Ca^{2+} channels, and by the selective involvement of VDAC1 in the transmission of apoptotic stimuli.

Overall, these data reveal a complex molecular organization underlying VDAC Ca^{2+} channelling properties, and allowing VDAC1 to exert its pro-apoptotic activity. The emerging picture reveals that VDACs represent a fundamental factor in mitochondria physiology, with similar channelling properties shared among its different variants, but also mediating diverse effects through isoform-specific protein-protein interactions and the assembly of highly specialized, higher-order protein complexes. This view accounts for most of experimental data available and finally reconciles apparently contrasting evidence, allowing a deeper insight on mitochondrial regulation of cell life and death.

3.2 PML regulates apoptosis at endoplasmic reticulum by modulating calcium release

Introduction

The promyelocytic leukemia (PML) protein is a tumor suppressor frequently lost or aberrant in hematopoietic malignancies and human solid tumors (229, 230). Its gene was originally identified at the break point of the t(15;17) chromosomal translocation of acute promyelocytic leukemia (APL), a distinct subtype of acute myeloid leukemia. As a consequence of this translocation, PML fuses to the retinoic acid (RA) receptor alpha (RARα) gene. Two fusion genes are generated encoding PML-RARα and RARα-PML fusion proteins, which coexist in the leukemic cells, blocking heamatopoietic differentiation. PML has, therefore, become the object of intense research on the basis of this premise. Since then, PML has been shown to regulate diverse cellular functions, such as transcriptional regulation, DNA-damage response, sumoylation process, cellular senescence, neoangiogenesis, and apoptosis (231).

PML belongs to a large family of proteins harboring a tripartite structure that contains a zinc-finger called the RING motif (R) located N-terminally followed by two additional zincfingers motifs (B-boxes; B) and an α-helical coiled-coil domain (CC), collectively referred to as the RBCC domain. The RBCC domain mediates protein-protein interactions and is responsible for PML multimerization and the formation of macromolecular complexes. The C-terminal region of PML is less structured and varies between PML isoforms. Alternative splicing of C-terminal exons is responsible for the existence of at least seven PML isoforms characterized by different C-terminal regions and functional specificity (232).

PML is typically concentrated in subnuclear macromolecular structures termed PML-nuclear bodies (PML-NBs), of which PML is the essential component. PML-NBs have a diameter of 0.2-1 μm and the shape of a doughnut. PML-NBs are multiprotein dynamic structures that undergo significant changes in number, size, and position, particularly in response to cellular stress (233). They critically depend on PML to be correctly assembled (234). PML functionally interacts with a large number of proteins within PML-NBs. Some are in direct physical contact with PML, while others are not (235). PML SUMOylation and noncovalent binding of PML to SUMOylated PML through the SUMO-binding motif constitutes the nucleation event for subsequent recruitment of SUMOylated proteins and/or proteins containing SUMO-binding motifs to the PML-NBs (234). In

the APL blasts, PML-RARα associates physically with PML and causes its delocalization into microspeckled nuclear structures with consequent disruption of the PML-NBs (236).

Pml null mice and cells are protected from multiple and diverse apoptotic stimuli (237). A possible explanation for why *Pml* null cells are resistant to many apoptotic stimuli can be ascribed to the fact that PML can act as a pleiotropic factor in the functional regulation of several pro- and antiapoptotic pathways. Indeed, PML is functioning as part of a complex tumour-suppressive network. For instance, it is well established that PML is an important factor in the regulation of both p53-dependent and -independent apoptotic pathways (238). Moreover, PML can act as a suppressor of other major oncogenic pathways, such as the PI3K/Akt pathway, through its ability to interact with the protein phosphatase 2a (PP2a) and inhibit the nuclear function of Akt, thus leading to suppression of its prosurvival and promitogenic functions (239). Finally, PML regulates the function of PTEN (phosphatase and tensin homolog deleted on chromosome 10), which is the main suppressor of the PI3K pathway (see Results, section 3.3). PML co-ordinate PTEN subcellular nuclear localization: this occurs through inhibition of PTEN de-ubiquitination by HAUSP (herpesvirus-associated ubiquitin-specific protease) and its nuclear retention. As a consequence, both in APL blasts and in PML-loss conditions, PTEN is excluded from the nucleus (240, 241).

Despite PML protein has been recognized as a critical and essential regulator of multiple apoptotic response, no unified mechanism appeared to explain the global resistance of *Pml* null cells to apoptosis. How PML would exert such broad and fundamental role in apoptosis remained for long time a mystery. Interestingly, many, if not all, PML isoforms have shown both cytoplasmic and nuclear localization (242, 243).

Therefore in this part of the PhD project, we aimed to understand how PML could regulate such broadly diverse apoptotic responses through its extranuclear localization. In particular, we analyzed PML intracellular localization by cell fractionation and found that extranuclear PML was specifically enriched at the ER and MAMs. So, we investigated the role of PML at MAMs in the control of the functional cross-talk between ER and mitochondria. We found PML in complexes of large molecular size with the IP3R, Akt and PP2a, and demonstrated that PML is essential for Akt- and PP2a-dependent modulation of IP3R phosphorylation and in turn for IP3R-mediated Ca^{2+} release from the ER to the mitochondria. Our findings provide a mechanistic explanation for the elusive mechanism whereby the PML tumour suppressor exerts its essential role in apoptosis triggered by Ca^{2+}-dependent stimuli and identify a novel unexplored pharmacological target for the modulation of Ca^{2+} signals and cell death.

Results

PML localizes at ER and MAMs regions and mediates Ca^{2+}-dependent apoptotic cell death

We fractionated homogenates of primary mouse embryonic fibroblasts (MEFs) by ultracentrifugation, focusing on the mitochondria, ER and MAMs, the structures that contain sites where the ER contacts mitochondria. All fraction markers were enriched in their respective compartments (we used β-tubulin as a general cytosolic marker, IP3R as ER marker, VDAC as mitochondrial marker, and PCNA as nuclear marker); moreover, the close apposition between ER and mitochondrial membranes at MAMs explained the presence of both VDAC and IP3R in these microdomains (139, 171). PML localized both to the nucleus and the cytosol and appeared to localize also to the ER, MAM, and crude mitochondrial fractions but not to "pure" mitochondrial fraction free of ER and nuclear markers (Figure 14A). These results were confirmed by immunogold labeling of ultrathin cryosections showing that PML associates with the surface of the ER (Figure 14B, a and b) and in the proximity of the mitochondrial membrane at contact sites between the ER and mitochondria (Figure 14B, d to g).

In view of the localization of PML at the ER and MAM, we investigated its requirement in apoptosis induced by ER stress (169). Matched wild-type ($Pml^{+/+}$) and $Pml^{-/-}$ MEFs were treated with ER stress inducers: H_2O_2 and menadione (MEN), two oxidizing agents that induce ER Ca^{2+} release; tunicamycin (TN) or an inhibitor of protein N-glycosylation; and thapsigargin (TG), an inhibitor of the SERCA. After 12 hours of treatment, the percentage of apoptotic cells in $Pml^{-/-}$ MEFs was much lower than that observed in $Pml^{+/+}$ MEFs under all treatment conditions (Figure 14C).

PML absence induces a smaller release of Ca^{2+} from ER, leading to reduced mitochondrial Ca^{2+} uptake after agonist or apoptotic stimulation

MAMs are specialized domains selectively enriched in critical Ca^{2+} signaling elements, which mediate Ca^{2+} transfer between ER and mitochondria, such as the IP3R (see Introduction, section 1.7). Ca^{2+} signaling has a major role in the regulation of cell death. Release of the ER Ca^{2+} pool through the IP3R3 appears to induce a sensitization of cells to apoptotic stimuli (see Introduction, section 1.6).

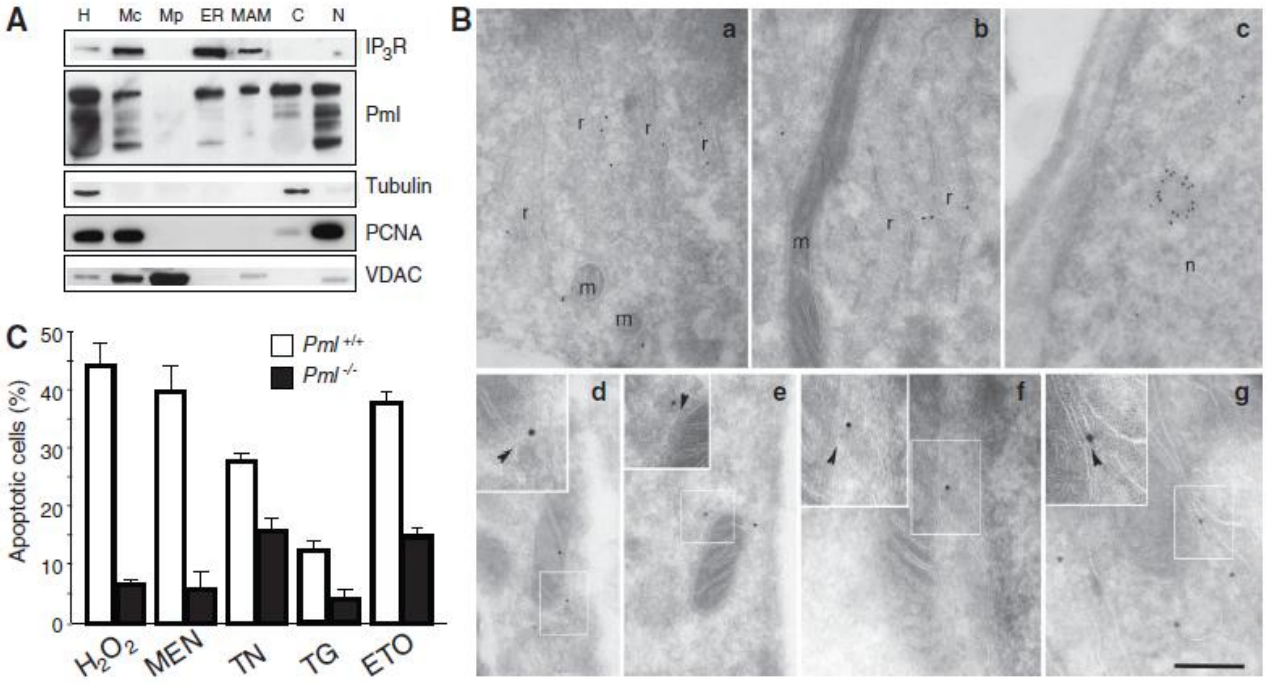

Figure 14. Identification of PML at ER and MAM regions and Ca^{2+}-mediated PML-dependent cell death. *(A) Detection of PML by immunoblotting in $Pml^{+/+}$ MEFs fractionation. IP3R, tubulin, proliferating cell nuclear antigen (PCNA), VDAC are used as markers. H: homogenate; Mc: crude mitochondria; Mp: pure mitochondria; ER; MAM; C: cytosol; N: nucleus. (B) Immunogold labeling of PML near the rough ER (r), mitochondria (m), and MAM (arrowheads) in $Pml^{+/+}$ MEFs. Gold particles (15 nm) are mostly associated with the surface of the ER (7.07 gold particles/μm^2) and more occasionally with mitochondrial membranes (3.08 gold particles/μm^2) (a and b). Specificity of the antibodies is demonstrated by labelling of nuclear bodies (n) (c). Morphologically identified MAM often demonstrated labeling at contacts between ER and mitochondria [(d) to (g), and arrowheads in insets therein]. Insets correspond to boxed areas. Bar: (a) 360 nm; (b) 340 nm; (c) 370 nm; (d) 188 nm, inset 120 nm; (e) 260 nm, inset 190 nm; (f) 340 nm, inset 180 nm; (g) 280 nm, inset 210 nm. (C) Apoptosis induced by 1 mM H_2O_2, 15 μM menadione (MEN), 6 μM tunicamycin (TN), 2 μM thapsigargin (TG), or 50 μM etoposide (ETO) in $Pml^{+/+}$ or $Pml^{-/-}$ MEFs treated for 12 hours. Data represent the mean SD of five independent experiments.*

To investigate the role of PML in Ca^{2+} homeostasis, we used recombinant Ca^{2+}-sensitive bioluminescent protein aequorin (244). In $Pml^{+/+}$ MEFs, the $[Ca^{2+}]$ in the lumen of the ER ($[Ca^{2+}]_{er}$) at steady state was ~450 μM, whereas in $Pml^{-/-}$ MEFs it was lower. When the cells were stimulated with ATP, the P2Y receptor agonist that causes release of Ca^{2+} from the ER, the decreases in the $[Ca^{2+}]_{er}$ observed in $Pml^{+/+}$ MEFs in quantitative and kinetic terms were larger and faster than in $Pml^{-/-}$ MEFs, reflecting a more rapid flow of Ca^{2+} through the IP3R (Figure 15A). In turn, the $[Ca^{2+}]$ increases evoked by stimulation with ATP in the cytosol ($[Ca^{2+}]_c$) and mitochondria ($[Ca^{2+}]_m$) were smaller in $Pml^{-/-}$ than in $Pml^{+/+}$ MEFs (Figure 15, B and C).

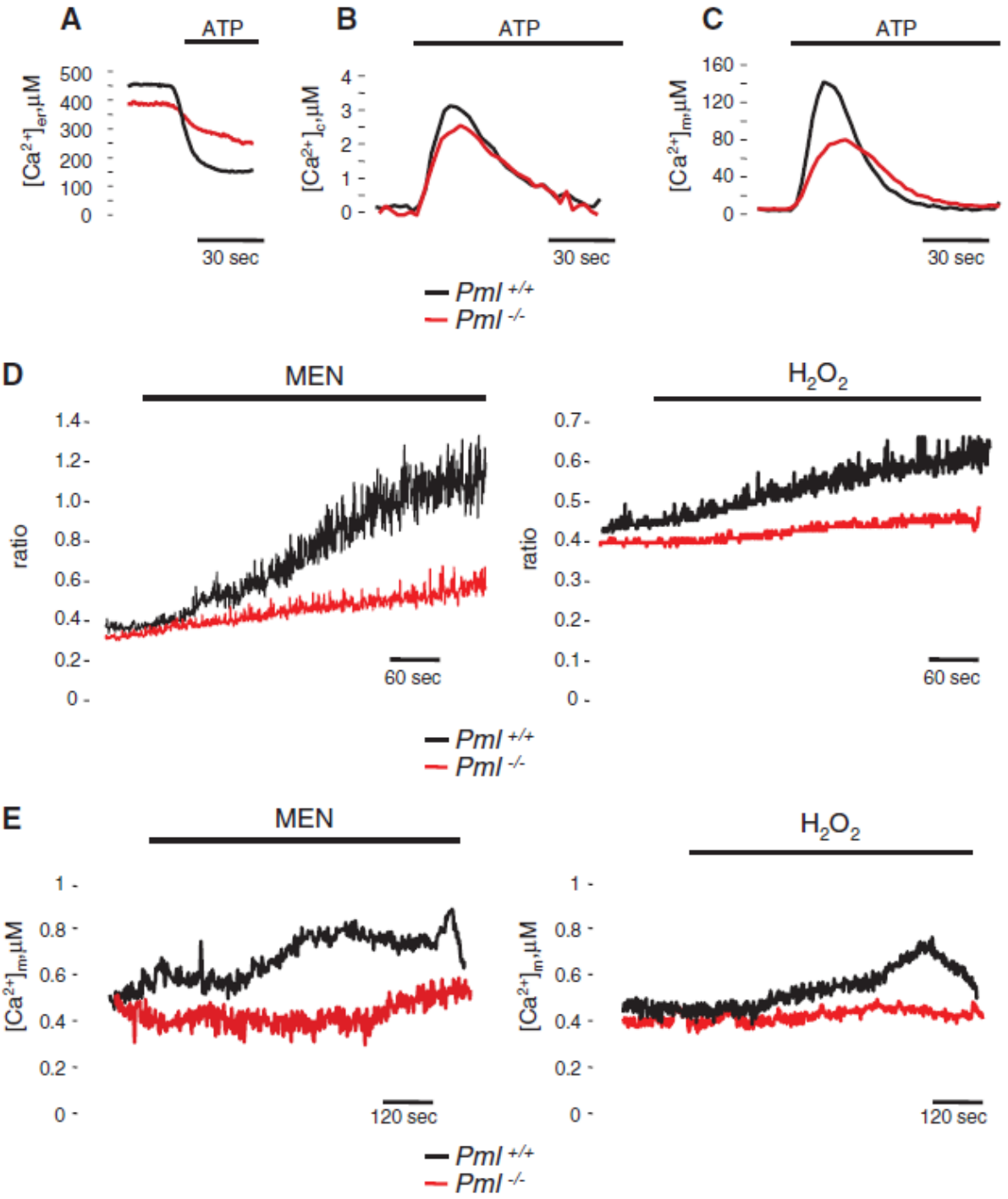

Figure 15. Intracellular Ca^{2+} homeostasis in $Pml^{+/+}$ and $Pml^{-/-}$ MEFs. *(A to C) ER (A), cytosolic (B), and mitochondrial (C) Ca^{2+} homeostasis measurements with aequorins. Where indicated, cells were treated with 100 μM ATP. $Pml^{+/+}$: $[Ca^{2+}]_{er}$ peak 448 ± 32 μM; $[Ca^{2+}]_c$ peak 3.3 ± 0.16 μM; $[Ca^{2+}]_m$ peak 138 ± 14 μM. $Pml^{-/-}$: $[Ca^{2+}]_{er}$ peak 386 ± 42 μM; $[Ca^{2+}]_c$ peak 2.65 ± 0.23 μM; $[Ca^{2+}]_m$ peak 78 ± 10 μM. n = 15 samples from five independent experiments, P < 0.01. (D) MEFs loaded with calcium-sensitive fluorescent dye Fura-2/AM were stimulated with menadione (MEN) or*
H_2O_2. The kinetic behaviour of the $[Ca^{2+}]_c$ response is presented as the ratio of fluorescence at 340 nm/380 nm. The traces are representative of at least 10 single-cell responses from three independent experiments. (E) Analysis of $[Ca^{2+}]_m$ during oxidative stress. Where indicated, cells were stimulated with 30 μM MEN or 2 mM H_2O_2. n = 10 samples from three independent experiments.

We then investigated whether the absence of *Pml* could alter the increases in $[Ca^{2+}]_c$ and $[Ca^{2+}]_m$ induced by apoptotic stimuli. In $Pml^{-/-}$ MEFs, the increases in $[Ca^{2+}]_c$ and $Ca^{2+}]_m$, evoked by the oxidative apoptotic stimuli, such as MEN and H_2O_2 that trigger both a progressive release of Ca^{2+} from the ER and an activation of the capacitative Ca^{2+} influx (142), were smaller as mentioned above (Figure 15, D and E).

The erPML chimera rescues Ca^{2+} homeostasis after physiological and apoptotic stimuli in $Pml^{-/-}$ MEFs

To determine whether the effects of PML on regulation of Ca^{2+} homeostasis depend on its localization to the ER and MAMs, we generated a chimeric protein containing the entire PML protein that was targeted to the outer surface of the ER (245).

This chimera, designated erPML, localized to the ER and MAMs in $Pml^{-/-}$ MEFs, as revealed by immunocytochemical staining (Figure 16A). The introduction of erPML in $Pml^{-/-}$ MEFs restored Ca^{2+} signals evoked by either agonist (Figure 16B) or apoptotic stimuli (MEN or H_2O_2) (Figure 16C) to values comparable to those in $Pml^{+/+}$ MEFs (Figure 15, C and D).

This effect was associated with a re-established sensitivity to apoptosis induced by ER stress but did not restore the sensitivity to etoposide (ETO) (Figure 16D), a DNA-damaging agent that triggers apoptotic death by a Ca^{2+}-independent process.

Overall, these experiments indicate that the absence of *Pml* causes a reduction in the amplitude of Ca^{2+} signals induced by ATP, other agents, or apoptotic stimuli, and that forcing PML to the ER rescues these defects. A PML protein targeted to the nucleus restored the formation of NBs, but did not restore the Ca^{2+} responses and the sensitivity to ER stress-dependent cell death, although it restored response to other apoptotic stimuli such as ETO (data not shown).

PML is essential for Akt- and PP2a-dependent modulation of IP3R phosphorylation and in turn for IP3R-mediated Ca^{2+} release from ER

To investigate the mechanism underlying these activities of PML, we tested whether PML could functionally and physically interact with the IP3R3. Immunoprecipitation of IP3R3 led to the co-precipitation of PML (Figure 17A) and vice versa (data not shown). Amounts of phosphorylated-IP3R3 (p-IP3R3) were higher in $Pml^{-/-}$ than in $Pml^{+/+}$ MEFs (Figure 17A).

Reduced cellular sensitivity to apoptotic stimuli was observed in cells with high activity of the protein kinase Akt, as a result of diminished Ca^{2+} flux from the ER through the IP3R (146, 147). The amount of phosphorylated Akt (pAkt) (that is, the active form of Akt) co-precipitated with

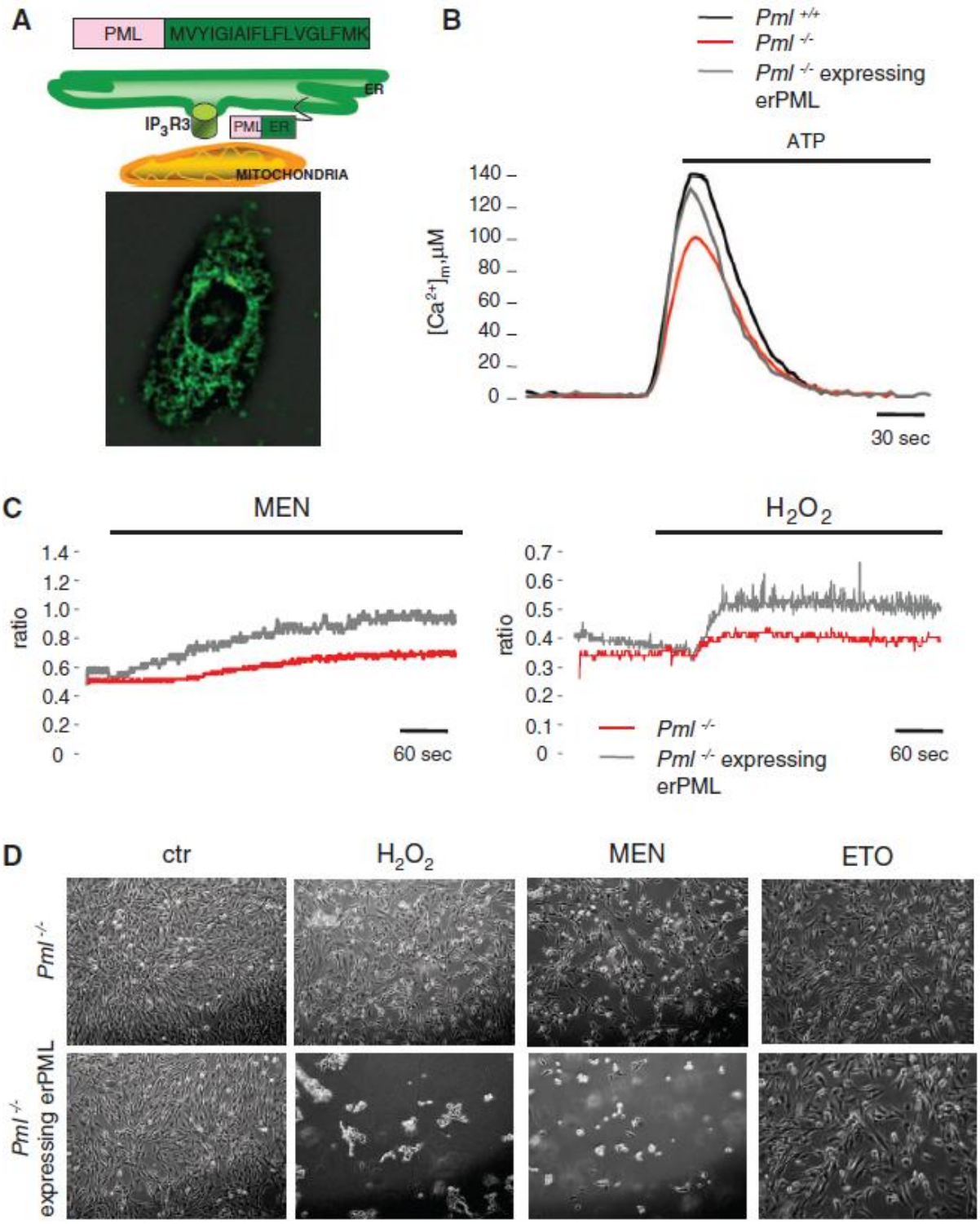

Figure 16. erPML chimera reestablishes the $[Ca^{2+}]_m$ and apoptotic responses in $Pml^{-/-}$ MEFs. *(A) Schematic map of the erPML chimera and immunofluorescence image, stained with the antibody to PML, of $Pml^{-/-}$ MEFs expressing erPML. (B) erPML re-establishes the agonist-dependent $[Ca^{2+}]_m$ response in $Pml^{-/-}$ MEFs ($[Ca^{2+}]_m$ peak 135 ± 12 μM) to values comparable to those of $Pml^{+/+}$ MEFs. (C) $Pml^{-/-}$ and $Pml^{-/-}$ MEFs expressing erPML previously incubated with Fura-2/AM were stimulated with menadione (MEN) or H_2O_2. The kinetic behaviour of the $[Ca^{2+}]_c$ response is presented as the ratio of fluorescence at 340 nm/380 nm. The traces are representative of at least 10 single-cell responses from three independent experiments. (D) Representative microscopic fields of $Pml^{-/-}$ MEFs and $Pml^{-/-}$ expressing erPML before and after treatment with 1 mM H_2O_2, 15 μM MEN, or 50 μM etoposide (ETO) for 16 hours.*

IP3R3 (Figure 17A) was higher in *Pml*$^{-/-}$ than in *Pml*$^{+/+}$ MEFs. Dephosphorylation of Akt at the MAM might occur through PML-mediated recruitment of the phosphatase PP2a. Indeed, PML interacts with PP2a in PML-NBs (239). Further, the amount of PP2a coprecipitated with IP3R3 (Figure 17A) was diminished in *Pml*$^{-/-}$ MEFs (Figure 17A). Thus, in the absence of *Pml*, reduced Ca^{2+} release could be caused by increased phosphorylation and activation of Akt at the ER due to an impaired PP2a activity, which in turn impair Ca^{2+} flux through the IP3R because of its hyperphosphorylated state.

We also demonstrated the localization of all these proteins at the ER and MAM through immunocytochemical staining and subfractionation (Figure 17, B and C).

We further investigated the correlation among PML, Akt, and PP2a at the ER and the regulation of the IP3R by a selective inhibition of either Akt or PP2a. Pretreatment of cells with okadaic acid (OA, a PP2a inhibitor) caused a reduction in $[Ca^{2+}]_m$ responses to ATP stimulation and a reduced H_2O_2- or MEN-induced death in *Pml*$^{+/+}$ MEFs **(**92 ± 21 μM vs 128 ± 33 μM in control cells, $p<0.01$) and in *Pml*$^{-/-}$ MEFs expressing erPML (102 ± 13 μM vs. 135 ± 17 μM in control cells, $p<0.05$**)**, but not in *Pml*$^{-/-}$MEFs (73 ± 22 μM vs 78 ± 14 μM in control cells) (Figure 17, D and E), in which PP2a activity is impaired. LY294002 (an inhibitor of Akt) had no effect on the agonist-dependent $[Ca^{2+}]_m$ transients and on apoptosis in *Pml*$^{+/+}$ (126 ± 16 μM vs 128 ± 33 μM in control cells) or *Pml*$^{-/-}$ MEFs expressing erPML (124 ± 13 μM vs 132 ± 18 μM in control cells), whereas it increased agonist dependent $[Ca^{2+}]_m$ responses and restored sensitivity to H_2O_2 or MEN (Figure 17, D and E) in *Pml*$^{-/-}$ MEFs (112 ± 15 μM vs 78 ± 14 μM in control cells, $p<0.01$**)** (in which high levels of pAkt are observed; Figure 17A).

Discussion

The PML tumor suppressor is a critical and essential regulator of multiple apoptotic responses. While the reported role of PML in the modulation of p53 transcription could explain some of its pro-apoptotic functions, it failed to reconcile the fundamental role played by PML in the transcription-independent early apoptotic response.

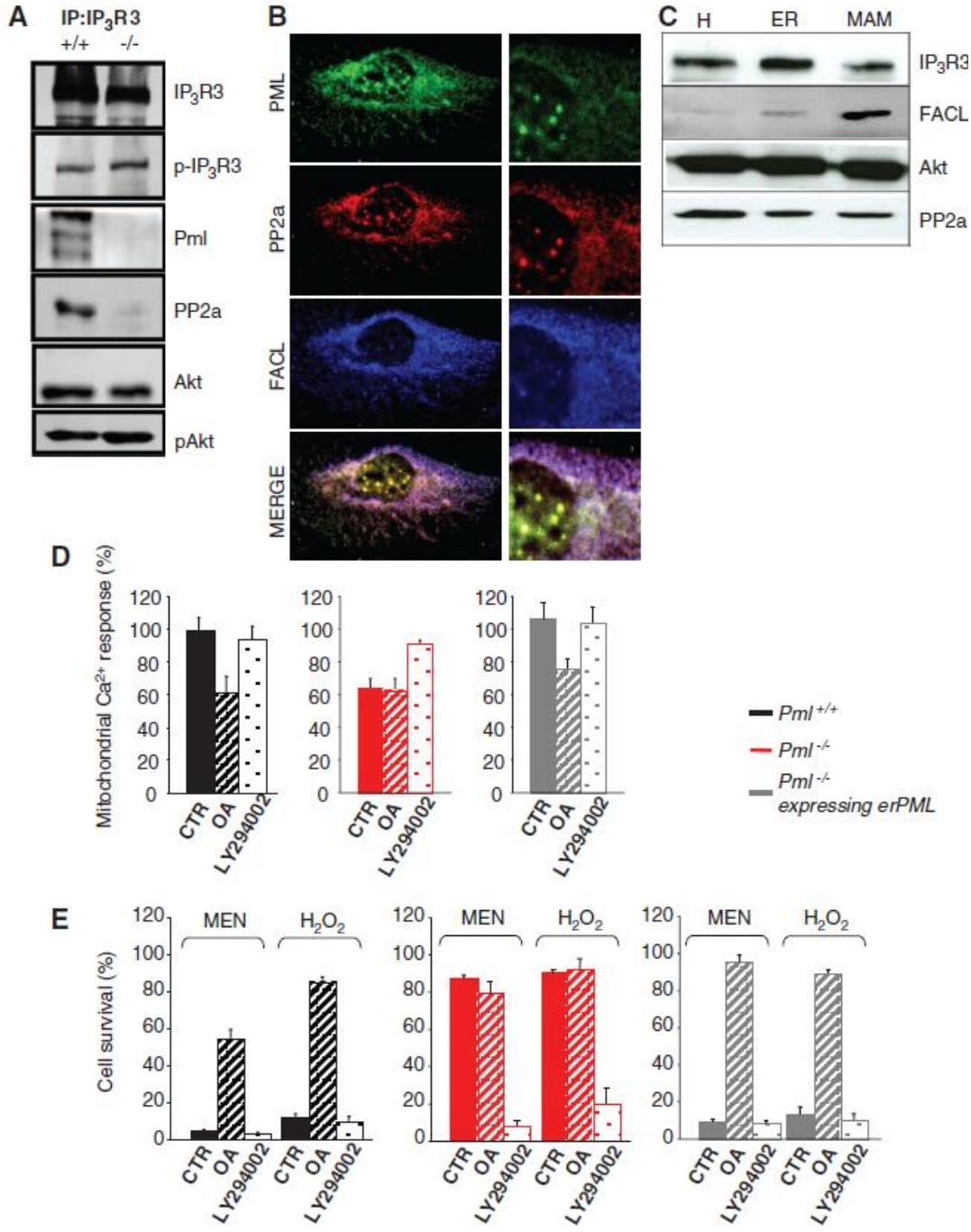

Figure 17. Modulation of $[Ca^{2+}]_m$ and apoptotic responses by PML through Akt- and PP2a-dependent phosphorylation of IP3R3. *(A) Coimmunoprecipitation of IP3R3 with PML, Akt, and PP2a in $Pml^{+/+}$ MEFs. In the same blot, the levels of p-IP3R3 and pAkt are shown. (B) Localization of PML (green) and PP2a (red) at ER and MAM sites in $Pml^{+/+}$ MEFs analyzed by immunofluorescence. FACL was used as MAM marker. (C) $Pml^{+/+}$ MEFs subcellular fractionation and identification of PP2a and Akt at ER and MAM fractions by immunoblot. (D) Effects of okadaic acid (OA, 1 μM for 1 hour) and LY294002 (5 μM for 30 min) on agonist-dependent $[Ca^{2+}]_m$ responses in $Pml^{+/+}$, $Pml^{-/-}$, and $Pml^{-/-}$ MEFs expressing erPML. $[Ca^{2+}]_m$ is represented as a percentage of the peak value of control cells. For all these experiments $n \geq 15$ of at least five independent experiments. (E) Quantification of cell survival of $Pml^{+/+}$, $Pml^{-/-}$, and $Pml^{-/-}$ MEFs expressing erPML, control (CTR, untreated) and treated first with OA (1 μM for 1 hour) or LY294002 (5 μM for 30 min) and then H_2O_2 or menadione (MEN) for 16 hours. The data show the percentage of living cells in the whole-cell population negative for annexin-V-fluorescein isothiocyanate and propidium iodide staining, analyzed by flow cytometry. Data show the means SD from three independent experiments.*

Here we elucidate, at list in part, the molecular basis for such a diverse proapoptotic role. By ultracentrifugation, immunogold labeling, and immunofluorescence, we revealed that extranuclear PML is specifically enriched at ER and at the MAMs, signaling domains involved in ER-to-mitochondria Ca^{2+} transport and in induction of apoptosis, suggesting that PML might have additional and yet unidentified functions independent from the PML-NB.

The most important molecular component of the Ca^{2+} handling machinery of the ER is represented by the IP3Rs. IP3Rs are ligand-gated channels that serve to discharge Ca^{2+} from ER stores in response to agonist stimulation. However, being directly responsible for mitochondrial Ca^{2+} overload, the release of Ca^{2+} from ER stores by IP3Rs is linked to multiple models of apoptosis. Recent data showed that IP3R3, localized in the MAMs, has a selective role in the induction of apoptosis by preferentially transmitting apoptotic Ca^{2+} signals to mitochondria. Accordingly, siRNA silencing of IP3R3 blocked apoptosis (246) and KO of IP3R3 significantly decreased agonist induced mitochondrial Ca^{2+} uptake (138). IP3Rs possess consensus sequences for phosphorylation by numerous kinases, including Akt, which is constitutively active in some cancer cells. In turn, the hyper-phosphorylation of IP3Rs by Akt inhibits ER Ca^{2+} release and reduces significantly cellular sensitivity to Ca^{2+}-mediated pro-apoptotic stimulation (146, 147).

We found Pml to physically interact with IP3R3, modulating its phosphorylation state by controlling the activity of Akt through the recruitment of the PP2a phosphatase at the ER/MAMs. In so doing, PML is able to regulate Ca^{2+} mobilization into the mitochondrion, which then triggers the cell death program. Conversely, in the absence of PML, PP2a does not accumulate in the complexes with IP3R and Akt, and this results in an accumulation of activated Akt (phospho-Akt). Once activated Akt can hyper-phosphorylate IP3R thus inhibiting the ER Ca^{2+} release towards the mitochondria. This was demonstrated to be mediated by a specific multi-protein complex, localized at ER/MAMs contact sites, including PML, IP3R3, the protein phosphatase PP2a, and Akt. In particular, PML appeared to be essential for the binding of PP2a to the IP3R3, hence favoring IP3R3 de-phosphorylation (Figure 18).

Strikingly, the final outcome of a PML functional loss at the cellular level is similar to the one observed in cells overexpressing Bcl-2 or lacking of Bax/Bak (albeit through a completely different molecular mechanism): a reduced mitochondrial Ca^{2+} overload upon pro-apoptotic stimuli that dramatically blunts the apoptotic response.

Our data highlight an extranuclear, transcriptionindependent function of PML that regulates cell survival through changes in Ca^{2+} signaling in the ER, cytosol, and mitochondria. This effect appears to be specific to Ca^{2+}-mediated apoptotic stimuli because alteration in *Pml* did not influence cell

death in cells treated with ETO, which activates the apoptotic pathway in a way largely independent of Ca^{2+}.

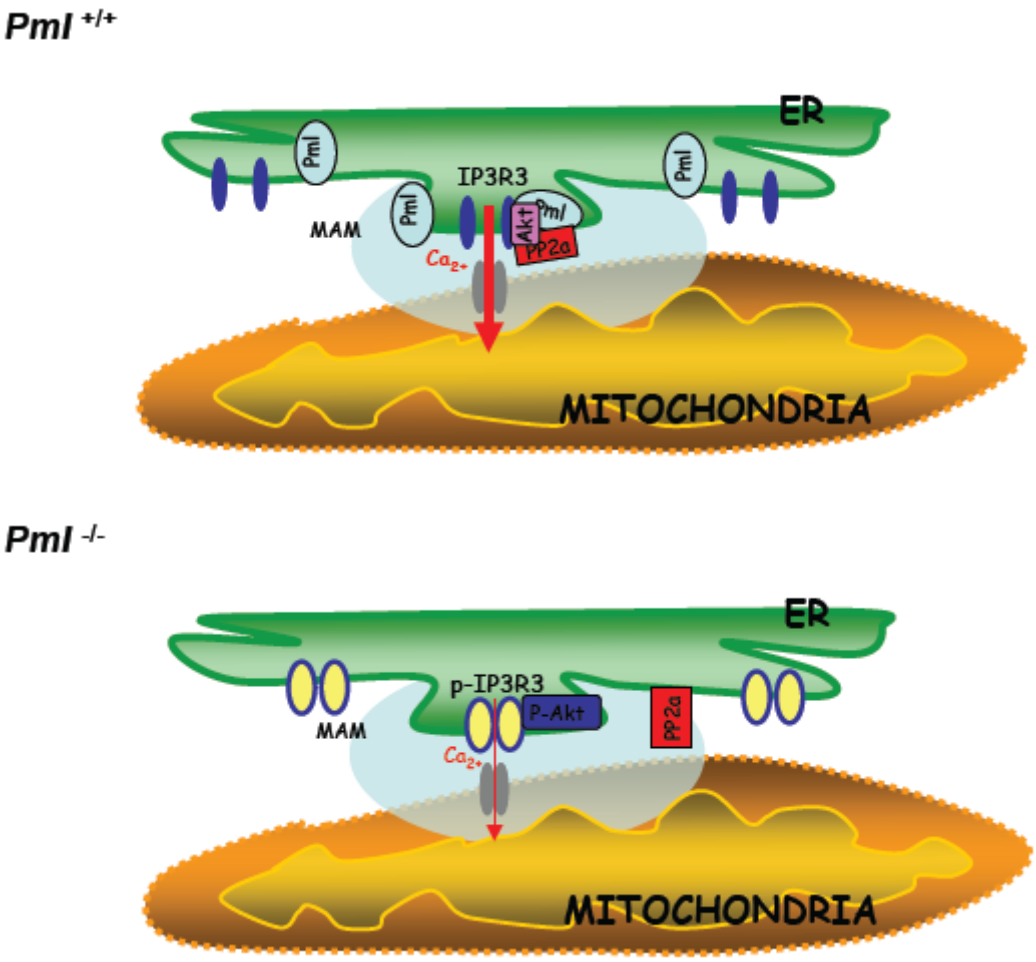

Figure 18. Schematic model of PML effects on Ca^{2+} homeostasis. *PML localized at the ER and MAM, to the outer surface of the ER, interacts with IP3R3, Akt and PP2a. This interaction is fundamental for the modulation of IP3R3-phosphorylation and in turn for IP3R dependent Ca^{2+} release*

This mechanism may explain how PML can so broadly regulate the early (and transcription independent) apoptotic response. This new apoptogenic mechanism, which appears to operate in parallel to those regulated at other sites such as the PML-NBs, demonstrates that the role of PML in apoptosis is broader than previously believed inasmuch as it does modulate apoptosis both in the nucleus as well as at the MAMs. Our findings may have implications in tumorigenesis where the function of PML is frequently lost, or in other pathophysiological conditions where PML is accumulated such as cell stress, or infection with viral or bacterial pathogens.

3.3 PTEN localization at the ER and MAMs regulates calcium signalling and apoptosis

Introduction

PTEN (phosphatase and tensin homolog deleted on chromosome 10) is among the most commonly lost or mutated tumour suppressors in human cancers (247, 248). PTEN acts as a haploinsufficient tumour suppressor, with somatic alterations of at least one allele frequently observed in glioma, breast, colon, lung and prostate tumours, whereas its complete loss occurs at highest frequency in glioblastoma and endometrial carcinomas, and is generally correlated with advanced cancer and metastases (249). Moreover, germline mutations of PTEN have been found in cancer-susceptibility syndromes (250).

PTEN is a phosphatase that has both a lipid (251) and a dual-specificity protein phosphatase activity (252). It dephosphorylates the plasma membrane lipid phosphatidylinositol 3,4,5-trisphosphate (PIP3) to generate phosphatidylinositol 4,5-bisphosphate (PIP2), thereby directly antagonizing the phosphatidylinositol 3-kinase (PI3K)-Akt pathway that is crucial for maintaining tissue homeostasis (253, 254). Loss of PTEN leads to elevated levels of PIP3 and consequent Akt hyperactivation, which promotes cell growth, proliferation, survival and other cellular processes (255, 256). Although the tumour-suppressive function of PTEN is mostly dependent on its PIP3 phosphatase activity, it has now been firmly established that PTEN also possesses additional novel biological functions that are independent of its lipid phosphatase activity (257-260). PTEN exerts such functions by its protein phosphatase activity and proposed non-enzymatic mechanisms, such as interaction with other proteins (261, 262). Recent advances have also proved that the cellular localization of PTEN plays a central role in its regulation (263). Several studies clearly demonstrate that nuclear PTEN has important tumour-suppressive functions (239, 264-266). Furthermore, PTEN has been found in mitochondria, in hippocampal neurons undergoing apoptosis (267) and in hearts exposed to ischemia-reperfusion (268), and has been proposed to be a crucial mediator of mitochondria-dependent apoptosis under certain circumstances.

Mitochondria and the ER have emerged as cellular targets of oncogenes and tumour suppressors, as they are crucial nodes where significant remodelling of Ca^{2+} signalling occurs in tumour cells to sustain proliferation and avoid cell death (see Introduction, section 1.6). Indeed, despite controlling many processes essential for life, the ER-mitochondrial Ca^{2+} transmission can be a potent death-inducing signal, since the enhancement of mitochondrial Ca^{2+}-uptake generally correlates with increased sensitivity to apoptosis. The ER supplies Ca^{2+} directly to mitochondria via IP3Rs at close

contacts between the two organelles, referred to as MAMs. Ca^{2+}-handling proteins of both organelles are highly compartmentalized at MAMs, providing a direct and proper mitochondrial Ca^{2+} signalling. Recently, numerous other proteins, including those involved in the pathogenesis of different disorders, have been characterized at MAMs, underling their importance for signalling cell fate choices (see Introduction, section 1.7).

In this part of the PhD project, we identify a novel intracellular localization of PTEN at ER and MAMs. We evaluate the effect of PTEN silencing, overexpression, and ER-targeting, in regulating ER-mitochondrial Ca^{2+} signal transmission and in the induction of apoptosis. Taken together, the present data demonstrate that ER-localized PTEN is specifically involved in increasing both Ca^{2+} transfer from the ER to mitochondria and cell sensitivity to Ca^{2+}-mediated apoptosis, suggesting an additional mechanism of action of this important tumour suppressor.

Results

PTEN is localized in different intracellular compartments including ER and MAMs

Besides the best-known cytoplasmic and nuclear pools, it has been reported that PTEN can accumulate in mitochondria. To further analyze the intracellular localization of PTEN, in particular its presence in the ER and MAMs, we performed detailed subcellular fractionation in HEK-293.

We isolated crude mitochondria, nuclei and a cytosolic fraction containing lysosomes and microsomes. Subsequent ultracentrifugation of the cytosolic fraction results in the separation of ER and cytosol, whereas the crude mitochondria preparation were further fractionated on a Percoll gradient to obtain purified mitochondria and MAMs. We evaluated total homogenate, cytosol, ER and MAMs fractions by immunoblot analyses (Figure 19) using β-tubulin as a general cytosolic marker, IP3R3 as ER marker, FACL4 as MAMs marker, VDAC as mitochondrial marker, and lamin B1 as nuclear marker (to exclude nuclear contamination during fractionation); all markers were enriched in their respective compartments. Using this protocol, PTEN was found enriched in the cytosol, as expected, but we also revealed its presence in the ER and MAMs fractions. We also confirmed the previously described localization of Akt, the major downstream target of PTEN, at ER and MAMs in HEK-293 cells (206). The same results were obtained by subcellular fractionation of primary MEFs (Figure 20). Localization of PTEN in the ER was also verified by immunocytochemical staining (Figure 22a, A-A’’).

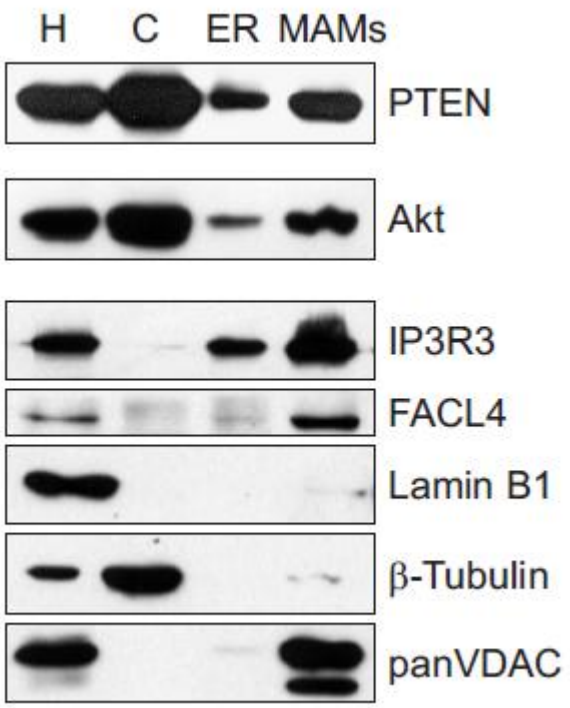

Figure 19. Identification of PTEN in ER and MAMs subcellular fractions. *HEK-293 cells were fractionated into cytosol, ER and MAMs, and protein components of subcellular fractions were subjected to immunoblotting. The presence of PTEN was shown by using a specific monoclonal antibody. Marker proteins indicate ER (IP3R3), MAMs (FACL4), cytosol (β-tubulin), mitochondria (panVDAC) and nucleus (lamin B1). VDAC and IP3R3 were both present in the MAMs, whereas all fractions were free of nuclear contamination. Akt presence was also verified in all fractions. H: homogenate; C: cytosol; ER; MAMs.*

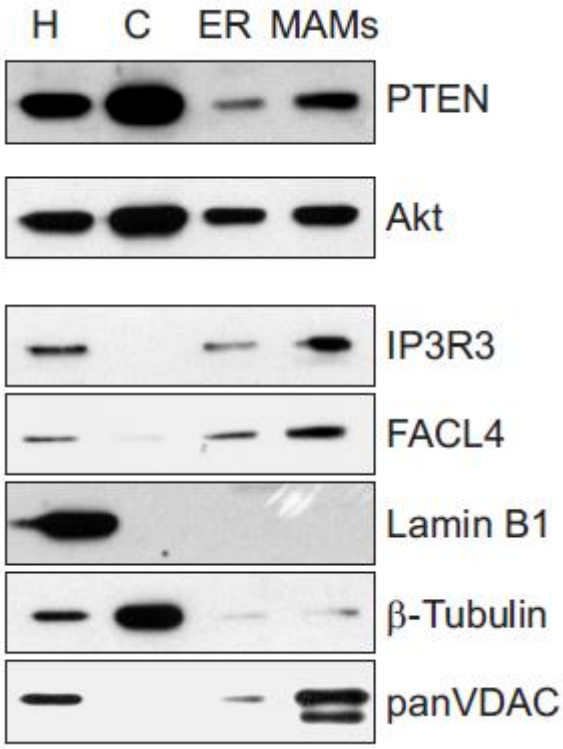

Figure 20. Identification of PTEN in the ER and MAMs upon MEFs fractionation. *Marker proteins indicate ER (IP3R3), MAMs (FACL4), cytosol (β-tubulin), mitochondria (panVDAC) and nucleus (lamin B1). Akt presence was also confirmed in all fractions. H: homogenate; C: cytosol; ER; MAMs*

We thus demonstrate that although PTEN is mainly localised in the cytosol, the nucleus and, in a smaller proportion, in mitochondria (our nuclear and mitochondrial fractions contained PTEN as well, data not shown), a significant amount of PTEN is present in the ER and MAMs.

PTEN silencing reduces ER Ca^{2+} release, thus impairing cytosolic and mitochondrial Ca^{2+} transients elicited by agonist stimulation

In view of the localization of PTEN at the ER and MAMs, we investigated whether it plays a role in regulating Ca^{2+} signalling between the ER and mitochondria. We analyzed intracellular Ca^{2+} homeostasis after downregulation of PTEN expression by RNA interference (RNAi) silencing. Two

different small interfering RNAs (siRNAs), siRNA-PTEN(1049) and siRNA-PTEN(219), were generated and tested for specific silencing efficiency and ability to increase the levels of activated, Ser473-phosphorylated Akt ($pAkt^{Ser473}$) (Figure 21a).

Ca^{2+} measurements were then carried out in HEK-293 cells co-transfected with the PTEN siRNAs and specific organelle-targeted aequorin probes (244). Cells were stimulated with ATP, the P2Y receptor agonist that induces the generation of IP3, thus activating the IP3R channels and causing Ca^{2+} release from ER stores.

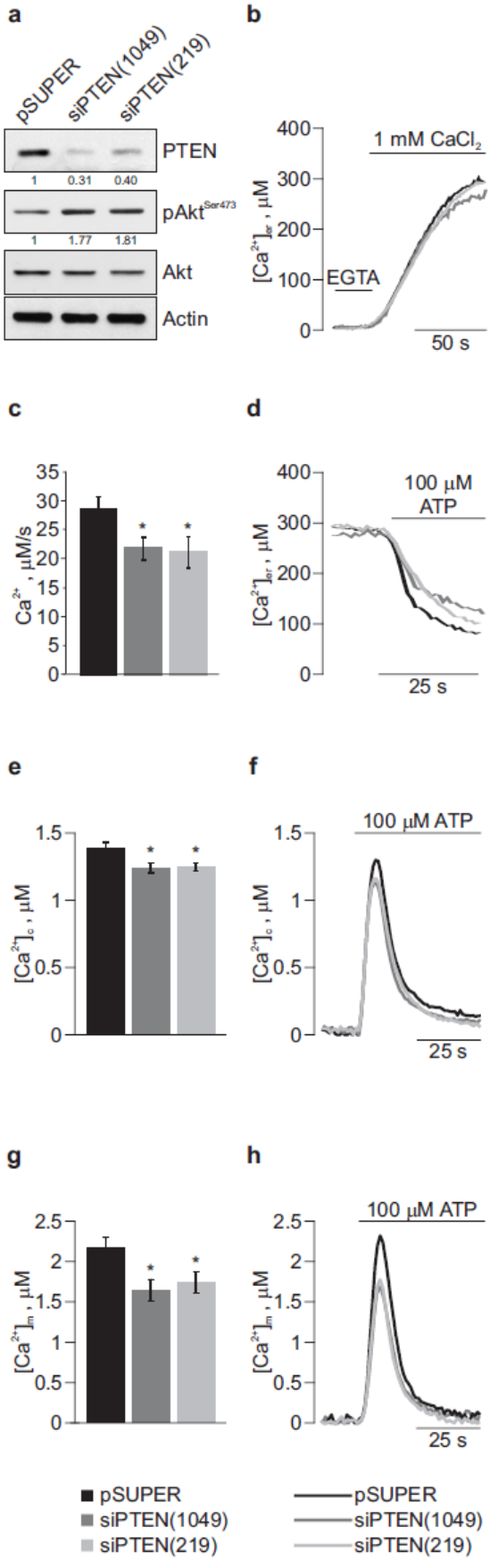

Figure 21. Effect of PTEN silencing on intracellular Ca^{2+} homeostasis. *(**a**) HEK-293 cells were transfected with siRNAs-PTEN encoding plasmid or mock transfected with empty vector (pSUPER) in control cells. Immunoblotting of total cell lysates shows that transfection with PTEN siRNAs effectively decreased PTEN protein levels and increased $pAkt^{S473}$ levels, reflecting an effective Akt activation without altering its expression. Numbers indicate densitometrically determined protein levels relative to actin for PTEN and to total Akt for $pAkt^{Ser473}$. The traces (**b**, **d**, **f**, **h**) show representative $[Ca^{2+}]$ measurements performed in PTEN-silenced HEK-293 cells co-transfected with the appropriate aequorin (AEQ) chimera (erAEQmut, cytAEQ and mtAEQ for monitoring the ER, cytosol and mitochondria, respectively). Where indicated, cells were challenged with 100 µM ATP to induce Ca^{2+} release from the ER. The bar graphs (**c**, **e**, **g**) are the average of all experiments performed. (**b**) $[Ca^{2+}]_{er}$ steady-state levels. (**c**) Mean rate of Ca^{2+} release. (**d**) ER Ca^{2+} release kinetics. (**e**) Average $[Ca^{2+}]_c$ peak. (**f**) Cytosolic Ca^{2+} transients. (**g**) Average $[Ca^{2+}]_m$ peak. (**h**) Mitochondrial Ca^{2+} transients. Transfection, aequorin reconstitution and measurements of luminescence were carried out and calibrated into $[Ca^{2+}]$ values as described in the Materials and Methods section. The traces and bar graphs of this figure are representatives of ≥ 10 samples from at least three independent experiments that yielded similar results.*

The effect of PTEN silencing on ER Ca^{2+} handling was first investigated (see Materials and Methods section for details). Silencing of PTEN did not alter significantly the Ca^{2+} loading kinetics, nor the steady state [Ca^{2+}] of the ER lumen ($[Ca^{2+}]_{er}$) (Figure 21b, $[Ca^{2+}]_{er}$: pSUPER, 321.1 ± 27.30 μM; siRNA-PTEN(1049), 286.7 ± 23.17 μM; siRNA-PTEN(219) 293.9 ± 27.59 μM; n ≥ 10). However, upon ATP stimulation, Ca^{2+} release kinetics from the ER were slower in PTEN-silenced cells (Figures 21c and d, Vmax: pSUPER, 28.68 ± 2.12 μM/s; siRNA-PTEN(1049) 21.89 ± 1.97 μM/s; siRNA-PTEN(219) 21.25 ± 2.69 μM/s; n ≥ 10, $p < 0.05$). Accordingly, ATP elicited a significantly smaller transient [Ca^{2+}] rise in the cytosol ($[Ca^{2+}]_c$) and in the mitochondrial matrix ($[Ca^{2+}]_m$) (Figures 21e and f, $[Ca^{2+}]_c$ peak values: pSUPER, 1.29 ± 0.04 μM; siRNA-PTEN(1049) 1.15 ± 0.04 μM; siRNA-PTEN(219) 1.16 ± 0.03 μM; n ≥ 30, $p < 0.05$; figures 21g and h, $[Ca^{2+}]_m$ peak values: pSUPER, 2.17 ± 0.14 μM; siRNA-PTEN(1049) 1.64 ± 0.13 μM; siRNA-PTEN(219) 1.74 ± 0.14 μM; n ≥ 18, $p < 0.05$). Taken together, these data show that downregulation of PTEN expression globally affects intracellular Ca^{2+} signalling acting on the ER Ca^{2+} release machinery.

ER-localized PTEN, but not wild-type PTEN, enhances the agonist-dependent mitochondrial Ca^{2+} response

In order to test whether the effects of PTEN on regulation of Ca^{2+} homeostasis were specifically dependent on its localization in the ER and MAMs, we generated a chimeric protein, designated ER-PTEN, that targets the entire PTEN protein to the cytoplasmic surface of the ER membrane (Figure 22b). We verified the intracellular distributions of endogenous, recombinant and ER-targeted PTEN in HEK-293 cells co-transfected with erGFP as a marker for the ER. Immunofluorescence analyses confirmed the presence of endogenous PTEN at the ER, where it slightly co-localize with erGFP (Figure 22a, A-A''). When analyzing the transfected wild-type PTEN staining pattern, we found a higher overlap with the ER, but PTEN was also found diffusely accumulated in the nucleus (Figure 22a, B-B''). Instead, ER-PTEN was predominantly localized in the ER and mostly excluded from the nucleus (Figure 22a, C-C''). We also analysed recombinant PTEN and ER-PTEN chimera expression levels and effects on Akt phosphorylation (Figure 22c).

We next determined whether overexpression of PTEN or ER-PTEN could differentially affect Ca^{2+} handling of mitochondria, the main proximal target of Ca^{2+} signals arising from the ER. Surprisingly, ER-PTEN significantly enhanced mitochondrial Ca^{2+} uptake evoked by agonist stimulation, while wild-type PTEN was indistinguishable from controls (Figure 22d and e, $[Ca^{2+}]_m$:

pcDNA3, 3.17 ± 0.19 μM; PTEN, 3.37 ± 0.22 μM, n = 18, p > 0.5; ER-PTEN 4.13 ± 0.22 μM, n = 18, p < 0.01).

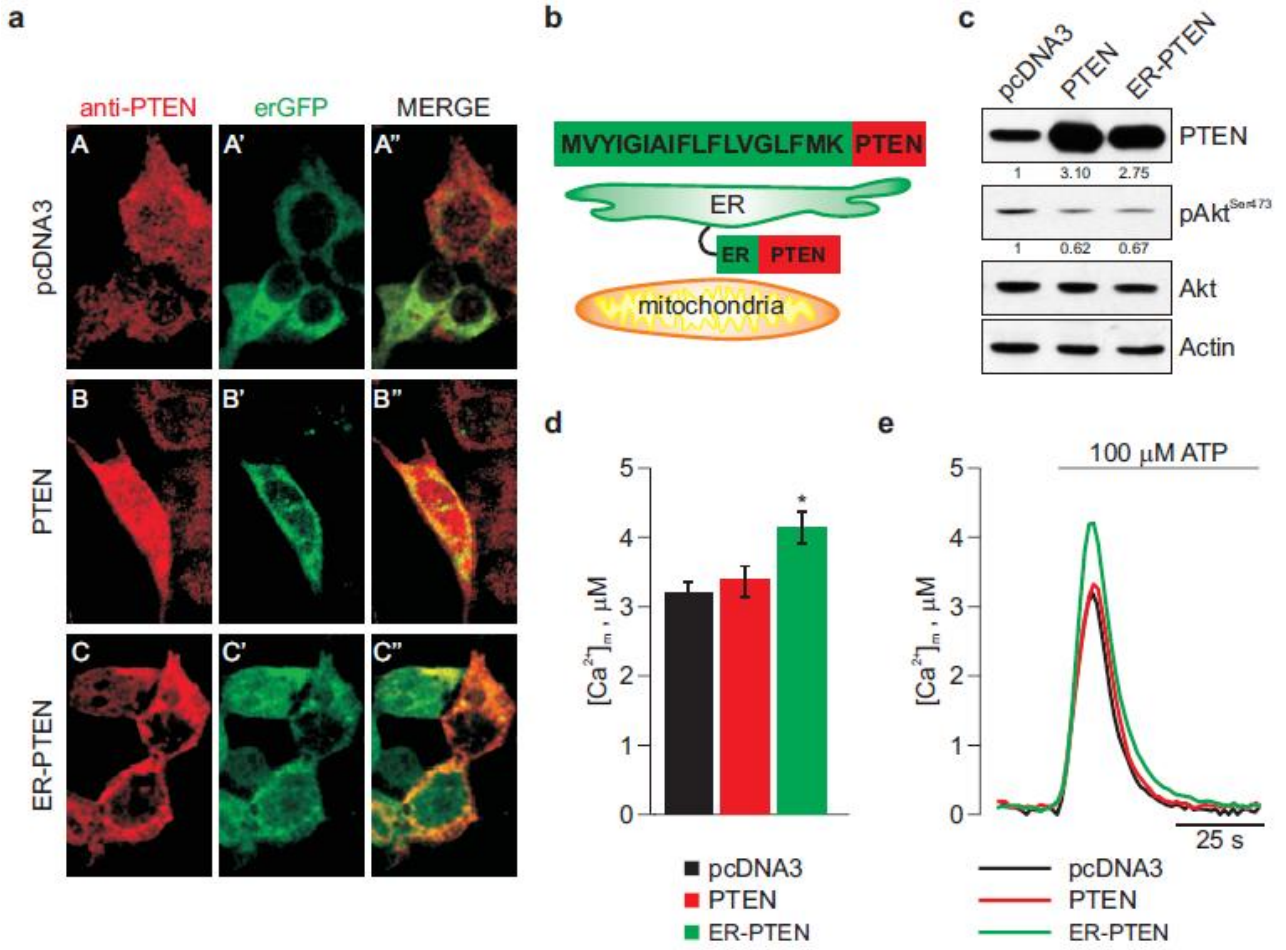

Figure 22. PTEN and ER-PTEN differentially affect mitochondrial Ca^{2+} uptake. ***(a)*** *Immunofluorescence to detect localization of PTEN and targeted ER-PTEN. HEK-293 cells transiently expressing empty vector (pcDNA3) (A), PTEN (B) or ER-PTEN (C), and co-transfected with erGFP (green images: A'-C'), were stained for PTEN (red images: A-C). Co-localisation of the green and red signals, yielding a yellow staining, is apparent in the merged images (merge: A''-C''). (**b**) Schematic map of the ER-PTEN chimera. (**c**) PTEN and ER-PTEN expression, and Akt phosphorylation were investigated by immunoblot of whole cell lysates using total and phospho-specific antibodies. Numbers indicate densitometrically determined protein levels relative to actin for PTEN and to total Akt for $pAkt^{Ser473}$. (**d**) Bar graph of the average $[Ca^{2+}]_m$ peak. (**e**) Mitochondrial Ca^{2+} homeostasis modulation after ER-PTEN overexpression. Traces and bar graphs are representatives of ≥ 18 samples from at least three independent experiments that yielded similar results.*

The same $[Ca^{2+}]_m$ increase was observed also using a different ER-targeting PTEN chimera (Figure 23). Collectively, these data indicate that a subpopulation of cellular PTEN localized at the ER is specifically involved in the regulation of the agonist-induced Ca^{2+} fluxes from the ER to mitochondria.

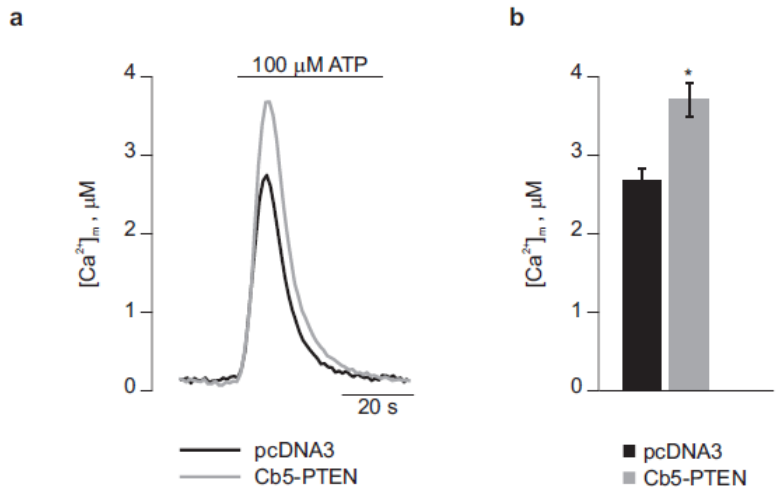

Figure 23 Effect of Cb5-PTEN chimera overexpression on mitochondrial Ca^{2+} uptake *(**a**) Representative traces of mitochondrial Ca^{2+} transients evoked by 100 µM ATP in Cb5-PTEN-overexpressing HEK-293 cells. (**b**) Average $[Ca^{2+}]_m$ peak (pcDNA3, 2.66 ± 0.16 µM; ER-PTEN 3.71 ± 0.22 µM, n = 20, p < 0.01).*

Ca^{2+} mobilization from intracellular stores evoked by arachidonic acid is impaired when PTEN is silenced and increased through targeting of PTEN to the ER

The transfer of Ca^{2+} from the ER to mitochondria not only controls a variety of physiological processes during cell activation, but can also be a potent death-inducing signal (135). In order to test whether PTEN is involved in remodelling ER-mitochondrial Ca^{2+} flux also during apoptosis-inducing Ca^{2+} signals, we investigated Ca^{2+} dynamics in response to the lipid mediator arachidonic acid (ArA) (269) after PTEN silencing, overexpression or targeting to the ER. ArA is proposed to initiate apoptotic death through a Ca^{2+}-controlled process: it progressively releases Ca^{2+} from intracellular stores, thereby directly causing a long-lasting $[Ca^{2+}]_c$ rise that finally leads to the mitochondrial permeability transition and release of caspase cofactor (143, 147). In our experiments, we measured the release of Ca^{2+} from intracellular stores by monitoring cytosolic Ca^{2+} responses over time with the dye Fura-2/AM (270). In order to identify transfected cells in single cell imaging experiments, HEK-293 cells were co-transfected with mtRFP; untransfected cells in the same sample were used to compare changes in the 340/380 Fura-2/AM ratio. Treatment of untransfected or mock-transfected cells with 80 µM ArA caused a cytosolic Ca^{2+} elevation that gradually increased over time. Consistent with the impaired release of ER Ca^{2+} in response to agonists coupled to IP3 mobilization, the increase in cytosolic Ca^{2+} induced by ArA was markedly blunted in PTEN-silenced cells (Figures 24a and b). The overexpression of PTEN did not cause any difference in the release of Ca^{2+} evoked by ArA, while ER-PTEN significantly increased the cytosolic Ca^{2+} responses (Figures 24c and d). Overall, these experiments indicate that the absence of PTEN causes a reduction in the cytosolic Ca^{2+} rise elicited by the discharge of intracellular Ca^{2+}

stores after apoptotic stimuli. Moreover, we confirmed that ER-localized PTEN can enhance the Ca^{2+}-dependent death signalling.

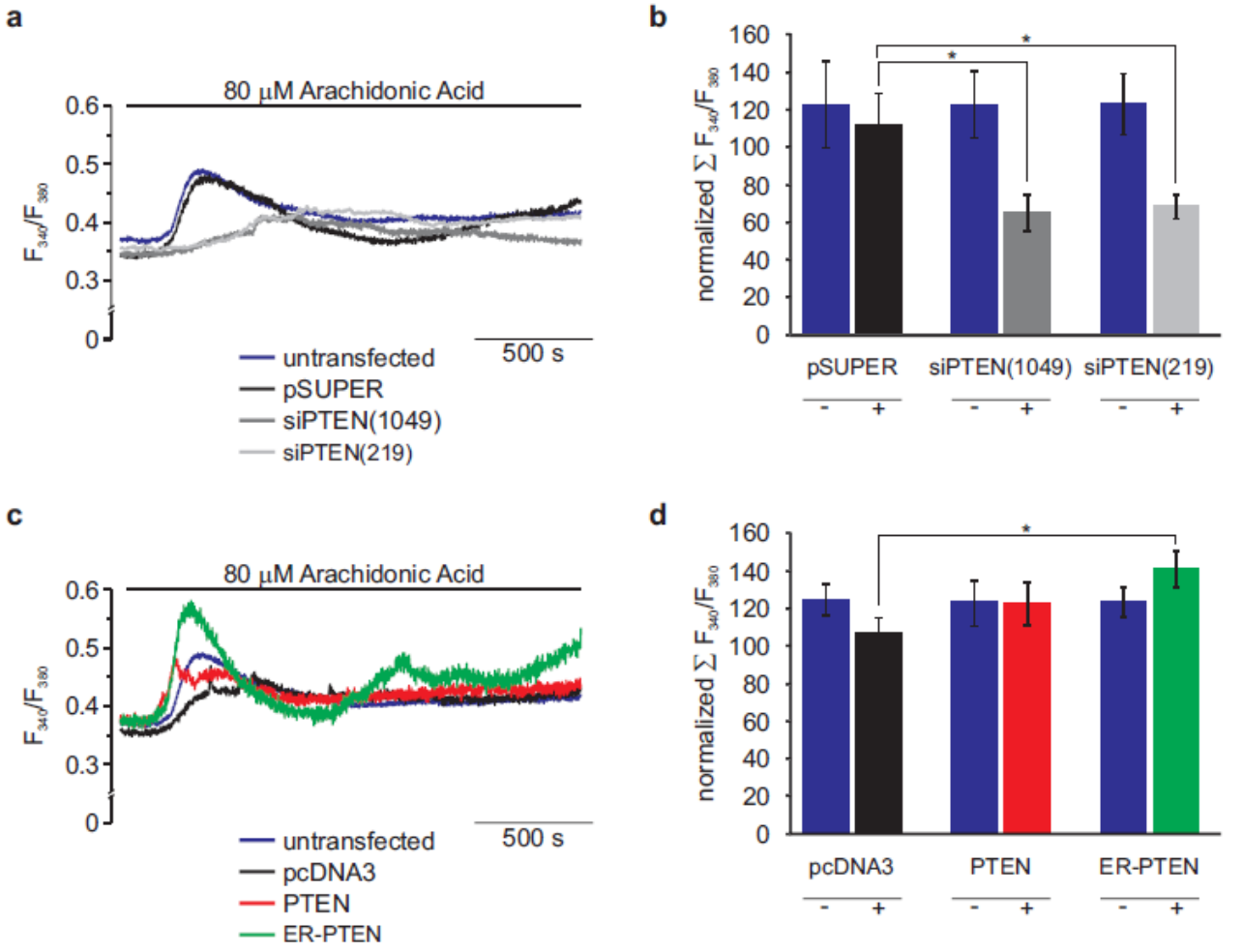

Figure 24. Effect of PTEN silencing or overexpression on cytosolic Ca^{2+} responses after exposure to 80 μM arachidonic acid. *HEK-293 cells were co-transfected with mtRFP and the indicated plasmid in a 1:1 ratio in order to distinguish transfected cells (positive). Untransfected cells (negative) were used to compare changes in the 340/380 Fura-2/AM ratio on the same sample as detailed in Materials and Methods. After loading with the Ca^{2+} indicator Fura-2/AM, cells were maintained in 1 mM Ca^{2+}/KRB and, where indicated, challenged with 80 μM ArA. The kinetics of the cytosolic Ca^{2+} response (**a** and **c**) are presented as the ratio of fluorescence at 340 nm/380 nm. In the bar graphs (**b** and **d**) every F_{340}/F_{380} value is normalized to the start value; the average of normalized $\Sigma(F_{340}/F_{380})$ over time in all the single cell imaging experiments performed was then calculated. (**a**) Representative traces of cytosolic Ca^{2+} responses in PTEN-silenced cells. (**b**) Statistics analysis of cytosolic Ca^{2+} increase in PTEN-silenced cells. Normalized $\Sigma(F_{340}/F_{380})$: pSUPER [negative 31.66 ± 5.94 (n=20 cells); positive 28.77 ± 4.43 (n=33 cells)]; siPTEN(1049) [negative 31.65 ± 4.60 (n=31 cells); positive 16.71 ± 2.51 (n=39 cells), $p < 0.05$ compared to pSUPER]; siPTEN(219) [negative 31.75 ± 4.17 (n=44 cells); positive 17.66 ± 1.62 (n=55 cells), $p < 0.05$ compared to pSUPER]. (**c**) Representative traces of cytosolic Ca^{2+} responses in cells overexpressing PTEN or targeted ER-PTEN chimera. (**d**) Statistics of cytosolic Ca^{2+} increase in PTEN or ER-PTEN overexpressing cells. Normalized $\Sigma(F_{340}/F_{380})$: pcDNA3 [negative 124.75 ± 8.50 (n=20 cells); positive 107.03 ± 8.56 (n=25 cells)]; PTEN [negative 123.13 ± 12.16 (n=18 cells); positive 123.01 ± 11.15 (n=24 cells)]; ER-PTEN [negative 123.62 ± 7.84 (n=26 cells); positive 141.14 ± 9.44 (n=36 cells), $p < 0.01$ compared to pcDNA3]. The traces and bar graphs are representative of at least three independent experiments that yielded similar results.*

Ca^{2+}-mediated apoptosis is prevented by PTEN silencing and enhanced through overexpression of ER-PTEN

ER-to-mitochondria Ca^{2+} transfer has been implicated in multiple models of apoptosis as being directly responsible for mitochondrial Ca^{2+} overload (142, 189), which sensitizes the organelle to apoptotic challenges and may result in the induction of cell death through PTP opening, mitochondria swelling and release of caspase cofactors (222). Previous studies have established that the reduction in the Ca^{2+} amount that can be released from the ER and accumulated in mitochondria decreases the probability of Ca^{2+}-dependent apoptosis (147, 194, 203, 206). Here, we tested whether PTEN, by affecting ER-mitochondria Ca^{2+} flux, could influence the apoptotic response to death stimuli that requires Ca^{2+} transfer between the two organelles. We used ArA since it triggers or enhances the release of Ca^{2+} from the ER and activates the intrinsic apoptotic pathway (143, 147, 269). The effects on cell fate were evaluated by monitoring the processing of effector caspase-3 into active cleaved caspase-3 fragments.

Immunoblot results showed that after ArA treatment a smaller amount of cleaved caspase-3 is present in PTEN-silenced cells than in control (mock-transfected) cells (Figures 25a and c). This indicates that the reduction of ER Ca^{2+} release observed in PTEN-silenced cells increases the threshold for Ca^{2+}-mediated apoptosis. After ArA treatment, cells also displayed a downregulation of PTEN expression in comparison to vehicle-treated cells, probably because during apoptotic cell death PTEN is cleaved by active caspase-3 (271, 272). We found a greater downregulation of PTEN expression in PTEN-silenced cells than in control cells, most likely due to their preferential survival (Figure 25b). Overexpression of wild type PTEN was unable to sensitize HEK-293 cells to ArA-induced apoptosis; indeed, the levels of cleaved caspase-3 were comparable to those observed in control cells (Figures 25d and f). Moreover, the reduction in PTEN protein levels is comparable to that observed in control cells (Figure 25e). Conversely, in cells overexpressing ER-PTEN, the sensitivity to apoptosis after ArA treatment was enhanced as indicated by the increased levels of cleaved caspase-3. These cells also displayed a greater reduction of PTEN levels, most likely due to increased apoptosis (Figures 25d-f).

In conclusion, ER-localized PTEN sensitizes cells to apoptotic death by stimuli that require Ca^{2+} transfer from ER to mitochondria.

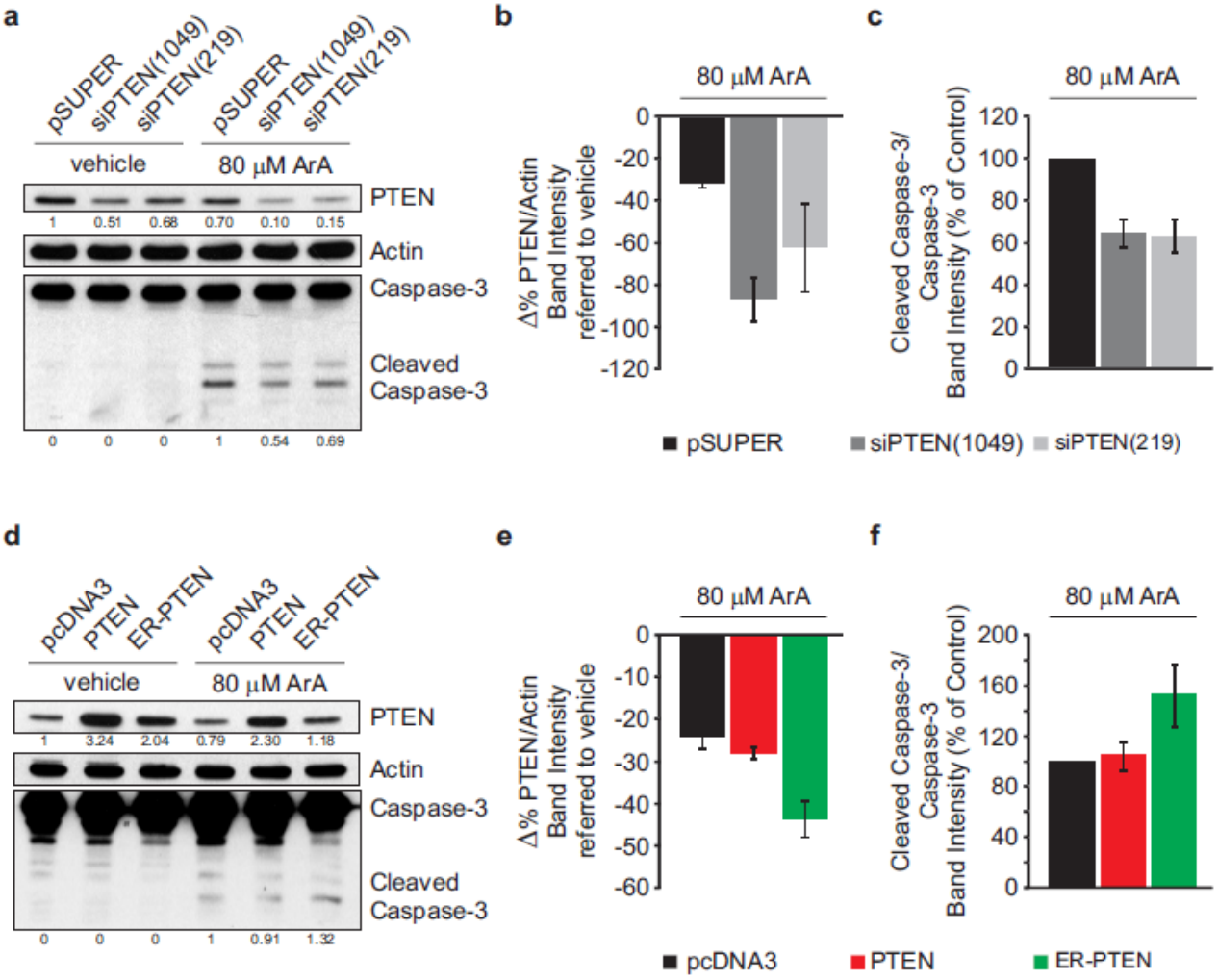

Figure 25. Effect of PTEN silencing or overexpression on sensitivity to Ca^{2+}-dependent apoptosis. *HEK-293 cells were transfected with PTEN siRNAs,mPTEN, ER-PTEN or the respective empty vector; 36 h after transfection the cells were treated with 80 μM arachidonic acid (ArA) or vehicle (EtOH) for 90 min; cell lysates were then prepared and analyzed by immunoblotting. Membranes were probed with antibodies against PTEN, actin and caspase-3 proteins. Representative immunoblots (**a** and **d**) from three independent experiments are shown. Numbers indicate densitometrically determined protein levels relative to actin for PTEN and to caspase-3 (35 kDa) for cleaved caspase-3 (17 kDa). The bar graphs show mean ± s.e.m. from densitometric analysis of normalized PTEN (**b** and **e**) and cleaved caspase-3 (**c** and **f**) protein levels. (**a**) PTEN silencing reduces caspase-3 activation after ArA challenge. (**b**) Reduction in PTEN expression compared to vehicle, in PTEN-silenced cells. Δ% PTEN/Actin: pSUPER –31.2 ± 2.1%; siRNA-PTEN(1049) –87.0 ± 10.3%; siRNA-PTEN(219) –62.4 ± 20.9%. (**c**) Caspase-3 activation expressed as percentage of control (mock-transfected) cells, after PTEN silencing. Cleaved caspase-3/caspase-3 band intensity: siRNA-PTEN(1049) 64.3 ± 6.7%, siRNA-PTEN(219) 63.0 ± 7.9%, vs control cells 100%. (**d**) ER-PTEN enhanced caspase-3 activation after ArA challenge. (**e**) Reduction in PTEN expression compared to vehicle, in cells overexpressing PTEN or ER-PTEN. Δ% PTEN/Actin: pcDNA3 –24.1 ± 2.8%; PTEN –28.0 ± 1.4%; ER-PTEN –43.6 ± 4.3%. (**f**) Caspase-3 activation expressed as percentage of control (mock-transfected) cells, after overexpression of PTEN or ER-PTEN. Cleaved caspase-3/caspase-3 band intensity: PTEN 104.5 ± 11.2%, ER-PTEN 152.3 ± 24.3%, vs control cells 100%.*

Discussion

PTEN is a phosphatase whose main tumour suppressor activity is likely to be caused by dephosphorylation of the lipid second messenger PIP3, which accumulates at the plasma membrane upon activation of PI3K (273). Even though PTEN has multiple domains for membrane association, in most mammalian cell types it does not show an obvious association with the plasma membrane (274). Differing results show PTEN localization distributed between cytosol and nucleus and there is evidence that it could operate as a tumour suppressor in both these compartments (275). PTEN could also accumulate in mitochondria in cells undergoing apoptosis and is implicated in the regulation of the intrinsic apoptotic pathway (267, 268). These findings highlight the importance of PTEN's subcellular localization in regulating its function and point out the possibility that different tumour-suppressive mechanisms of action may occur in well-defined cellular compartments.

In this part of the PhD project, we investigated in greater detail the intracellular distribution of PTEN using an established fractionation protocol (160). Our results showed that, in addition to cytosolic, nuclear and mitochondrial pools, PTEN is also present in the ER and MAMs. Since a major area of functional interaction between the ER and mitochondria is the control of Ca^{2+} signalling, and growing evidence indicates that the Ca^{2+} uptake into mitochondria is controlled by specific proteins residing at the ER and MAMs (see Introduction, section 1.7), our finding raises the possibility that PTEN could act as a tumour suppressor, at least in part, by modulating the transmission of Ca^{2+} from the ER to mitochondria. We confirm this possibility by showing a reduction in the kinetics of Ca^{2+} release from the ER in PTEN-silenced cells, that significantly blunted also the cytosolic and the mitochondrial Ca^{2+} responses. Previous experiments ruled out the possibility that our results could be a consequence of decreased production of IP3 on phospholipase C activation (276, 277). To outline the functional relevance of PTEN localization in the ER and MAMs in modulating Ca^{2+} signalling, we generated an ER-targeted PTEN chimera and demonstrated that its transient overexpression significantly increased the agonist-induced mitochondrial Ca^{2+} transient, which is a proximal sensor of Ca^{2+} release through IP3Rs (30), while wild-type PTEN overexpression had no effect. We concluded that PTEN's regulation of Ca^{2+} homeostasis relied specifically on its localization in the ER and MAMs.

Ca^{2+} signalling is an important regulator of both cell proliferation and apoptosis (5). Broad evidence has established that mitochondrial Ca^{2+} loading favours apoptosis; reducing or increasing the Ca^{2+} amount that can be released from the ER to mitochondria protects from or enhances apoptosis, respectively (see Introduction, section 1.6). There is an increasing number of reports supporting the

role of Ca^{2+} signalling remodelling for cancer cell proliferation and survival (3). Our results confirm this possibility for PTEN, as decreased release of Ca^{2+} from the ER in PTEN-silenced cells accounts for reduced sensitivity to apoptosis. Moreover, we demonstrated that only ER-localized PTEN is able to increase ER Ca^{2+} release in response to ER death stimuli, in turn engaging mitochondria in a Ca^{2+}-dependent apoptotic process. Therefore, PTEN in the ER and MAMs is critical for cell death regulation by this tumour suppressor, and loss of PTEN function could limit apoptosis-inducing Ca^{2+} signals during cancer. The tumour-suppressive function of PTEN at the ER and MAMs can also explain why the E307K mutation in MDA-MB-453 breast carcinoma cell line lead to higher PTEN plasma membrane localization which confers a greater ability in suppressing pAkt levels (278); it is possible that this mutation results in the inability of PTEN to be targeted to the ER and MAMs, and so limits Ca^{2+}-dependent death signalling.

At present, the precise molecular mechanism by which PTEN localizes to the ER and MAMs, and regulates ER-to-mitochondria Ca^{2+} transport remains unclear, but several possibilities exist (Figure 26). The major site of PIP2 and PIP3 accumulation is the plasma membrane. Lindsay et al. estimated that intracellular membranes accounted for no more than 10-20% of total PIP3 and suggest that PTEN is only active as a lipid phosphatase when targeted to plasma membranes (279). However, both PIP2 (280, 281) and PIP3 (282) have been detected in intracellular organelles including the ER, and Sato emphasized how signalling pathways downstream of PIP3, including Akt, are activated at intracellular compartments remote from the plasma membrane. This could explain both recruitment and potential functional consequence of PTEN in the ER, since PTEN association with membranes depends on their composition, in particular on the presence of PIP2 (283, 284). Since PTEN is known to be involved in forming gradients of PIP3 necessary for sustaining cell polarity during motility (285), our data suggests that it could function in a spatially restricted manner and regulate PIP2/PIP3 turnover for generating microdomains of activated Akt on the ER surface. In this way, PTEN may modulate Akt-dependent phosphorylation of IP3Rs, which reduced their Ca^{2+} release activity (66, 146, 147), through the efficient localization to specific ER and MAMs sites where its activity is needed. However, there are also other possibilities that we cannot exclude at present. PTEN also possesses multiple biological functions independent of its lipid phosphatase activity. It is likely that it exerts such functions by protein-protein interaction or by its protein phosphatase activity. A number of PTEN-interacting proteins are known (286), including PP2a (287), PML (241) and PP1 (288). All these proteins are also known interactors and functional modulators of IP3R phosphorylation and, in turn, regulate IP3R-mediated Ca^{2+} release from the ER (206, 289). Several possibilities exist regarding these PTEN-interacting proteins: (i)

they could associate with a subpopulation of PTEN to guide it to the ER and MAMs and thus to a specific target; (ii) they could regulate PTEN function, including its enzymatic activity, or conversely (iii) PTEN could regulate the function of this binding partners; (iv) moreover, since several substrates for PTEN's protein phosphatase activity have been proposed, it could also act in the ER and MAMs as a protein phosphatase on still unidentified substrates. Future experiments will be required to determine the precise molecular mechanism by which ER- and MAMs-localized PTEN controls Ca^{2+} flux from the ER to mitochondria.

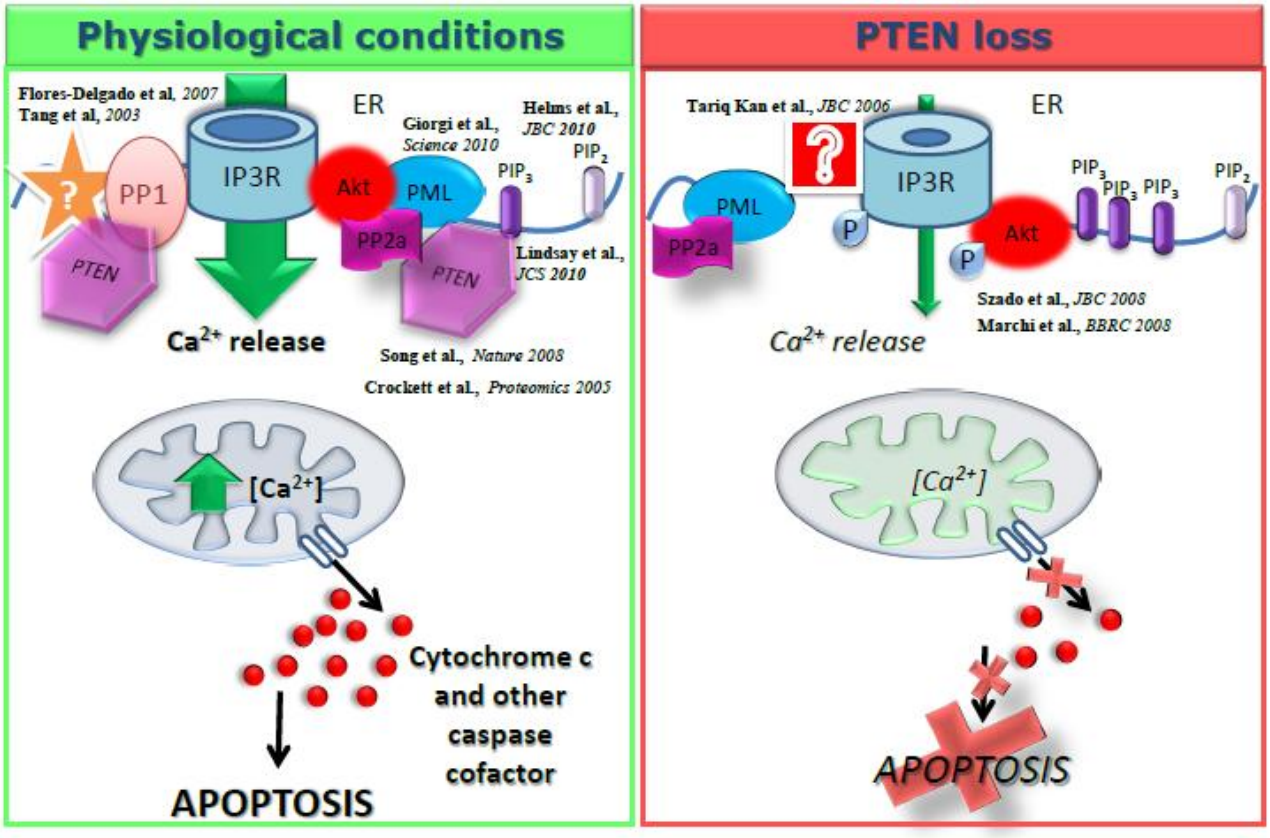

Figure 26. PTEN effects on Ca^{2+} homeostasis: schematic model of the possible molecular mechanisms.

PTEN is a multifunctional protein that, in addition to its canonical PIP3 phosphatase-dependent functions, can exert multiple biological functions at the same time. Several findings suggest that the subcellular localization of PTEN may be a regulatory mechanism for separating certain specific functions simultaneously conducted in the same cells (263, 265). Overall, the data presented in this thesis reveal that a subpopulation of PTEN is localized at the ER-MAMs interface with mitochondria, where it regulates the ER-mitochondria interorganelle Ca^{2+} signalling and exerts a

pro-apoptotic activity. This novel function may integrate its previously reported roles in tumour suppression and serve as a novel strategy for targeted therapeutic intervention.

4.MATERIALS AND METHODS:

Cells culture and Transfection

HeLa and HEK-293 cells were grown in Dulbecco's modified Eagle's medium (DMEM) (Euroclone), supplemented with 10% fetal bovine serum (FBS). Primary MEFs were prepared from embryos at day 13.5 of development (E13.5). Early passage (P2–P5) MEFs were grown in DMEM supplemented with 10% FCS. HEK-293 cells were seeded 48 h before transfection onto glass coverslips coated with poly-L-lysine (Sigma), 13-mm in diameter for aequorin experiments, or 24-mm for Fura-2/AM measurements and immunofluorescence. For immunoblot and cell death experiments, cells were seeded on 10-cm Petri dishes or 24-mm coverlip.

HeLa and HEK-293 cells were allowed to grow to 50% confluence, transfected with a standard calcium-phosphate procedure and used in the experiments 36 h post-transfection. MEFs were transfected with different constructs using the MicroPorator (Digital Bio).

Plasmid cloning

For selective VDAC silencing several sequences were cloned and tested for specific silencing efficiency without upregulation of the other isoforms. The most effective sequences were: 50-AAGCGGGAGCACATTAACCTG-30 for hVDAC1; 50-AAGGATGATCTCAACAAGAGC-30 for hVDAC2; 50-AAGGGTGGCTTGCTGGCTATC-30 for hVDAC3. To silence PTEN specific siRNA were designed: siPTEN(1049): nucleotides 1049–1067 of the corresponding mRNA (5'-AGTAGAGGAGCCGTCAAAT-3'); siPTEN(219): nucleotides 219–237 of the corresponding mRNA (5'-AGACATTATGACACCGCCA-3'). Oligonucleotides containing the selected sequences were purchased from Sigma-Aldrich and cloned into pSUPER (Oligoengine) according to the manufacturer's instructions.

ErPML chimera was addressed to the external surface of ER by fusing sequence from the yeast UBC6 protein (245) to the C-terminal end of the human PML isoform IV.

Human PTEN was cloned into pcDNA3 (Invitrogen) and PTEN chimeras were targeted to the external surface of the ER by fusing sequences from UBC6 (ER-PTEN) (245) or cytochrome b5 (Cb5) (Cb5-PTEN) (290) to the N-terminus of PTEN.

Subcellular Fractionation

Subcellular fractionation of cells and Percoll purification of MAMs were performed as described previously (160, 206).

Briefly, cells (10^9) were harvested, washed by centrifugation at 500 g for 5 min with PBS, resuspended in homogenization buffer (225 mM mannitol, 75 mM sucrose, 30 mM Tris-HCl pH 7.4, 0.1 mM EGTA, and PMSF) and gently disrupted by dounce homogenisation. The homogenate was centrifuged twice at 600 g for 5min to remove nuclei and unbroken cells, and then the supernatant was centrifuged at 10,300 g for 10 min to pellet crude mitochondria. The resultant supernatant was centrifuged at 100,000 g for 90 min (70-Ti rotor, Beckman) at 4 °C to pellet the ER fraction. The crude mitochondrial fraction, resuspended in isolation buffer (250 mM mannitol, 5 mM HEPES pH 7.4 and 0.5 mM EGTA), was subjected to Percoll gradient centrifugation (Percoll medium: 225 mM mannitol, 25 mM HEPES pH 7.4, 1 mM EGTA and 30% vol/vol Percoll) in a 10-ml polycarbonate ultracentrifuge tube. After centrifugation at 95,000 g for 30 min a dense band containing purified mitochondria was recovered approximately at the bottom of the gradient (and further processed as described in (160)), whereas MAMs was retrieved as a diffuse white band located above the mitochondria. MAMs were diluted in isolation buffer and centrifuged at 6,300 g for 10 min. To pellet the MAMs fraction the supernatant was centrifuged at 100,000 g for 90 min (70-Ti rotor, Beckman) at 4 °C.

Co-immunoprecipitation

Co-immunoprecipitations were carried out by using protein A- or protein G-coated sepharose beads (GE Healthcare) following manufacturer's instructions. Different protein extraction buffers were used in order to minimize non-specific binding while maximizing antigen extraction. IP3R3 and IP3R1 were extracted in a modified RIPA buffer (150mM NaCl, 1% NP-40, 0.05% SDS, Tris 50 mM, pH=8) while HA and grp75 were purified in a NP-40 buffer (150mM NaCl, 1% NP-40, Tris 50 mM, pH=8), all supplemented with proteases and phosphatases inhibitors (2 mM Na_3VO_4, 2 mM NaF, 1 mM PMSF and Protease Inhibitor Cocktail). Extracted proteins (700 μg) were first precleared by incubating lysates with sepharose beads for 1 h at 4 °C and the supernatant (referred as Input) was incubated overnight with the antibody at 4 °C. Precipitation of the immune complexes was carried for 2 h at 4 °C and washed three times with the extraction buffer.

Pml$^{+/+}$ and *Pml*$^{-/-}$ MEFs extracts were prepared using lysis buffer containing: 50 mM NaCl, 50 mM Tris-HCl pH 7.4, 0.1% NP-40 supplemented with 1 mM PMSF and proteases/phosphatases inhibitors. Protein extracts were pre-cleared with protein G/A beads (Pierce) than precipitated with

IP3R3, PML, Akt and PP2a antibodies overnight at 4°C. Protein G beads were added and rocked 5 hours at 4°C. Afterwards, beads were washed with 50 mM NaCl, 50 mM Tris-HCl pH 7.4, 0.1% NP-40 4°C.

Samples were proceed by SDS-PAGE and analyzed by standard mmunoblot technique.

Immunoblot

Total cell lysates were prepared in RIPA buffer (50 mM Tris-HCl pH 7.8, 150 mM NaCl, 1% IGEPAL CA-630, 0.5% sodium deoxycholate, 0.1% SDS, 1 mM DTT) supplemented with proteases and phosphatases inhibitors (2 mM Na_3VO_4, 2 mM NaF, 1 mM PMSF and Protease Inhibitor Cocktail). Proteins (30 μg) were quantified using the Bradford assay (Bio-Rad Laboratories), separated by SDS-PAGE and transferred to nitrocellulose membranes for standard western blotting. Antibodies were purchased from the following sources and used at the indicated dilutions: PTEN (1:1000), Akt (1:1000), $pAkt^{Ser473}$ (1:500), Caspase-3 (1:250) and PARP (1:2000) from Cell Signaling; actin (1:5000), β–tubulin (1:3000) and αHA (1:5000) from Sigma-Aldrich; αIP3R3 (1:250) from BD Biosciences; FACL4 (1:250), HK-I (1:1000) and grp75 (1:10 000) from Santa Cruz; lamin B1 (1:1000), αVDAC2 (1:1000), αVDAC3 (1:1000) and αIP3R1 (1:1000) from Abcam, αVDAC1 (1:10 000) from Calbiochem, anti-hPML (1:1000), anti-PML (1:1000) from Chemicon.

Densitometric analysis of protein levels were performed with ImageJ software .

Immunofluorescence

MEFs were fixed in 4% paraformaldehyde in PBS for 15 min, washed three times with PBS, permeabilized for 10 min with 0.1% Triton X-100 in PBS and blocked in PBS containing 1% BSA for 20 min. Cells were then incubated O/N at 4°C in a wet chamber with the following antibodies: anti-PML (H-238, Santa Cruz) for erPML, or with the anti-PML (for endogenous PML), anti-FACL, anti-PP2a, dilute 1:100 with 2% BSA in PBS. Staining was then carried out with Alexa 488 anti-rabbit for hPML (erPML), with Alexa 488 anti-mouse for Pml, with Alexa 543 anti-rabbit for PP2a and with Alexa 633 anti-goat for FACL secondary antibodies.

HEK-293 cells were grown on 24-mm coverslips and co-transfected with 4 μg of the indicated plasmids and 4 μg of erGFP. After 36 h, cells were fixed, washed, permeabilized and blocked in PBS containing 1% BSA for 20 min (as described above). Cells were then incubated O/N at 4°C with the PTEN antibody (1:100), and subsequent staining was carried out with AlexaFluor-conjugated 546 (Invitrogen).

After each antibody incubation, cells were washed three times with 0.1% Triton X-100 in PBS. Samples were mounted in ProLong Gold antifade (Invitrogen) and images were obtained by high-speed confocal fluorescence microscopy (Nikon LiveScan Swept Field Confocal Microscope).

Immunoelectron microscopy

MEF cells are fixed with 2% paraformaldehyde and 0.2% glutaraldehyde in PBS, embedded in 12% gelatin, 2,3 M sucrose and frozen in liquid nitrogen. Ultrathin cryosections, obtained by a Reichert-Jung Ultracut E with FC4E cryoattachment, were collected on copper-formvar-carbon-coated grids. Immunogold localization was revealed using the PML Chemicon antibody for endogenous mouse PML and PML (H-238) Santa Cruz for erPML chimera, and 10 nm proteinA-gold conjugated, according published protocols (291, 292). All samples were examined in a Philips CM10 or a FEI Tecnai 12G2 electron microscopes.

Aequorin measurements

Cells grown on 13-mm round glass coverslips were co-transfected with 1 μg of aequorin (erAEQmut, cytAEQ, or mtAEQ) and 3 μg of the indicated siRNA or plasmid. After 36 h, cells were reconstituted and placed in a perfused thermostated chamber where the light signal was collected in a purpose-built luminometer and calibrated into $[Ca^{2+}]$ values as previously described (244). For $[Ca^{2+}]_{er}$ measurements in HeLa and MEF cells, erAEQmut-transfected cells were reconstituted with coelenterazine n, following ER Ca^{2+} depletion in a solution containing 0 $[Ca^{2+}]$, 500 μM EGTA, 1 μM ionomycin, as previously described. After three washes with KRB supplemented with 2% BSA and 1 mM EGTA, cells were perfused with Krebs-Ringer buffer (KRB: 135 mM NaCl, 5 mM KCl, 1 mM $MgSO_4$, 0.4 mM KH_2PO_4, 5.5 mM glucose, 20 mM HEPES, pH 7.4) containing 100 μM EGTA. HEK-293 cells transfected with erAEQmut were reconstituted with coelenterazine n (Tebu-Bio), after ER Ca^{2+} depletion by incubating cells for 1 h at 4°C in KRB supplemented with 100 μM EGTA, and 40 μM tBHQ (2,5-Di-*tert*-butylhydroquinone) (Sigma); cells were then washed with KRB supplemented with 2% BSA and 1 mM EGTA. ER refilling was then triggered by perfusing KRB buffer supplemented with 1mM $CaCl_2$ until equilibrium (steady state) was reached. Cells transfected with cytAEQ and mtAEQ were reconstituted with coelenterazine (Synchem) for 2 h in KRB supplemented with 1 mM $CaCl_2$. All aequorin measurements were carried out in 1 mM Ca^{2+}/KRB (cytAEQ and mtAEQ) or 100 μM EGTA/KRB (erAEQmut). Agonist was added to the same medium, as specified in the figures. The

experiments were concluded by lysing the cells with 100 μM digitonin in a hypotonic Ca^{2+}-rich solution (10 mM $CaCl_2$ in H_2O).

Fura-2/AM measurements

Cytosolic Ca^{2+} response was evaluated using the fluorescent Ca^{2+} indicator Fura-2/AM (Invitrogen). Cells were grown on 24-mm coverslips and co-transfected with 4 μg of the indicated siRNA or plasmid and 4 μg of mtRFP. After 36 h, cells were incubated at 37°C for 30 min in 1 mM Ca^{2+}/KRB supplemented with 2.5 μM Fura-2/AM, 0.02% Pluronic F-68 (Sigma), 0.1 mM Sulfinpyrazone (Sigma). Cells were then washed and supplied with 1 mM Ca^{2+}/KRB. To determine cytosolic Ca^{2+} response cells were placed in an open Leyden chamber on a 37°C thermostatted stage and exposed to 340/380 wavelength light using the Olympus xcellence multiple wavelength high-resolution fluorescence microscopy system. The fluorescence data collected were expressed as emission ratios.

Induction of Apoptosis

HeLa cells grown on 24-mm coverlip at 30% confluence were co-transfected with GFP and control or siRNA-hVDACs containing plasmids in a 1:1 ratio. The effect on cell fate was evaluated by applying an apoptotic challenge (20 μM C2-ceramide or 100 μM H_2O_2) and comparing the survival of transfected and non-transfected cells. In these experiments, the percentage of GFP-positive cells was calculated before and after applying an apoptotic stimulus (C2-ceramide or H_2O_2). In mock-transfected cells, although the total number of cells is reduced after cell death induction, the apparent transfection efficiency was maintained (i.e., transfected and nontransfected cells have the same sensitivity to the apoptotic stimulus and thus die to the same extent). However, when cells are transfected with a construct influencing their sensitivity to apoptosis, this will be reflected by a change in the fraction of fluorescent cells, that is, in the 'apparent' transfection efficiency. Thus, protection from apoptosis results into an apparent increase of transfection, whereas a decrease reflects a higher sensitivity to apoptosis. Data are reported as the mean percentage change in the apparent transfection efficiency after apoptotic challenge compared with vehicle-treated cells. Cells were extensively washed with PBS, stained with DAPI, and two images per field (blue and green fluorescence) were taken at × 10 magnification (mean transfection efficiency were roughly 30% for all conditions). At least 10 fields per coverslip were randomly imaged and counted. Data presented are the sum of at least two different wells per experimental condition carried out in three different independent experiments.

MEFs *Pml*$^{+/+}$ and *Pml*$^{-/-}$ apoptosis was determined by FACS analysis of cells stained with Annexin-V FITC/Propidium Iodide (BioVision). For cell death induction cells were treated as indicated in the text with 1 mM H_2O_2, 15 μM MEN, 6 μM TN, 2 μM TG and 50 μM ETO in DMEM, supplemented with 10% FCS.

HEK-293 cells were grown on 10-cm Petri dishes and transfected with the indicated siRNA, plasmid or empty vector. After 36 h, cells were washed and growth media was replaced with 1 mM Ca^{2+}/KRB containing 80 μM arachidonic acid (ArA) (Santa Cruz) for 90 min. Cells in the media were retained and pooled with remaining adherent cells that were harvested by scraping, collected by centrifugation at 200 *g* for 5 min and lysed as described above.

Statistical analyses

Statistical analyses were performed using Student's t-test. A *p*-value ≤ 0.05 was considered significant. All data are reported as mean ± s.e.m., or means ± SD where indicated.

REFERENCES:

1. Berridge MJ, Lipp P, Bootman MD. The versatility and universality of calcium signalling. Nat Rev Mol Cell Biol. 2000;1(1):11-21. Epub 2001/06/20.

2. Rizzuto R, Pozzan T. When calcium goes wrong: genetic alterations of a ubiquitous signaling route. Nat Genet. 2003;34(2):135-41. Epub 2003/05/31.

3. Roderick HL, Cook SJ. Ca2+ signalling checkpoints in cancer: remodelling Ca2+ for cancer cell proliferation and survival. Nat Rev Cancer. 2008;8(5):361-75. Epub 2008/04/25.

4. Berridge MJ, Bootman MD, Roderick HL. Calcium signalling: dynamics, homeostasis and remodelling. Nat Rev Mol Cell Biol. 2003;4(7):517-29. Epub 2003/07/03.

5. Rizzuto R, Marchi S, Bonora M, Aguiari P, Bononi A, De Stefani D, et al. Ca(2+) transfer from the ER to mitochondria: when, how and why. Biochim Biophys Acta. 2009;1787(11):1342-51. Epub 2009/04/04.

6. Brini M, Carafoli E. Calcium pumps in health and disease. Physiol Rev. 2009;89(4):1341-78. Epub 2009/10/01.

7. Blaustein MP, Lederer WJ. Sodium/calcium exchange: its physiological implications. Physiol Rev. 1999;79(3):763-854. Epub 1999/07/03.

8. Bertolino M, Llinas RR. The central role of voltage-activated and receptor-operated calcium channels in neuronal cells. Annu Rev Pharmacol Toxicol. 1992;32:399-421. Epub 1992/01/01.

9. McFadzean I, Gibson A. The developing relationship between receptor-operated and store-operated calcium channels in smooth muscle. Br J Pharmacol. 2002;135(1):1-13. Epub 2002/01/12.

10. Meldolesi J, Pozzan T. Pathways of Ca2+ influx at the plasma membrane: voltage-, receptor-, and second messenger-operated channels. Exp Cell Res. 1987;171(2):271-83. Epub 1987/08/01.

11. Foskett JK, White C, Cheung KH, Mak DO. Inositol trisphosphate receptor Ca2+ release channels. Physiol Rev. 2007;87(2):593-658. Epub 2007/04/13.

12. Sutko JL, Airey JA. Ryanodine receptor Ca2+ release channels: does diversity in form equal diversity in function? Physiol Rev. 1996;76(4):1027-71. Epub 1996/10/01.

13. Patel S, Joseph SK, Thomas AP. Molecular properties of inositol 1,4,5-trisphosphate receptors. Cell Calcium. 1999;25(3):247-64. Epub 1999/06/23.

14. Patterson RL, Boehning D, Snyder SH. Inositol 1,4,5-trisphosphate receptors as signal integrators. Annu Rev Biochem. 2004;73:437-65. Epub 2004/06/11.

15. Berridge MJ. Calcium microdomains: organization and function. Cell Calcium. 2006;40(5-6):405-12. Epub 2006/10/13.

16. Berridge MJ. Inositol trisphosphate and calcium signalling mechanisms. Biochim Biophys Acta. 2009;1793(6):933-40. Epub 2008/11/18.

17. John LM, Lechleiter JD, Camacho P. Differential modulation of SERCA2 isoforms by calreticulin. J Cell Biol. 1998;142(4):963-73. Epub 1998/08/29.

18. Varnai P, Hunyady L, Balla T. STIM and Orai: the long-awaited constituents of store-operated calcium entry. Trends Pharmacol Sci. 2009;30(3):118-28. Epub 2009/02/04.

19. Saris NE, Carafoli E. A historical review of cellular calcium handling, with emphasis on mitochondria. Biochemistry (Mosc). 2005;70(2):187-94. Epub 2005/04/06.

20. Pinton P, Pozzan T, Rizzuto R. The Golgi apparatus is an inositol 1,4,5-trisphosphate-sensitive Ca2+ store, with functional properties distinct from those of the endoplasmic reticulum. EMBO J. 1998;17(18):5298-308. Epub 1998/09/16.

21. Mitchell KJ, Pinton P, Varadi A, Tacchetti C, Ainscow EK, Pozzan T, et al. Dense core secretory vesicles revealed as a dynamic Ca(2+) store in neuroendocrine cells with a vesicle-associated membrane protein aequorin chimaera. J Cell Biol. 2001;155(1):41-51. Epub 2001/09/26.

22. Rodriguez A, Webster P, Ortego J, Andrews NW. Lysosomes behave as Ca2+-regulated exocytic vesicles in fibroblasts and epithelial cells. J Cell Biol. 1997;137(1):93-104. Epub 1997/04/07.

23. Gerasimenko JV, Tepikin AV, Petersen OH, Gerasimenko OV. Calcium uptake via endocytosis with rapid release from acidifying endosomes. Curr Biol. 1998;8(24):1335-8. Epub 1998/12/09.

24. Drago I, Giacomello M, Pizzo P, Pozzan T. Calcium dynamics in the peroxisomal lumen of living cells. J Biol Chem. 2008;283(21):14384-90. Epub 2008/03/26.

25. Lasorsa FM, Pinton P, Palmieri L, Scarcia P, Rottensteiner H, Rizzuto R, et al. Peroxisomes as novel players in cell calcium homeostasis. J Biol Chem. 2008;283(22):15300-8. Epub 2008/03/28.

26. Rizzuto R, Pozzan T. Microdomains of intracellular Ca2+: molecular determinants and functional consequences. Physiol Rev. 2006;86(1):369-408. Epub 2005/12/24.

27. Carafoli E. Historical review: mitochondria and calcium: ups and downs of an unusual relationship. Trends Biochem Sci. 2003;28(4):175-81. Epub 2003/04/26.

28. Mitchell P. Chemiosmotic coupling in oxidative and photosynthetic phosphorylation. Biol Rev Camb Philos Soc. 1966;41(3):445-502. Epub 1966/08/01.

29. Rizzuto R, Simpson AW, Brini M, Pozzan T. Rapid changes of mitochondrial Ca2+ revealed by specifically targeted recombinant aequorin. Nature. 1992;358(6384):325-7. Epub 1992/07/23.

30. Rizzuto R, Brini M, Murgia M, Pozzan T. Microdomains with high Ca2+ close to IP3-sensitive channels that are sensed by neighboring mitochondria. Science. 1993;262(5134):744-7. Epub 1993/10/29.

31. Csordas G, Thomas AP, Hajnoczky G. Quasi-synaptic calcium signal transmission between endoplasmic reticulum and mitochondria. EMBO J. 1999;18(1):96-108. Epub 1999/01/07.

32. Palmer AE, Tsien RY. Measuring calcium signaling using genetically targetable fluorescent indicators. Nat Protoc. 2006;1(3):1057-65. Epub 2007/04/05.

33. Rizzuto R, Pinton P, Carrington W, Fay FS, Fogarty KE, Lifshitz LM, et al. Close contacts with the endoplasmic reticulum as determinants of mitochondrial Ca2+ responses. Science. 1998;280(5370):1763-6. Epub 1998/06/20.

34. Giacomello M, Drago I, Bortolozzi M, Scorzeto M, Gianelle A, Pizzo P, et al. Ca2+ hot spots on the mitochondrial surface are generated by Ca2+ mobilization from stores, but not by activation of store-operated Ca2+ channels. Mol Cell. 2010;38(2):280-90. Epub 2010/04/27.

35. Palmer AE, Giacomello M, Kortemme T, Hires SA, Lev-Ram V, Baker D, et al. Ca2+ indicators based on computationally redesigned calmodulin-peptide pairs. Chem Biol. 2006;13(5):521-30. Epub 2006/05/25.

36. Csordas G, Varnai P, Golenar T, Roy S, Purkins G, Schneider TG, et al. Imaging interorganelle contacts and local calcium dynamics at the ER-mitochondrial interface. Mol Cell. 2010;39(1):121-32. Epub 2010/07/07.

37. Inoue T, Heo WD, Grimley JS, Wandless TJ, Meyer T. An inducible translocation strategy to rapidly activate and inhibit small GTPase signaling pathways. Nat Methods. 2005;2(6):415-8. Epub 2005/05/24.

38. Voeltz GK, Prinz WA, Shibata Y, Rist JM, Rapoport TA. A class of membrane proteins shaping the tubular endoplasmic reticulum. Cell. 2006;124(3):573-86. Epub 2006/02/14.

39. Shibata Y, Voeltz GK, Rapoport TA. Rough sheets and smooth tubules. Cell. 2006;126(3):435-9. Epub 2006/08/12.

40. English AR, Zurek N, Voeltz GK. Peripheral ER structure and function. Curr Opin Cell Biol. 2009;21(4):596-602. Epub 2009/05/19.

41. Shibata Y, Shemesh T, Prinz WA, Palazzo AF, Kozlov MM, Rapoport TA. Mechanisms determining the morphology of the peripheral ER. Cell. 2010;143(5):774-88. Epub 2010/11/30.

42. Chevet E, Cameron PH, Pelletier MF, Thomas DY, Bergeron JJ. The endoplasmic reticulum: integration of protein folding, quality control, signaling and degradation. Curr Opin Struct Biol. 2001;11(1):120-4. Epub 2001/02/17.

43. Palade G. Intracellular aspects of the process of protein synthesis. Science. 1975;189(4200):347-58. Epub 1975/08/01.

44. Bootman MD, Petersen OH, Verkhratsky A. The endoplasmic reticulum is a focal point for co-ordination of cellular activity. Cell Calcium. 2002;32(5-6):231-4. Epub 2003/01/25.

45. Verkhratsky A, Petersen OH. The endoplasmic reticulum as an integrating signalling organelle: from neuronal signalling to neuronal death. Eur J Pharmacol. 2002;447(2-3):141-54. Epub 2002/08/02.

46. Jobsis FF, O'Connor MJ. Calcium release and reabsorption in the sartorius muscle of the toad. Biochem Biophys Res Commun. 1966;25(2):246-52. Epub 1966/10/20.

47. Ridgway EB, Ashley CC. Calcium transients in single muscle fibers. Biochem Biophys Res Commun. 1967;29(2):229-34. Epub 1967/10/26.

48. Ashley CC, Ridgway EB. On the relationships between membrane potential, calcium transient and tension in single barnacle muscle fibres. J Physiol. 1970;209(1):105-30. Epub 1970/07/01.

49. MacKrill JJ. Protein-protein interactions in intracellular Ca2+-release channel function. Biochem J. 1999;337 (Pt 3):345-61. Epub 1999/01/23.

50. Rebecchi MJ, Pentyala SN. Structure, function, and control of phosphoinositide-specific phospholipase C. Physiol Rev. 2000;80(4):1291-335. Epub 2000/10/04.

51. Litjens T, Nguyen T, Castro J, Aromataris EC, Jones L, Barritt GJ, et al. Phospholipase C-gamma1 is required for the activation of store-operated Ca2+ channels in liver cells. Biochem J. 2007;405(2):269-76. Epub 2007/04/17.

52. Mikoshiba K. IP3 receptor/Ca2+ channel: from discovery to new signaling concepts. J Neurochem. 2007;102(5):1426-46. Epub 2007/08/19.

53. Iwai M, Tateishi Y, Hattori M, Mizutani A, Nakamura T, Futatsugi A, et al. Molecular cloning of mouse type 2 and type 3 inositol 1,4,5-trisphosphate receptors and identification of a novel type 2 receptor splice variant. J Biol Chem. 2005;280(11):10305-17. Epub 2005/01/06.

54. Iwai M, Michikawa T, Bosanac I, Ikura M, Mikoshiba K. Molecular basis of the isoform-specific ligand-binding affinity of inositol 1,4,5-trisphosphate receptors. J Biol Chem. 2007;282(17):12755-64. Epub 2007/03/01.

55. Parker I, Choi J, Yao Y. Elementary events of InsP3-induced Ca2+ liberation in Xenopus oocytes: hot spots, puffs and blips. Cell Calcium. 1996;20(2):105-21. Epub 1996/08/01.

56. Rooney TA, Thomas AP. Intracellular calcium waves generated by Ins(1,4,5)P3-dependent mechanisms. Cell Calcium. 1993;14(10):674-90. Epub 1993/11/01.

57. Allbritton NL, Meyer T. Localized calcium spikes and propagating calcium waves. Cell Calcium. 1993;14(10):691-7. Epub 1993/11/01.

58. Hirata M, Suematsu E, Hashimoto T, Hamachi T, Koga T. Release of Ca2+ from a non-mitochondrial store site in peritoneal macrophages treated with saponin by inositol 1,4,5-trisphosphate. Biochem J. 1984;223(1):229-36. Epub 1984/10/01.

59. Iino M. Biphasic Ca2+ dependence of inositol 1,4,5-trisphosphate-induced Ca release in smooth muscle cells of the guinea pig taenia caeci. J Gen Physiol. 1990;95(6):1103-22. Epub 1990/06/01.

60. Missiaen L, Taylor CW, Berridge MJ. Luminal Ca2+ promoting spontaneous Ca2+ release from inositol trisphosphate-sensitive stores in rat hepatocytes. J Physiol. 1992;455:623-40. Epub 1992/09/01.

61. Hajnoczky G, Hager R, Thomas AP. Mitochondria suppress local feedback activation of inositol 1,4, 5-trisphosphate receptors by Ca2+. J Biol Chem. 1999;274(20):14157-62. Epub 1999/05/13.

62. Smith JB, Smith L, Higgins BL. Temperature and nucleotide dependence of calcium release by myo-inositol 1,4,5-trisphosphate in cultured vascular smooth muscle cells. J Biol Chem. 1985;260(27):14413-6. Epub 1985/11/25.

63. Bezprozvanny I, Ehrlich BE. ATP modulates the function of inositol 1,4,5-trisphosphate-gated channels at two sites. Neuron. 1993;10(6):1175-84. Epub 1993/06/01.

64. Iino M. Effects of adenine nucleotides on inositol 1,4,5-trisphosphate-induced calcium release in vascular smooth muscle cells. J Gen Physiol. 1991;98(4):681-98. Epub 1991/10/01.

65. Vanderheyden V, Devogelaere B, Missiaen L, De Smedt H, Bultynck G, Parys JB. Regulation of inositol 1,4,5-trisphosphate-induced Ca2+ release by reversible phosphorylation and dephosphorylation. Biochim Biophys Acta. 2009;1793(6):959-70. Epub 2009/01/10.

66. Khan MT, Wagner L, 2nd, Yule DI, Bhanumathy C, Joseph SK. Akt kinase phosphorylation of inositol 1,4,5-trisphosphate receptors. J Biol Chem. 2006;281(6):3731-7. Epub 2005/12/08.

67. Bugrim AE. Regulation of Ca2+ release by cAMP-dependent protein kinase. A mechanism for agonist-specific calcium signaling? Cell Calcium. 1999;25(3):219-26. Epub 1999/06/23.

68. Murthy KS, Zhou H. Selective phosphorylation of the IP3R-I in vivo by cGMP-dependent protein kinase in smooth muscle. Am J Physiol Gastrointest Liver Physiol. 2003;284(2):G221-30. Epub 2003/01/17.

69. Bagni C, Mannucci L, Dotti CG, Amaldi F. Chemical stimulation of synaptosomes modulates alpha -Ca2+/calmodulin-dependent protein kinase II mRNA association to polysomes. J Neurosci. 2000;20(10):RC76. Epub 2000/04/28.

70. Vermassen E, Fissore RA, Nadif Kasri N, Vanderheyden V, Callewaert G, Missiaen L, et al. Regulation of the phosphorylation of the inositol 1,4,5-trisphosphate receptor by protein kinase C. Biochem Biophys Res Commun. 2004;319(3):888-93. Epub 2004/06/09.

71. Jayaraman T, Ondrias K, Ondriasova E, Marks AR. Regulation of the inositol 1,4,5-trisphosphate receptor by tyrosine phosphorylation. Science. 1996;272(5267):1492-4. Epub 1996/06/07.

72. Dyall SD, Brown MT, Johnson PJ. Ancient invasions: from endosymbionts to organelles. Science. 2004;304(5668):253-7. Epub 2004/04/10.

73. Mokranjac D, Neupert W. Protein import into mitochondria. Biochem Soc Trans. 2005;33(Pt 5):1019-23. Epub 2005/10/26.

74. Mannella CA. Structure and dynamics of the mitochondrial inner membrane cristae. Biochim Biophys Acta. 2006;1763(5-6):542-8. Epub 2006/05/30.

75. Mitchell P, Moyle J. Chemiosmotic hypothesis of oxidative phosphorylation. Nature. 1967;213(5072):137-9. Epub 1967/01/14.

76. Rimessi A, Giorgi C, Pinton P, Rizzuto R. The versatility of mitochondrial calcium signals: from stimulation of cell metabolism to induction of cell death. Biochim Biophys Acta. 2008;1777(7-8):808-16. Epub 2008/06/25.

77. Drago I, Pizzo P, Pozzan T. After half a century mitochondrial calcium in- and efflux machineries reveal themselves. EMBO J. 2011;30(20):4119-25. Epub 2011/09/22.

78. Rapizzi E, Pinton P, Szabadkai G, Wieckowski MR, Vandecasteele G, Baird G, et al. Recombinant expression of the voltage-dependent anion channel enhances the transfer of Ca2+ microdomains to mitochondria. J Cell Biol. 2002;159(4):613-24. Epub 2002/11/20.

79. Shoshan-Barmatz V, Israelson A, Brdiczka D, Sheu SS. The voltage-dependent anion channel (VDAC): function in intracellular signalling, cell life and cell death. Curr Pharm Des. 2006;12(18):2249-70. Epub 2006/06/22.

80. Shoshan-Barmatz V, Gincel D. The voltage-dependent anion channel: characterization, modulation, and role in mitochondrial function in cell life and death. Cell Biochem Biophys. 2003;39(3):279-92. Epub 2004/01/13.

81. Wu S, Sampson MJ, Decker WK, Craigen WJ. Each mammalian mitochondrial outer membrane porin protein is dispensable: effects on cellular respiration. Biochim Biophys Acta. 1999;1452(1):68-78. Epub 1999/10/19.

82. Xu X, Decker W, Sampson MJ, Craigen WJ, Colombini M. Mouse VDAC isoforms expressed in yeast: channel properties and their roles in mitochondrial outer membrane permeability. J Membr Biol. 1999;170(2):89-102. Epub 1999/08/03.

83. Ujwal R, Cascio D, Colletier JP, Faham S, Zhang J, Toro L, et al. The crystal structure of mouse VDAC1 at 2.3 A resolution reveals mechanistic insights into metabolite gating. Proc Natl Acad Sci U S A. 2008;105(46):17742-7. Epub 2008/11/08.

84. Hiller S, Garces RG, Malia TJ, Orekhov VY, Colombini M, Wagner G. Solution structure of the integral human membrane protein VDAC-1 in detergent micelles. Science. 2008;321(5893):1206-10. Epub 2008/08/30.

85. Bayrhuber M, Meins T, Habeck M, Becker S, Giller K, Villinger S, et al. Structure of the human voltage-dependent anion channel. Proc Natl Acad Sci U S A. 2008;105(40):15370-5. Epub 2008/10/04.

86. De Pinto V, Reina S, Guarino F, Messina A. Structure of the voltage dependent anion channel: state of the art. J Bioenerg Biomembr. 2008;40(3):139-47. Epub 2008/08/01.

87. Colombini M. VDAC: the channel at the interface between mitochondria and the cytosol. Mol Cell Biochem. 2004;256-257(1-2):107-15. Epub 2004/02/24.

88. Lee AC, Xu X, Colombini M. The role of pyridine dinucleotides in regulating the permeability of the mitochondrial outer membrane. J Biol Chem. 1996;271(43):26724-31. Epub 1996/10/25.

89. Vander Heiden MG, Li XX, Gottleib E, Hill RB, Thompson CB, Colombini M. Bcl-xL promotes the open configuration of the voltage-dependent anion channel and metabolite passage through the outer mitochondrial membrane. J Biol Chem. 2001;276(22):19414-9. Epub 2001/03/22.

90. Pastorino JG, Hoek JB. Regulation of hexokinase binding to VDAC. J Bioenerg Biomembr. 2008;40(3):171-82. Epub 2008/08/07.

91. Schwarzer C, Barnikol-Watanabe S, Thinnes FP, Hilschmann N. Voltage-dependent anion-selective channel (VDAC) interacts with the dynein light chain Tctex1 and the heat-shock protein PBP74. Int J Biochem Cell Biol. 2002;34(9):1059-70. Epub 2002/05/16.

92. Rostovtseva TK, Sheldon KL, Hassanzadeh E, Monge C, Saks V, Bezrukov SM, et al. Tubulin binding blocks mitochondrial voltage-dependent anion channel and regulates respiration. Proc Natl Acad Sci U S A. 2008;105(48):18746-51. Epub 2008/11/27.

93. Rostovtseva TK, Tan W, Colombini M. On the role of VDAC in apoptosis: fact and fiction. J Bioenerg Biomembr. 2005;37(3):129-42. Epub 2005/09/17.

94. Tan W, Colombini M. VDAC closure increases calcium ion flux. Biochim Biophys Acta. 2007;1768(10):2510-5. Epub 2007/07/10.

95. Baines CP, Kaiser RA, Sheiko T, Craigen WJ, Molkentin JD. Voltage-dependent anion channels are dispensable for mitochondrial-dependent cell death. Nat Cell Biol. 2007;9(5):550-5. Epub 2007/04/10.

96. Chiara F, Castellaro D, Marin O, Petronilli V, Brusilow WS, Juhaszova M, et al. Hexokinase II detachment from mitochondria triggers apoptosis through the permeability transition pore independent of voltage-dependent anion channels. PLoS One. 2008;3(3):e1852. Epub 2008/03/20.

97. Rostovtseva TK, Antonsson B, Suzuki M, Youle RJ, Colombini M, Bezrukov SM. Bid, but not Bax, regulates VDAC channels. J Biol Chem. 2004;279(14):13575-83. Epub 2004/01/20.

98. Litsky ML, Pfeiffer DR. Regulation of the mitochondrial Ca2+ uniporter by external adenine nucleotides: the uniporter behaves like a gated channel which is regulated by nucleotides and divalent cations. Biochemistry. 1997;36(23):7071-80. Epub 1997/06/10.

99. Montero M, Lobaton CD, Hernandez-Sanmiguel E, Santodomingo J, Vay L, Moreno A, et al. Direct activation of the mitochondrial calcium uniporter by natural plant flavonoids. Biochem J. 2004;384(Pt 1):19-24. Epub 2004/08/25.

100. Perocchi F, Gohil VM, Girgis HS, Bao XR, McCombs JE, Palmer AE, et al. MICU1 encodes a mitochondrial EF hand protein required for Ca(2+) uptake. Nature. 2010;467(7313):291-6. Epub 2010/08/10.

101. Pagliarini DJ, Calvo SE, Chang B, Sheth SA, Vafai SB, Ong SE, et al. A mitochondrial protein compendium elucidates complex I disease biology. Cell. 2008;134(1):112-23. Epub 2008/07/11.

102. De Stefani D, Raffaello A, Teardo E, Szabo I, Rizzuto R. A forty-kilodalton protein of the inner membrane is the mitochondrial calcium uniporter. Nature. 2011. Epub 2011/06/21.

103. Baughman JM, Perocchi F, Girgis HS, Plovanich M, Belcher-Timme CA, Sancak Y, et al. Integrative genomics identifies MCU as an essential component of the mitochondrial calcium uniporter. Nature. 2011. Epub 2011/06/21.

104. Bernardi P. Mitochondrial transport of cations: channels, exchangers, and permeability transition. Physiol Rev. 1999;79(4):1127-55. Epub 1999/10/03.

105. Brierley GP, Baysal K, Jung DW. Cation transport systems in mitochondria: Na+ and K+ uniports and exchangers. J Bioenerg Biomembr. 1994;26(5):519-26. Epub 1994/10/01.

106. Palty R, Silverman WF, Hershfinkel M, Caporale T, Sensi SL, Parnis J, et al. NCLX is an essential component of mitochondrial Na+/Ca2+ exchange. Proc Natl Acad Sci U S A. 2010;107(1):436-41. Epub 2009/12/19.

107. Baines CP. The molecular composition of the mitochondrial permeability transition pore. J Mol Cell Cardiol. 2009;46(6):850-7. Epub 2009/02/24.

108. Rasola A, Bernardi P. The mitochondrial permeability transition pore and its involvement in cell death and in disease pathogenesis. Apoptosis. 2007;12(5):815-33. Epub 2007/02/13.

109. Rasola A, Sciacovelli M, Pantic B, Bernardi P. Signal transduction to the permeability transition pore. FEBS Lett. 2010;584(10):1989-96. Epub 2010/02/16.

110. McCormack JG, Halestrap AP, Denton RM. Role of calcium ions in regulation of mammalian intramitochondrial metabolism. Physiol Rev. 1990;70(2):391-425. Epub 1990/04/01.

111. Carafoli E. The fateful encounter of mitochondria with calcium: how did it happen? Biochim Biophys Acta. 2010;1797(6-7):595-606. Epub 2010/04/14.

112. Jouaville LS, Pinton P, Bastianutto C, Rutter GA, Rizzuto R. Regulation of mitochondrial ATP synthesis by calcium: evidence for a long-term metabolic priming. Proc Natl Acad Sci U S A. 1999;96(24):13807-12. Epub 1999/11/26.

113. Maes K, Missiaen L, De Smet P, Vanlingen S, Callewaert G, Parys JB, et al. Differential modulation of inositol 1,4,5-trisphosphate receptor type 1 and type 3 by ATP. Cell Calcium. 2000;27(5):257-67. Epub 2000/06/22.

114. Betzenhauser MJ, Wagner LE, 2nd, Iwai M, Michikawa T, Mikoshiba K, Yule DI. ATP modulation of Ca2+ release by type-2 and type-3 inositol (1, 4, 5)-triphosphate receptors. Differing ATP sensitivities and molecular determinants of action. J Biol Chem. 2008;283(31):21579-87. Epub 2008/05/29.

115. Walsh C, Barrow S, Voronina S, Chvanov M, Petersen OH, Tepikin A. Modulation of calcium signalling by mitochondria. Biochim Biophys Acta. 2009;1787(11):1374-82. Epub 2009/04/07.

116. Arnaudeau S, Kelley WL, Walsh JV, Jr., Demaurex N. Mitochondria recycle Ca(2+) to the endoplasmic reticulum and prevent the depletion of neighboring endoplasmic reticulum regions. J Biol Chem. 2001;276(31):29430-9. Epub 2001/05/19.

117. Tinel H, Cancela JM, Mogami H, Gerasimenko JV, Gerasimenko OV, Tepikin AV, et al. Active mitochondria surrounding the pancreatic acinar granule region prevent spreading of inositol trisphosphate-evoked local cytosolic Ca(2+) signals. EMBO J. 1999;18(18):4999-5008. Epub 1999/09/16.

118. Goetz JG, Genty H, St-Pierre P, Dang T, Joshi B, Sauve R, et al. Reversible interactions between smooth domains of the endoplasmic reticulum and mitochondria are regulated by physiological cytosolic Ca2+ levels. J Cell Sci. 2007;120(Pt 20):3553-64. Epub 2007/09/27.

119. Wang HJ, Guay G, Pogan L, Sauve R, Nabi IR. Calcium regulates the association between mitochondria and a smooth subdomain of the endoplasmic reticulum. J Cell Biol. 2000;150(6):1489-98. Epub 2000/09/20.

120. Yi M, Weaver D, Hajnoczky G. Control of mitochondrial motility and distribution by the calcium signal: a homeostatic circuit. J Cell Biol. 2004;167(4):661-72. Epub 2004/11/17.

121. Westermann B. Mitochondrial fusion and fission in cell life and death. Nat Rev Mol Cell Biol. 2010;11(12):872-84. Epub 2010/11/26.

122. Rintoul GL, Filiano AJ, Brocard JB, Kress GJ, Reynolds IJ. Glutamate decreases mitochondrial size and movement in primary forebrain neurons. J Neurosci. 2003;23(21):7881-8. Epub 2003/08/29.

123. Germain M, Mathai JP, McBride HM, Shore GC. Endoplasmic reticulum BIK initiates DRP1-regulated remodelling of mitochondrial cristae during apoptosis. EMBO J. 2005;24(8):1546-56. Epub 2005/03/26.

124. Alirol E, James D, Huber D, Marchetto A, Vergani L, Martinou JC, et al. The mitochondrial fission protein hFis1 requires the endoplasmic reticulum gateway to induce apoptosis. Mol Biol Cell. 2006;17(11):4593-605. Epub 2006/08/18.

125. Szabadkai G, Simoni AM, Chami M, Wieckowski MR, Youle RJ, Rizzuto R. Drp-1-dependent division of the mitochondrial network blocks intraorganellar Ca2+ waves and protects against Ca2+-mediated apoptosis. Mol Cell. 2004;16(1):59-68. Epub 2004/10/08.

126. Ichas F, Jouaville LS, Mazat JP. Mitochondria are excitable organelles capable of generating and conveying electrical and calcium signals. Cell. 1997;89(7):1145-53. Epub 1997/06/27.

127. Fulda S, Debatin KM. Extrinsic versus intrinsic apoptosis pathways in anticancer chemotherapy. Oncogene. 2006;25(34):4798-811. Epub 2006/08/08.

128. Kroemer G, Galluzzi L, Brenner C. Mitochondrial membrane permeabilization in cell death. Physiol Rev. 2007;87(1):99-163. Epub 2007/01/24.

129. Tait SW, Green DR. Mitochondria and cell death: outer membrane permeabilization and beyond. Nat Rev Mol Cell Biol. 2010;11(9):621-32. Epub 2010/08/05.

130. Armstrong JS. The role of the mitochondrial permeability transition in cell death. Mitochondrion. 2006;6(5):225-34. Epub 2006/08/29.

131. Basso E, Fante L, Fowlkes J, Petronilli V, Forte MA, Bernardi P. Properties of the permeability transition pore in mitochondria devoid of Cyclophilin D. J Biol Chem. 2005;280(19):18558-61. Epub 2005/03/29.

132. Shoshan-Barmatz V, De Pinto V, Zweckstetter M, Raviv Z, Keinan N, Arbel N. VDAC, a multi-functional mitochondrial protein regulating cell life and death. Mol Aspects Med. 2010;31(3):227-85. Epub 2010/03/30.

133. Rong Y, Distelhorst CW. Bcl-2 protein family members: versatile regulators of calcium signaling in cell survival and apoptosis. Annu Rev Physiol. 2008;70:73-91. Epub 2007/08/08.

134. Joseph SK, Hajnoczky G. IP3 receptors in cell survival and apoptosis: Ca2+ release and beyond. Apoptosis. 2007;12(5):951-68. Epub 2007/02/13.

135. Pinton P, Giorgi C, Siviero R, Zecchini E, Rizzuto R. Calcium and apoptosis: ER-mitochondria Ca2+ transfer in the control of apoptosis. Oncogene. 2008;27(50):6407-18. Epub 2008/10/29.

136. Sugawara H, Kurosaki M, Takata M, Kurosaki T. Genetic evidence for involvement of type 1, type 2 and type 3 inositol 1,4,5-trisphosphate receptors in signal transduction through the B-cell antigen receptor. EMBO J. 1997;16(11):3078-88. Epub 1997/06/02.

137. Jayaraman T, Marks AR. T cells deficient in inositol 1,4,5-trisphosphate receptor are resistant to apoptosis. Mol Cell Biol. 1997;17(6):3005-12. Epub 1997/06/01.

138. Hayashi T, Su TP. Sigma-1 receptor chaperones at the ER-mitochondrion interface regulate Ca(2+) signaling and cell survival. Cell. 2007;131(3):596-610. Epub 2007/11/06.

139. Mendes CC, Gomes DA, Thompson M, Souto NC, Goes TS, Goes AM, et al. The type III inositol 1,4,5-trisphosphate receptor preferentially transmits apoptotic Ca2+ signals into mitochondria. J Biol Chem. 2005;280(49):40892-900. Epub 2005/09/30.

140. Khan AA, Soloski MJ, Sharp AH, Schilling G, Sabatini DM, Li SH, et al. Lymphocyte apoptosis: mediation by increased type 3 inositol 1,4,5-trisphosphate receptor. Science. 1996;273(5274):503-7. Epub 1996/07/26.

141. Boehning D, Patterson RL, Sedaghat L, Glebova NO, Kurosaki T, Snyder SH. Cytochrome c binds to inositol (1,4,5) trisphosphate receptors, amplifying calcium-dependent apoptosis. Nat Cell Biol. 2003;5(12):1051-61. Epub 2003/11/11.

142. Pinton P, Ferrari D, Rapizzi E, Di Virgilio F, Pozzan T, Rizzuto R. The Ca2+ concentration of the endoplasmic reticulum is a key determinant of ceramide-induced apoptosis: significance for the molecular mechanism of Bcl-2 action. EMBO J. 2001;20(11):2690-701. Epub 2001/06/02.

143. Scorrano L, Oakes SA, Opferman JT, Cheng EH, Sorcinelli MD, Pozzan T, et al. BAX and BAK regulation of endoplasmic reticulum Ca2+: a control point for apoptosis. Science. 2003;300(5616):135-9. Epub 2003/03/08.

144. Pinton P, Ferrari D, Magalhaes P, Schulze-Osthoff K, Di Virgilio F, Pozzan T, et al. Reduced loading of intracellular Ca(2+) stores and downregulation of capacitative Ca(2+) influx in Bcl-2-overexpressing cells. J Cell Biol. 2000;148(5):857-62. Epub 2000/03/08.

145. Oakes SA, Scorrano L, Opferman JT, Bassik MC, Nishino M, Pozzan T, et al. Proapoptotic BAX and BAK regulate the type 1 inositol trisphosphate receptor and calcium leak from the endoplasmic reticulum. Proc Natl Acad Sci U S A. 2005;102(1):105-10. Epub 2004/12/23.

146. Szado T, Vanderheyden V, Parys JB, De Smedt H, Rietdorf K, Kotelevets L, et al. Phosphorylation of inositol 1,4,5-trisphosphate receptors by protein kinase B/Akt inhibits Ca2+ release and apoptosis. Proc Natl Acad Sci U S A. 2008;105(7):2427-32. Epub 2008/02/06.

147. Marchi S, Rimessi A, Giorgi C, Baldini C, Ferroni L, Rizzuto R, et al. Akt kinase reducing endoplasmic reticulum Ca2+ release protects cells from Ca2+-dependent apoptotic stimuli. Biochem Biophys Res Commun. 2008;375(4):501-5. Epub 2008/08/30.

148. Copeland DE, Dalton AJ. An association between mitochondria and the endoplasmic reticulum in cells of the pseudobranch gland of a teleost. J Biophys Biochem Cytol. 1959;5(3):393-6. Epub 1959/05/25.

149. Lewis JA, Tata JR. A rapidly sedimenting fraction of rat liver endoplasmic reticulum. J Cell Sci. 1973;13(2):447-59. Epub 1973/09/01.

150. Morre DJ, Merritt WD, Lembi CA. Connections between mitochondria and endoplasmic reticulum in rat liver and onion stem. Protoplasma. 1971;73(1):43-9. Epub 1971/01/01.

151. Mannella CA, Buttle K, Rath BK, Marko M. Electron microscopic tomography of rat-liver mitochondria and their interaction with the endoplasmic reticulum. Biofactors. 1998;8(3-4):225-8. Epub 1999/01/23.

152. Soltys BJ, Gupta RS. Interrelationships of endoplasmic reticulum, mitochondria, intermediate filaments, and microtubules--a quadruple fluorescence labeling study. Biochem Cell Biol. 1992;70(10-11):1174-86. Epub 1992/10/01.

153. Mannella CA, Marko M, Penczek P, Barnard D, Frank J. The internal compartmentation of rat-liver mitochondria: tomographic study using the high-voltage transmission electron microscope. Microsc Res Tech. 1994;27(4):278-83. Epub 1994/03/01.

154. Achleitner G, Gaigg B, Krasser A, Kainersdorfer E, Kohlwein SD, Perktold A, et al. Association between the endoplasmic reticulum and mitochondria of yeast facilitates interorganelle transport of phospholipids through membrane contact. Eur J Biochem. 1999;264(2):545-53. Epub 1999/09/22.

155. Csordas G, Renken C, Varnai P, Walter L, Weaver D, Buttle KF, et al. Structural and functional features and significance of the physical linkage between ER and mitochondria. J Cell Biol. 2006;174(7):915-21. Epub 2006/09/20.

156. de Brito OM, Scorrano L. Mitofusin 2 tethers endoplasmic reticulum to mitochondria. Nature. 2008;456(7222):605-10. Epub 2008/12/05.

157. Dennis EA, Kennedy EP. Intracellular sites of lipid synthesis and the biogenesis of mitochondria. J Lipid Res. 1972;13(2):263-7. Epub 1972/03/01.

158. Vance JE. Phospholipid synthesis in a membrane fraction associated with mitochondria. J Biol Chem. 1990;265(13):7248-56. Epub 1990/05/05.

159. Vance JE, Stone SJ, Faust JR. Abnormalities in mitochondria-associated membranes and phospholipid biosynthetic enzymes in the mnd/mnd mouse model of neuronal ceroid lipofuscinosis. Biochim Biophys Acta. 1997;1344(3):286-99. Epub 1997/02/18.

160. Wieckowski MR, Giorgi C, Lebiedzinska M, Duszynski J, Pinton P. Isolation of mitochondria-associated membranes and mitochondria from animal tissues and cells. Nat Protoc. 2009;4(11):1582-90. Epub 2009/10/10.

161. Pichler H, Gaigg B, Hrastnik C, Achleitner G, Kohlwein SD, Zellnig G, et al. A subfraction of the yeast endoplasmic reticulum associates with the plasma membrane and has a high capacity to synthesize lipids. Eur J Biochem. 2001;268(8):2351-61. Epub 2001/04/12.

162. Wu MM, Buchanan J, Luik RM, Lewis RS. Ca2+ store depletion causes STIM1 to accumulate in ER regions closely associated with the plasma membrane. J Cell Biol. 2006;174(6):803-13. Epub 2006/09/13.

163. Frieden M, Arnaudeau S, Castelbou C, Demaurex N. Subplasmalemmal mitochondria modulate the activity of plasma membrane Ca2+-ATPases. J Biol Chem. 2005;280(52):43198-208. Epub 2005/10/12.

164. Koziel K, Lebiedzinska M, Szabadkai G, Onopiuk M, Brutkowski W, Wierzbicka K, et al. Plasma membrane associated membranes (PAM) from Jurkat cells contain STIM1 protein is PAM involved in the capacitative calcium entry? Int J Biochem Cell Biol. 2009;41(12):2440-9. Epub 2009/07/23.

165. Piccini M, Vitelli F, Bruttini M, Pober BR, Jonsson JJ, Villanova M, et al. FACL4, a new gene encoding long-chain acyl-CoA synthetase 4, is deleted in a family with Alport syndrome, elliptocytosis, and mental retardation. Genomics. 1998;47(3):350-8. Epub 1998/04/16.

166. Stone SJ, Vance JE. Phosphatidylserine synthase-1 and -2 are localized to mitochondria-associated membranes. J Biol Chem. 2000;275(44):34534-40. Epub 2000/08/12.

167. Lebiedzinska M, Szabadkai G, Jones AW, Duszynski J, Wieckowski MR. Interactions between the endoplasmic reticulum, mitochondria, plasma membrane and other subcellular organelles. Int J Biochem Cell Biol. 2009;41(10):1805-16. Epub 2009/08/26.

168. Hayashi T, Rizzuto R, Hajnoczky G, Su TP. MAM: more than just a housekeeper. Trends Cell Biol. 2009;19(2):81-8. Epub 2009/01/16.

169. Giorgi C, De Stefani D, Bononi A, Rizzuto R, Pinton P. Structural and functional link between the mitochondrial network and the endoplasmic reticulum. Int J Biochem Cell Biol. 2009;41(10):1817-27. Epub 2009/04/25.

170. Decuypere JP, Monaco G, Bultynck G, Missiaen L, De Smedt H, Parys JB. The IP(3) receptor-mitochondria connection in apoptosis and autophagy. Biochim Biophys Acta. 2011;1813(5):1003-13. Epub 2010/12/15.

171. Szabadkai G, Bianchi K, Varnai P, De Stefani D, Wieckowski MR, Cavagna D, et al. Chaperone-mediated coupling of endoplasmic reticulum and mitochondrial Ca2+ channels. J Cell Biol. 2006;175(6):901-11. Epub 2006/12/21.

172. De Stefani D, Bononi A, Romagnoli A, Messina A, De Pinto V, Pinton P, et al. VDAC1 selectively transfers apoptotic Ca(2+) signals to mitochondria. Cell Death Differ. 2011. Epub 2011/07/02.

173. Roderick HL, Lechleiter JD, Camacho P. Cytosolic phosphorylation of calnexin controls intracellular Ca(2+) oscillations via an interaction with SERCA2b. J Cell Biol. 2000;149(6):1235-48. Epub 2000/06/13.

174. Camacho P, Lechleiter JD. Calreticulin inhibits repetitive intracellular Ca2+ waves. Cell. 1995;82(5):765-71. Epub 1995/09/08.

175. Michalak M, Groenendyk J, Szabo E, Gold LI, Opas M. Calreticulin, a multi-process calcium-buffering chaperone of the endoplasmic reticulum. Biochem J. 2009;417(3):651-66. Epub 2009/01/13.

176. Molinari M, Eriksson KK, Calanca V, Galli C, Cresswell P, Michalak M, et al. Contrasting functions of calreticulin and calnexin in glycoprotein folding and ER quality control. Mol Cell. 2004;13(1):125-35. Epub 2004/01/21.

177. Simmen T, Aslan JE, Blagoveshchenskaya AD, Thomas L, Wan L, Xiang Y, et al. PACS-2 controls endoplasmic reticulum-mitochondria communication and Bid-mediated apoptosis. EMBO J. 2005;24(4):717-29. Epub 2005/02/05.

178. Kottgen M, Benzing T, Simmen T, Tauber R, Buchholz B, Feliciangeli S, et al. Trafficking of TRPP2 by PACS proteins represents a novel mechanism of ion channel regulation. EMBO J. 2005;24(4):705-16. Epub 2005/02/05.

179. Myhill N, Lynes EM, Nanji JA, Blagoveshchenskaya AD, Fei H, Carmine Simmen K, et al. The subcellular distribution of calnexin is mediated by PACS-2. Mol Biol Cell. 2008;19(7):2777-88. Epub 2008/04/18.

180. Breckenridge DG, Stojanovic M, Marcellus RC, Shore GC. Caspase cleavage product of BAP31 induces mitochondrial fission through endoplasmic reticulum calcium signals, enhancing cytochrome c release to the cytosol. J Cell Biol. 2003;160(7):1115-27. Epub 2003/04/02.

181. Bui M, Gilady SY, Fitzsimmons RE, Benson MD, Lynes EM, Gesson K, et al. Rab32 modulates apoptosis onset and mitochondria-associated membrane (MAM) properties. J Biol Chem. 2010;285(41):31590-602. Epub 2010/07/31.

182. Maurice T, Su TP. The pharmacology of sigma-1 receptors. Pharmacol Ther. 2009;124(2):195-206. Epub 2009/07/22.

183. Aydar E, Palmer CP, Djamgoz MB. Sigma receptors and cancer: possible involvement of ion channels. Cancer Res. 2004;64(15):5029-35. Epub 2004/08/04.

184. Marrazzo A, Caraci F, Salinaro ET, Su TP, Copani A, Ronsisvalle G. Neuroprotective effects of sigma-1 receptor agonists against beta-amyloid-induced toxicity. Neuroreport. 2005;16(11):1223-6. Epub 2005/07/14.

185. Vagnerova K, Hurn PD, Bhardwaj A, Kirsch JR. Sigma 1 receptor agonists act as neuroprotective drugs through inhibition of inducible nitric oxide synthase. Anesth Analg. 2006;103(2):430-4, table of contents. Epub 2006/07/25.

186. Spruce BA, Campbell LA, McTavish N, Cooper MA, Appleyard MV, O'Neill M, et al. Small molecule antagonists of the sigma-1 receptor cause selective release of the death program in tumor and self-reliant cells and inhibit tumor growth in vitro and in vivo. Cancer Res. 2004;64(14):4875-86. Epub 2004/07/17.

187. Higo T, Hattori M, Nakamura T, Natsume T, Michikawa T, Mikoshiba K. Subtype-specific and ER lumenal environment-dependent regulation of inositol 1,4,5-trisphosphate receptor type 1 by ERp44. Cell. 2005;120(1):85-98. Epub 2005/01/18.

188. Li G, Mongillo M, Chin KT, Harding H, Ron D, Marks AR, et al. Role of ERO1-alpha-mediated stimulation of inositol 1,4,5-triphosphate receptor activity in endoplasmic reticulum stress-induced apoptosis. J Cell Biol. 2009;186(6):783-92. Epub 2009/09/16.

189. Szalai G, Krishnamurthy R, Hajnoczky G. Apoptosis driven by IP(3)-linked mitochondrial calcium signals. EMBO J. 1999;18(22):6349-61. Epub 1999/11/24.

190. Gilady SY, Bui M, Lynes EM, Benson MD, Watts R, Vance JE, et al. Ero1alpha requires oxidizing and normoxic conditions to localize to the mitochondria-associated membrane (MAM). Cell Stress Chaperones. 2010;15(5):619-29. Epub 2010/02/27.

191. Cartoni R, Martinou JC. Role of mitofusin 2 mutations in the physiopathology of Charcot-Marie-Tooth disease type 2A. Exp Neurol. 2009;218(2):268-73. Epub 2009/05/12.

192. Guo X, Chen KH, Guo Y, Liao H, Tang J, Xiao RP. Mitofusin 2 triggers vascular smooth muscle cell apoptosis via mitochondrial death pathway. Circ Res. 2007;101(11):1113-22. Epub 2007/09/29.

193. Vecchione A, Fassan M, Anesti V, Morrione A, Goldoni S, Baldassarre G, et al. MITOSTATIN, a putative tumor suppressor on chromosome 12q24.1, is downregulated in human bladder and breast cancer. Oncogene. 2009;28(2):257-69. Epub 2008/10/22.

194. Cerqua C, Anesti V, Pyakurel A, Liu D, Naon D, Wiche G, et al. Trichoplein/mitostatin regulates endoplasmic reticulum-mitochondria juxtaposition. EMBO Rep. 2010;11(11):854-60. Epub 2010/10/12.

195. Iwasawa R, Mahul-Mellier AL, Datler C, Pazarentzos E, Grimm S. Fis1 and Bap31 bridge the mitochondria-ER interface to establish a platform for apoptosis induction. EMBO J. 2011;30(3):556-68. Epub 2010/12/25.

196. Celsi F, Pizzo P, Brini M, Leo S, Fotino C, Pinton P, et al. Mitochondria, calcium and cell death: a deadly triad in neurodegeneration. Biochim Biophys Acta. 2009;1787(5):335-44. Epub 2009/03/10.

197. Contreras L, Drago I, Zampese E, Pozzan T. Mitochondria: the calcium connection. Biochim Biophys Acta. 2010;1797(6-7):607-18. Epub 2010/05/18.

198. Area-Gomez E, de Groof AJ, Boldogh I, Bird TD, Gibson GE, Koehler CM, et al. Presenilins are enriched in endoplasmic reticulum membranes associated with mitochondria. Am J Pathol. 2009;175(5):1810-6. Epub 2009/10/17.

199. Zampese E, Fasolato C, Kipanyula MJ, Bortolozzi M, Pozzan T, Pizzo P. Presenilin 2 modulates endoplasmic reticulum (ER)-mitochondria interactions and Ca2+ cross-talk. Proc Natl Acad Sci U S A. 2011;108(7):2777-82. Epub 2011/02/03.

200. Smith IF, Green KN, LaFerla FM. Calcium dysregulation in Alzheimer's disease: recent advances gained from genetically modified animals. Cell Calcium. 2005;38(3-4):427-37. Epub 2005/08/30.

201. Small DH. Dysregulation of calcium homeostasis in Alzheimer's disease. Neurochem Res. 2009;34(10):1824-9. Epub 2009/04/02.

202. Yu JT, Chang RC, Tan L. Calcium dysregulation in Alzheimer's disease: from mechanisms to therapeutic opportunities. Prog Neurobiol. 2009;89(3):240-55. Epub 2009/08/12.

203. Sano R, Annunziata I, Patterson A, Moshiach S, Gomero E, Opferman J, et al. GM1-ganglioside accumulation at the mitochondria-associated ER membranes links ER stress to Ca(2+)-dependent mitochondrial apoptosis. Mol Cell. 2009;36(3):500-11. Epub 2009/11/18.

204. d'Azzo A, Tessitore A, Sano R. Gangliosides as apoptotic signals in ER stress response. Cell Death Differ. 2006;13(3):404-14. Epub 2006/01/07.

205. Wu G, Lu ZH, Obukhov AG, Nowycky MC, Ledeen RW. Induction of calcium influx through TRPC5 channels by cross-linking of GM1 ganglioside associated with alpha5beta1 integrin initiates neurite outgrowth. J Neurosci. 2007;27(28):7447-58. Epub 2007/07/13.

206. Giorgi C, Ito K, Lin HK, Santangelo C, Wieckowski MR, Lebiedzinska M, et al. PML regulates apoptosis at endoplasmic reticulum by modulating calcium release. Science. 2010;330(6008):1247-51. Epub 2010/10/30.

207. Trinei M, Berniakovich I, Beltrami E, Migliaccio E, Fassina A, Pelicci P, et al. P66Shc signals to age. Aging (Albany NY). 2009;1(6):503-10. Epub 2010/02/17.

208. Lebiedzinska M, Duszynski J, Rizzuto R, Pinton P, Wieckowski MR. Age-related changes in levels of p66Shc and serine 36-phosphorylated p66Shc in organs and mouse tissues. Arch Biochem Biophys. 2009;486(1):73-80. Epub 2009/03/31.

209. Pinton P, Rimessi A, Marchi S, Orsini F, Migliaccio E, Giorgio M, et al. Protein kinase C beta and prolyl isomerase 1 regulate mitochondrial effects of the life-span determinant p66Shc. Science. 2007;315(5812):659-63. Epub 2007/02/03.

210. Bozidis P, Williamson CD, Colberg-Poley AM. Mitochondrial and secretory human cytomegalovirus UL37 proteins traffic into mitochondrion-associated membranes of human cells. J Virol. 2008;82(6):2715-26. Epub 2008/01/18.

211. Sheikh MY, Choi J, Qadri I, Friedman JE, Sanyal AJ. Hepatitis C virus infection: molecular pathways to metabolic syndrome. Hepatology. 2008;47(6):2127-33. Epub 2008/05/01.

212. Xu X, Forbes JG, Colombini M. Actin modulates the gating of Neurospora crassa VDAC. J Membr Biol. 2001;180(1):73-81. Epub 2001/04/04.

213. Rostovtseva TK, Bezrukov SM. VDAC regulation: role of cytosolic proteins and mitochondrial lipids. J Bioenerg Biomembr. 2008;40(3):163-70. Epub 2008/07/26.

214. Ren D, Kim H, Tu HC, Westergard TD, Fisher JK, Rubens JA, et al. The VDAC2-BAK rheostat controls thymocyte survival. Sci Signal. 2009;2(85):ra48. Epub 2009/08/27.

215. Roy SS, Madesh M, Davies E, Antonsson B, Danial N, Hajnoczky G. Bad targets the permeability transition pore independent of Bax or Bak to switch between Ca2+-dependent cell survival and death. Mol Cell. 2009;33(3):377-88. Epub 2009/02/17.

216. Roy SS, Ehrlich AM, Craigen WJ, Hajnoczky G. VDAC2 is required for truncated BID-induced mitochondrial apoptosis by recruiting BAK to the mitochondria. EMBO Rep. 2009;10(12):1341-7. Epub 2009/10/13.

217. Verrier F, Deniaud A, Lebras M, Metivier D, Kroemer G, Mignotte B, et al. Dynamic evolution of the adenine nucleotide translocase interactome during chemotherapy-induced apoptosis. Oncogene. 2004;23(49):8049-64. Epub 2004/09/21.

218. Cheng EH, Sheiko TV, Fisher JK, Craigen WJ, Korsmeyer SJ. VDAC2 inhibits BAK activation and mitochondrial apoptosis. Science. 2003;301(5632):513-7. Epub 2003/07/26.

219. Tomasello F, Messina A, Lartigue L, Schembri L, Medina C, Reina S, et al. Outer membrane VDAC1 controls permeability transition of the inner mitochondrial membrane in cellulo during stress-induced apoptosis. Cell Res. 2009;19(12):1363-76. Epub 2009/08/12.

220. Sampson MJ, Decker WK, Beaudet AL, Ruitenbeek W, Armstrong D, Hicks MJ, et al. Immotile sperm and infertility in mice lacking mitochondrial voltage-dependent anion channel type 3. J Biol Chem. 2001;276(42):39206-12. Epub 2001/08/17.

221. Weeber EJ, Levy M, Sampson MJ, Anflous K, Armstrong DL, Brown SE, et al. The role of mitochondrial porins and the permeability transition pore in learning and synaptic plasticity. J Biol Chem. 2002;277(21):18891-7. Epub 2002/03/22.

222. Baumgartner HK, Gerasimenko JV, Thorne C, Ferdek P, Pozzan T, Tepikin AV, et al. Calcium elevation in mitochondria is the main Ca2+ requirement for mitochondrial permeability transition pore (mPTP) opening. J Biol Chem. 2009;284(31):20796-803. Epub 2009/06/12.

223. Yamamoto T, Yamada A, Watanabe M, Yoshimura Y, Yamazaki N, Yamauchi T, et al. VDAC1, having a shorter N-terminus than VDAC2 but showing the same migration in an SDS-polyacrylamide gel, is the predominant form expressed in mitochondria of various tissues. J Proteome Res. 2006;5(12):3336-44. Epub 2006/12/02.

224. Graham BH, Craigen WJ. Genetic approaches to analyzing mitochondrial outer membrane permeability. Curr Top Dev Biol. 2004;59:87-118. Epub 2004/02/21.

225. Abu-Hamad S, Sivan S, Shoshan-Barmatz V. The expression level of the voltage-dependent anion channel controls life and death of the cell. Proc Natl Acad Sci U S A. 2006;103(15):5787-92. Epub 2006/04/06.

226. Yagoda N, von Rechenberg M, Zaganjor E, Bauer AJ, Yang WS, Fridman DJ, et al. RAS-RAF-MEK-dependent oxidative cell death involving voltage-dependent anion channels. Nature. 2007;447(7146):864-8. Epub 2007/06/15.

227. Voehringer DW, Hirschberg DL, Xiao J, Lu Q, Roederer M, Lock CB, et al. Gene microarray identification of redox and mitochondrial elements that control resistance or sensitivity to apoptosis. Proc Natl Acad Sci U S A. 2000;97(6):2680-5. Epub 2000/03/16.

228. Neumann D, Buckers J, Kastrup L, Hell SW, Jakobs S. Two-color STED microscopy reveals different degrees of colocalization between hexokinase-I and the three human VDAC isoforms. PMC Biophys. 2010;3(1):4. Epub 2010/03/09.

229. Salomoni P, Pandolfi PP. The role of PML in tumor suppression. Cell. 2002;108(2):165-70. Epub 2002/02/08.

230. Gurrieri C, Capodieci P, Bernardi R, Scaglioni PP, Nafa K, Rush LJ, et al. Loss of the tumor suppressor PML in human cancers of multiple histologic origins. J Natl Cancer Inst. 2004;96(4):269-79. Epub 2004/02/19.

231. Salomoni P, Ferguson BJ, Wyllie AH, Rich T. New insights into the role of PML in tumour suppression. Cell Res. 2008;18(6):622-40. Epub 2008/05/28.

232. Jensen K, Shiels C, Freemont PS. PML protein isoforms and the RBCC/TRIM motif. Oncogene. 2001;20(49):7223-33. Epub 2001/11/13.

233. Lallemand-Breitenbach V, de The H. PML nuclear bodies. Cold Spring Harb Perspect Biol. 2010;2(5):a000661. Epub 2010/05/11.

234. Shen TH, Lin HK, Scaglioni PP, Yung TM, Pandolfi PP. The mechanisms of PML-nuclear body formation. Mol Cell. 2006;24(3):331-9. Epub 2006/11/04.

235. Bernardi R, Pandolfi PP. Structure, dynamics and functions of promyelocytic leukaemia nuclear bodies. Nat Rev Mol Cell Biol. 2007;8(12):1006-16. Epub 2007/10/12.

236. Melnick A, Licht JD. Deconstructing a disease: RARalpha, its fusion partners, and their roles in the pathogenesis of acute promyelocytic leukemia. Blood. 1999;93(10):3167-215. Epub 1999/05/11.

237. Wang ZG, Ruggero D, Ronchetti S, Zhong S, Gaboli M, Rivi R, et al. PML is essential for multiple apoptotic pathways. Nat Genet. 1998;20(3):266-72. Epub 1998/11/07.

238. Bernardi R, Papa A, Pandolfi PP. Regulation of apoptosis by PML and the PML-NBs. Oncogene. 2008;27(48):6299-312. Epub 2008/10/22.

239. Trotman LC, Alimonti A, Scaglioni PP, Koutcher JA, Cordon-Cardo C, Pandolfi PP. Identification of a tumour suppressor network opposing nuclear Akt function. Nature. 2006;441(7092):523-7. Epub 2006/05/09.

240. Trotman LC, Wang X, Alimonti A, Chen Z, Teruya-Feldstein J, Yang H, et al. Ubiquitination regulates PTEN nuclear import and tumor suppression. Cell. 2007;128(1):141-56. Epub 2007/01/16.

241. Song MS, Salmena L, Carracedo A, Egia A, Lo-Coco F, Teruya-Feldstein J, et al. The deubiquitinylation and localization of PTEN are regulated by a HAUSP-PML network. Nature. 2008;455(7214):813-7. Epub 2008/08/22.

242. Lin HK, Bergmann S, Pandolfi PP. Cytoplasmic PML function in TGF-beta signalling. Nature. 2004;431(7005):205-11. Epub 2004/09/10.

243. Condemine W, Takahashi Y, Zhu J, Puvion-Dutilleul F, Guegan S, Janin A, et al. Characterization of endogenous human promyelocytic leukemia isoforms. Cancer Res. 2006;66(12):6192-8. Epub 2006/06/17.

244. Pinton P, Rimessi A, Romagnoli A, Prandini A, Rizzuto R. Biosensors for the detection of calcium and pH. Methods Cell Biol. 2007;80:297-325. Epub 2007/04/21.

245. Yang M, Ellenberg J, Bonifacino JS, Weissman AM. The transmembrane domain of a carboxyl-terminal anchored protein determines localization to the endoplasmic reticulum. J Biol Chem. 1997;272(3):1970-5. Epub 1997/01/17.

246. Blackshaw S, Sawa A, Sharp AH, Ross CA, Snyder SH, Khan AA. Type 3 inositol 1,4,5-trisphosphate receptor modulates cell death. FASEB J. 2000;14(10):1375-9. Epub 2000/07/06.

247. Li J, Yen C, Liaw D, Podsypanina K, Bose S, Wang SI, et al. PTEN, a putative protein tyrosine phosphatase gene mutated in human brain, breast, and prostate cancer. Science. 1997;275(5308):1943-7. Epub 1997/03/28.

248. Steck PA, Pershouse MA, Jasser SA, Yung WK, Lin H, Ligon AH, et al. Identification of a candidate tumour suppressor gene, MMAC1, at chromosome 10q23.3 that is mutated in multiple advanced cancers. Nat Genet. 1997;15(4):356-62. Epub 1997/04/01.

249. Salmena L, Carracedo A, Pandolfi PP. Tenets of PTEN tumor suppression. Cell. 2008;133(3):403-14. Epub 2008/05/06.

250. Hobert JA, Eng C. PTEN hamartoma tumor syndrome: an overview. Genet Med. 2009;11(10):687-94. Epub 2009/08/12.

251. Maehama T, Dixon JE. The tumor suppressor, PTEN/MMAC1, dephosphorylates the lipid second messenger, phosphatidylinositol 3,4,5-trisphosphate. J Biol Chem. 1998;273(22):13375-8. Epub 1998/06/05.

252. Myers MP, Stolarov JP, Eng C, Li J, Wang SI, Wigler MH, et al. P-TEN, the tumor suppressor from human chromosome 10q23, is a dual-specificity phosphatase. Proc Natl Acad Sci U S A. 1997;94(17):9052-7. Epub 1997/08/19.

253. Stambolic V, Suzuki A, de la Pompa JL, Brothers GM, Mirtsos C, Sasaki T, et al. Negative regulation of PKB/Akt-dependent cell survival by the tumor suppressor PTEN. Cell. 1998;95(1):29-39. Epub 1998/10/20.

254. Haas-Kogan D, Shalev N, Wong M, Mills G, Yount G, Stokoe D. Protein kinase B (PKB/Akt) activity is elevated in glioblastoma cells due to mutation of the tumor suppressor PTEN/MMAC. Curr Biol. 1998;8(21):1195-8. Epub 1998/11/04.

255. Carracedo A, Pandolfi PP. The PTEN-PI3K pathway: of feedbacks and cross-talks. Oncogene. 2008;27(41):5527-41. Epub 2008/09/17.

256. Chalhoub N, Baker SJ. PTEN and the PI3-kinase pathway in cancer. Annu Rev Pathol. 2009;4:127-50. Epub 2008/09/05.

257. Tamura M, Gu J, Matsumoto K, Aota S, Parsons R, Yamada KM. Inhibition of cell migration, spreading, and focal adhesions by tumor suppressor PTEN. Science. 1998;280(5369):1614-7. Epub 1998/06/11.

258. Maier D, Jones G, Li X, Schonthal AH, Gratzl O, Van Meir EG, et al. The PTEN lipid phosphatase domain is not required to inhibit invasion of glioma cells. Cancer Res. 1999;59(21):5479-82. Epub 1999/12/20.

259. Gildea JJ, Herlevsen M, Harding MA, Gulding KM, Moskaluk CA, Frierson HF, et al. PTEN can inhibit in vitro organotypic and in vivo orthotopic invasion of human bladder cancer cells even in the absence of its lipid phosphatase activity. Oncogene. 2004;23(40):6788-97. Epub 2004/07/27.

260. Leslie NR, Yang X, Downes CP, Weijer CJ. PtdIns(3,4,5)P(3)-dependent and -independent roles for PTEN in the control of cell migration. Curr Biol. 2007;17(2):115-25. Epub 2007/01/24.

261. Raftopoulou M, Etienne-Manneville S, Self A, Nicholls S, Hall A. Regulation of cell migration by the C2 domain of the tumor suppressor PTEN. Science. 2004;303(5661):1179-81. Epub 2004/02/21.

262. Okumura K, Zhao M, Depinho RA, Furnari FB, Cavenee WK. Cellular transformation by the MSP58 oncogene is inhibited by its physical interaction with the PTEN tumor suppressor. Proc Natl Acad Sci U S A. 2005;102(8):2703-6. Epub 2005/01/22.

263. Wang X, Jiang X. Post-translational regulation of PTEN. Oncogene. 2008;27(41):5454-63. Epub 2008/09/17.

264. Shen WH, Balajee AS, Wang J, Wu H, Eng C, Pandolfi PP, et al. Essential role for nuclear PTEN in maintaining chromosomal integrity. Cell. 2007;128(1):157-70. Epub 2007/01/16.

265. Chung JH, Eng C. Nuclear-cytoplasmic partitioning of phosphatase and tensin homologue deleted on chromosome 10 (PTEN) differentially regulates the cell cycle and apoptosis. Cancer Res. 2005;65(18):8096-100. Epub 2005/09/17.

266. Song MS, Carracedo A, Salmena L, Song SJ, Egia A, Malumbres M, et al. Nuclear PTEN regulates the APC-CDH1 tumor-suppressive complex in a phosphatase-independent manner. Cell. 2011;144(2):187-99. Epub 2011/01/19.

267. Zhu Y, Hoell P, Ahlemeyer B, Krieglstein J. PTEN: a crucial mediator of mitochondria-dependent apoptosis. Apoptosis. 2006;11(2):197-207. Epub 2006/02/28.

268. Zu L, Zheng X, Wang B, Parajuli N, Steenbergen C, Becker LC, et al. Ischemic preconditioning attenuates mitochondrial localization of PTEN induced by ischemia-reperfusion. Am J Physiol Heart Circ Physiol. 2011;300(6):H2177-86. Epub 2011/03/23.

269. Fleming N, Mellow L. Arachidonic acid stimulates intracellular calcium mobilization and regulates protein synthesis, ATP levels, and mucin secretion in submandibular gland cells. J Dent Res. 1995;74(6):1295-302. Epub 1995/06/01.

270. Grynkiewicz G, Poenie M, Tsien RY. A new generation of Ca2+ indicators with greatly improved fluorescence properties. J Biol Chem. 1985;260(6):3440-50. Epub 1985/03/25.

271. Torres J, Rodriguez J, Myers MP, Valiente M, Graves JD, Tonks NK, et al. Phosphorylation-regulated cleavage of the tumor suppressor PTEN by caspase-3: implications for the control of protein stability and PTEN-protein interactions. J Biol Chem. 2003;278(33):30652-60. Epub 2003/06/06.

272. Andres-Pons A, Valiente M, Torres J, Gil A, Rogla I, Ripoll F, et al. Functional definition of relevant epitopes on the tumor suppressor PTEN protein. Cancer Lett. 2005;223(2):303-12. Epub 2005/05/18.

273. Cantley LC. The phosphoinositide 3-kinase pathway. Science. 2002;296(5573):1655-7. Epub 2002/06/01.

274. Vazquez F, Matsuoka S, Sellers WR, Yanagida T, Ueda M, Devreotes PN. Tumor suppressor PTEN acts through dynamic interaction with the plasma membrane. Proc Natl Acad Sci U S A. 2006;103(10):3633-8. Epub 2006/03/16.

275. Planchon SM, Waite KA, Eng C. The nuclear affairs of PTEN. J Cell Sci. 2008;121(Pt 3):249-53. Epub 2008/01/25.

276. Morimoto AM, Tomlinson MG, Nakatani K, Bolen JB, Roth RA, Herbst R. The MMAC1 tumor suppressor phosphatase inhibits phospholipase C and integrin-linked kinase activity. Oncogene. 2000;19(2):200-9. Epub 2000/01/25.

277. Razzini G, Brancaccio A, Lemmon MA, Guarnieri S, Falasca M. The role of the pleckstrin homology domain in membrane targeting and activation of phospholipase Cbeta(1). J Biol Chem. 2000;275(20):14873-81. Epub 2000/05/16.

278. Singh G, Odriozola L, Guan H, Kennedy CR, Chan AM. Characterization of a novel PTEN mutation in MDA-MB-453 breast carcinoma cell line. BMC Cancer. 2011;11(1):490. Epub 2011/11/23.

279. Lindsay Y, McCoull D, Davidson L, Leslie NR, Fairservice A, Gray A, et al. Localization of agonist-sensitive PtdIns(3,4,5)P3 reveals a nuclear pool that is insensitive to PTEN expression. J Cell Sci. 2006;119(Pt 24):5160-8. Epub 2006/12/13.

280. Helms JB, de Vries KJ, Wirtz KW. Synthesis of phosphatidylinositol 4,5-bisphosphate in the endoplasmic reticulum of Chinese hamster ovary cells. J Biol Chem. 1991;266(32):21368-74. Epub 1991/11/15.

281. Watt SA, Kular G, Fleming IN, Downes CP, Lucocq JM. Subcellular localization of phosphatidylinositol 4,5-bisphosphate using the pleckstrin homology domain of phospholipase C delta1. Biochem J. 2002;363(Pt 3):657-66. Epub 2002/04/20.

282. Sato M, Ueda Y, Takagi T, Umezawa Y. Production of PtdInsP3 at endomembranes is triggered by receptor endocytosis. Nat Cell Biol. 2003;5(11):1016-22. Epub 2003/10/07.

283. McConnachie G, Pass I, Walker SM, Downes CP. Interfacial kinetic analysis of the tumour suppressor phosphatase, PTEN: evidence for activation by anionic phospholipids. Biochem J. 2003;371(Pt 3):947-55. Epub 2003/01/22.

284. Campbell RB, Liu F, Ross AH. Allosteric activation of PTEN phosphatase by phosphatidylinositol 4,5-bisphosphate. J Biol Chem. 2003;278(36):33617-20. Epub 2003/07/15.

285. Leslie NR, Batty IH, Maccario H, Davidson L, Downes CP. Understanding PTEN regulation: PIP2, polarity and protein stability. Oncogene. 2008;27(41):5464-76. Epub 2008/09/17.

286. Gericke A, Munson M, Ross AH. Regulation of the PTEN phosphatase. Gene. 2006;374:1-9. Epub 2006/05/06.

287. Crockett DK, Fillmore GC, Elenitoba-Johnson KS, Lim MS. Analysis of phosphatase and tensin homolog tumor suppressor interacting proteins by in vitro and in silico proteomics. Proteomics. 2005;5(5):1250-62. Epub 2005/02/18.

288. Flores-Delgado G, Liu CW, Sposto R, Berndt N. A limited screen for protein interactions reveals new roles for protein phosphatase 1 in cell cycle control and apoptosis. J Proteome Res. 2007;6(3):1165-75. Epub 2007/02/06.

289. Tang TS, Tu H, Wang Z, Bezprozvanny I. Modulation of type 1 inositol (1,4,5)-trisphosphate receptor function by protein kinase a and protein phosphatase 1alpha. J Neurosci. 2003;23(2):403-15. Epub 2003/01/21.

290. Zhu W, Cowie A, Wasfy GW, Penn LZ, Leber B, Andrews DW. Bcl-2 mutants with restricted subcellular location reveal spatially distinct pathways for apoptosis in different cell types. EMBO J. 1996;15(16):4130-41. Epub 1996/08/15.

291. Slot JW, Geuze HJ, Gigengack S, Lienhard GE, James DE. Immuno-localization of the insulin regulatable glucose transporter in brown adipose tissue of the rat. J Cell Biol. 1991;113(1):123-35. Epub 1991/04/01.

292. Confalonieri S, Salcini AE, Puri C, Tacchetti C, Di Fiore PP. Tyrosine phosphorylation of Eps15 is required for ligand-regulated, but not constitutive, endocytosis. J Cell Biol. 2000;150(4):905-12. Epub 2000/08/23.